



UNIVERSITAT_{DE}
BARCELONA

**Preclinical evaluation of the antitumor activity
of a new CXCR4 inhibitor: a novel therapeutic approach
in diffuse large B-cell lymphoma**

Clara Recasens Zorzo



Aquesta tesi doctoral està subjecta a la llicència **Reconeixement- NoComercial – SenseObraDerivada 3.0. Espanya de Creative Commons.**

Esta tesis doctoral está sujeta a la licencia **Reconocimiento - NoComercial – SinObraDerivada 3.0. España de Creative Commons.**

This doctoral thesis is licensed under the **Creative Commons Attribution-NonCommercial-NoDerivs 3.0. Spain License.**

DOCTORAL THESIS

Preclinical evaluation of the antitumor activity of
a new CXCR4 inhibitor: a novel therapeutic
approach in diffuse large B-cell lymphoma

Clara Recasens Zorzo

Barcelona 2018

DOCTORAL PROGRAMME IN BIOMEDICINE
Research line - Molecular and cellular biology of cancer

2014 - 2018



University of Barcelona - Faculty of Medicine

Preclinical evaluation of the antitumor activity of a new CXCR4 inhibitor: a novel therapeutic approach in diffuse large B-cell lymphoma

Doctoral thesis presented by:

Clara Recasens Zorzo

Institut d'Investigacions Biomèdiques August Pi i Sunyer (IDIBAPS)
Hematology-Oncology department

Gaël Roué

Thesis director

Patricia Pérez Galán

Thesis director

Elías Campo Güerri

Thesis tutor

Clara Recasens Zorzo

Doctorand

Barcelona, April 2018

Clara Recasens Zorzo: PRECLINICAL EVALUATION OF THE ANTITUMOR ACTIVITY OF A NEW CXCR4 INHIBITOR: A NOVEL THERAPEUTIC APPROACH IN DIFFUSE LARGE B-CELL LYMPHOMA, Doctoral Thesis.

Doctoral programme in BIOMEDICINE, University of Barcelona.

Funded by: European Regional Development Fund (ERDF) “Una manera de hacer Europa”, Integrated Excellence Grant from the Instituto de Salud Carlos III (ISCIII) PIE1313/00033.

Barcelona, April 2018

DOCTORAL THESIS

Preclinical evaluation of the antitumor activity of
a new CXCR4 inhibitor: a novel therapeutic
approach in diffuse large B-cell lymphoma

Clara Recasens Zorzo

Barcelona 2018

To my parents,
Maria and Jordi

Contents

Table of contents

Contents	vii
Table of contents	ix
List of figures	xv
List of tables	xvii
Abbreviations	xviii
1 Introduction	1
1.1 B cell lymphoid neoplasms.....	4
1.2 Normal B-cell development	4
1.3 B-cell lymphomagenesis.....	6
1.3.1 Genomic transforming events.....	6
1.3.2 Tumor Microenvironment.....	7
1.4 Diffuse large B-cell lymphoma, NOS.....	7
1.4.1 Taxonomy.....	7
1.4.2 Clinical presentation at diagnosis	8
1.4.3 Staging and Risk assessment	10
1.4.4 Pathobiology	11
1.4.4.1 Genetic alterations.....	13
GCB-DLBCL	13
ABC-DLBCL	14
Genetic alterations shared across subtypes	14
1.4.4.2 DLBCL microenvironment.....	16
1.4.5 Treatment.....	16
1.4.5.1 Immunochemotherapy	17
1.4.5.2 Cell-of-origin based therapies	18
Proteasome inhibitors	18
Immunomodulatory drugs	19

CONTENTS

BTK inhibitors	19
EZH2 inhibitors	19
1.4.5.3 Other novel therapies	19
PI3K inhibitors	20
BCL2 inhibitors	20
BCL6 inhibitors	20
CAR-T cells	20
1.5 CXCR4.....	21
1.5.1 The CXCL12 - CXCR4 pathway.....	22
1.5.2 The role of CXCL12 - CXCR4 in healthy biological processes	23
1.5.3 The role of CXCL12 - CXCR4 in cancer	24
1.5.4 The role of CXCL12 - CXCR4 in DLBCL.....	26
1.5.5 CXCR4 inhibition	26
1.5.6 CXCR4 inhibitors in the clinic or in development	27
1.5.6.1 AMD3100	28
Limitations of AMD3100.....	30
1.5.6.2 Other CXCR4 inhibitors in clinical trials	30
1.5.6.3 IQS-01.01.....	31
1.6 MYC.....	33
1.6.1 The role of MYC in healthy biological processes	33
1.6.2 The role of MYC in cancer and DLBCL	34
1.6.3 MYC inhibition	34
1.6.3.1 BET inhibitors.....	34
CPI203.....	36
1.7 CXCR4 and MYC.....	37
1.7.1 MYC stability	37
1.7.2 The CXCR4 - ERK1/2 - MYC signaling loop.....	38
2 Hypothesis & Aims	41
2.1 Hypothesis	43

2.2	General aim and specific objectives	44
3	Methods	45
3.1	Cell lines, cell culture and patient samples	47
3.1.1	DLBCL cell lines.....	47
3.1.2	Generation of SUDHL6-GFP+/Luc+	48
3.1.2.1	Plasmid amplification.....	48
3.1.2.2	Lentivirus generation	48
3.1.2.3	Infection of SUDHL6 and sorting of GFP+ cells.....	48
3.1.3	StromaNKtert	48
3.1.4	Isolation and culture of DLBCL primary cells	49
3.1.5	Isolation and culture of PBMCs	49
3.2	Drugs	50
3.3	cAMP-based CXCR4 activity assay	50
3.4	MTT assay	51
3.5	Chemotaxis assay	52
3.6	Docking study	52
3.7	Flow cytometry analysis	53
3.7.1	CXCR4 staining	53
3.7.2	Occupancy assay	53
3.7.3	Annexin V staining	53
3.8	Protein isolation and Western blot	53
	Western blot antibodies.....	54
	Blots quantification	54
3.9	Protein stability assay.....	54
3.10	RNA isolation and real-time PCR.....	55
3.11	<i>In vivo</i> experiments	55
3.11.1	NOD/SCID-IL2rynull strain	55
3.11.2	Drug administration.....	56
3.11.2.1	Toxicity assay.....	56

3.11.2.2	Doses	56
3.11.3	Systemic model	56
3.11.4	Subcutaneous model.....	57
3.12	IHC.....	57
3.13	Statistics.....	58
4	Results.....	59
4.1	Description of IQS-01.01 and its stereoisomers.....	61
4.1.1	IQS-01.01RS stereoisomer is the most potent CXCR4 inhibitor ..	61
4.1.2	Differential CXCR4 binding properties of IQS-01.01RS over other stereoisomers	62
4.2	IQS-01.01RS holds better pharmacological properties than AMD3100	63
4.2.1	IQS-01.01RS binds to a deeper area in CXCR4 than AMD3100 ...	63
4.2.2	IQS-01.01RS blocks migration of DLBCL tumor cells	65
4.2.3	IQS-01.01RS increases mobilization of DLBCL tumor cells.....	65
4.2.4	IQS-01.01RS inhibits DLBCL tumor growth	67
4.2.4.1	IQS-01.01RS anti-proliferative activity does not correlate with CXCR4 expression levels.....	70
4.2.4.2	IQS-01.01RS presents selectivity towards tumor cells	71
4.2.5	IQS-01.01RS potently inhibits CXCR4 downstream signaling.....	72
4.3	IQS-01.01RS destabilizes MYC protein.....	73
4.3.1	CXCL12 mediates MYC upregulation	73
4.3.2	IQS-01.01RS sustainably downregulates MYC	73
4.3.3	IQS-01.01RS destabilizes MYC protein via AKT	75
4.4	IQS-01.01RS cooperates with BET bromodomain inhibition <i>in vitro</i>	76
4.4.1	CPI203 enhances IQS-01.01RS toxicity in DLBCL	76
4.4.2	IQS-01.01RS and CPI203 cooperate by reducing MYC protein expression	77
4.4.3	CXCR4 levels are not affected by CPI203	79
4.5	IQS-01.01RS cooperates with BET-bromodomain inhibition <i>in vivo</i>	80

4.5.1	IQS-01.01RS and CPI203 combination reduces tumor burden ...	80
4.5.2	<i>In vivo</i> activity of IQS-01.01RS/CPI203 combination relies on CXCR4 downstream signaling blockade and subsequent triggering of apoptosis	82
5	Discussion	83
6	Conclusions	95
7	References	99
	<i>Acknowledgements</i>	123
ANNEX	A-I
	Scientific publications produced during this thesis.....	A-III

List of figures

- Figure 1.- Estimated cancer mortality worldwide in 2012.
- Figure 2.- Schematic representation of B-cell development.
- Figure 3.- Origin of GCB and ABC DLBCL.
- Figure 4.- Kaplan Mayer plot of overall survival of GCB and ABC DLBCL subgroups.
- Figure 5.- CXCR4 structure.
- Figure 6.- CXCR4 signaling pathway.
- Figure 7.- Role of the CXCL12 - CXCR4 axis in cancer.
- Figure 8.- Molecular structure of AMD3100.
- Figure 9.- Molecular structure of IQS-01.01.
- Figure 10.- MYC-MAX heterodimer and DNA binding.
- Figure 11.- BET inhibition.
- Figure 12.- Molecular structure of the BRD4 inhibitor CPI203.
- Figure 13.- Regulation of MYC protein stability.
- Figure 14.- CXCR4 - ERK1/2 - MYC signaling loop.
- Figure 15.- Schematic representation of the HitHunter cAMP Assay Principle.
- Figure 16.- Schematic representation of the transwell chemotaxis assay system.
- Figure 17.- Design of a new potent CXCR4 inhibitor.
- Figure 18.- Docking model.
- Figure 19.- Docking model.
- Figure 20.- Anti-CXCL12 induced chemotaxis activity of IQS-01.01RS and AMD3100.
- Figure 21.- Protein-protein blast.

CONTENTS

Figure 22.-Homing of SUDHL6 and SUDHL6-GFP+/Luc+ injected intravenously in NSG mice.

Figure 23.- Comparison of IQS-01.01RS vs AMD3100 in a systemic mouse model.

Figure 24.- Anti-tumor effect of IQS-01.01RS.

Figure 25.- Apoptosis induction by IQS-01.01RS.

Figure 26.- IQS-01.01RS antitumor effect vs CXCR4 expression dot plot in DLBCL cell lines.

Figure 27.- IQS-01.01RS selectivity.

Figure 28.- Effect of IQS-01.01RS and AMD3100 on CXCR4 signaling.

Figure 29. Relative MYC transcript levels in SUDHL6 cells upon stimulation with CXCL12.

Figure 30.- Modulation of CXCR4 signaling.

Figure 31.- MYC protein stability assay.

Figure 32.- Antitumor effect of the combination in DLBCL cell lines.

Figure 33.- Effects of the combination on signaling.

Figure 34.- Effect of the treatment on *MYC* transcription.

Figure 35.- Effect of CPI203 on CXCR4 levels.

Figure 36.- IQS-01.01RS and CPI203 cooperate to reduce tumor growth in a subcutaneous mouse model of DLBCL.

Figure 37.- Molecular effects underlying the combination of IQS-01.01RS and CPI203 in a subcutaneous model of DLBCL.

List of tables

- Table 1.- World Health Organization classification of aggressive mature B-cell lymphomas.
- Table 2.- Ann Arbor staging classification.
- Table 3.- International prognostic index.
- Table 4.- Age adjusted international prognostic index (aaIPI) in patients ≤ 60 years.
- Table 5.- Genetic alterations in DLBCL.
- Table 6.- Ongoing clinical trials with AMD3100 as an antitumor drug.
- Table 7.- CXCR4 inhibitors in clinical trials.
- Table 8.- Main characteristics of the DLBCL cell lines used in this study.
- Table 9.- Patients characteristics.
- Table 10.- Description of primary antibodies used for western blotting.
- Table 11.- Characteristics of the immune system of NSG mice.
- Table 12.- In vivo route of administration and doses.
- Table 13.- Description of the antibodies used for IHC.
- Table 14.- Sensitivity of DLBCL cell lines to CXCR4 and BET bromodomain inhibition.

Abbreviations

aaIPI: age adjusted IPI

ABC: Activated B-cell

Ac-Lys: Acetylated lysine

ADCC: Antibody-dependent cell-mediated cytotoxicity

AHSCT: Autologous HSC transplantation

ALL: Acute lymphoblastic leukemia

AML: Acute myeloid leukemia

APC: Antigen presenting cell

BCR: B-cell receptor

BCR-DLBCL: BCR/proliferation cluster

BD: Bromodomain

BET: Bromodomain and extra-terminal

bHLH-LZ: Basic-helix-loop-helix-leucine zipper

BL: Burkitt lymphoma

BLI: Bioluminescence imaging

BM: Bone marrow

BTK: Bruton's tyrosine kinase

CAM-DR: Cell adhesion mediated drug resistance

CAR T-cells: Chimeric Antigen Receptor T-cells

CCC: Consensus clustering classification

CD: Cluster of differentiation

CDC: Complement Dependent Cytotoxicity

CHOP: Cyclophosphamide, doxorubicin, vincristine, prednisolone

CHX: Cycloheximide

CI: Combination index

CI: Confidence interval

CLL: Chronic lymphocytic leukemia

COO: Cell of origin

CSR: Class switch recombination

Ct: C terminal

DH: "Double hit". High-grade B-cell lymphoma with MYC and BCL2 and/or BCL6 rearrangements

DLBCL, NOS: DLBCL, not otherwise specified

DLBCL: Diffuse large B-cell lymphoma

EA: Enzyme acceptor

ECL: Enhanced chemiluminescence

ECOG: Eastern Cooperative Oncology Group

ED: Enzyme donor

EMA: European Medicine Agency

ET: Extra-terminal

FBS: Fetal bovine serum

FDA: U.S. Food and Drug Administration

FFPE: Formalin-fixed paraffin wax-embedded

FL: Follicular lymphoma

GC: Germinal center

GCB: Germinal center B-cell

G-CSF: Granulocyte colony stimulating factor

GELA: Groupe d'Etudes des Lymphomes de l'Adulte

GEM: Molecular Engineering group

GEP: Gene expression profiling

GFP: Green fluorescence protein

GPCR: G-protein coupled receptor

H3: Histone 3

ABBREVIATIONS

- HE:** Hematoxylin and eosin
- HIV:** Human immunodeficiency virus
- HLA-I:** Human leukocyte antigen I
- HR:** Host response cluster
- HRP:** Horseradish peroxidase
- HSC:** Hematopoietic stem cells
- i.p.:** intraperitoneal administration
- IARC:** Agency for Research on Cancer
- IARC:** International Agency for Research on Cancer
- iCXCR4:** Intracellular CXCR4
- Ig:** Immunoglobulin
- IHC:** Immunohistochemistry
- IPI:** International prognostic index
- IQS:** Institut Químic de Sarrià
- IQS:** Institut Químic de Sarrià
- LDH:** Lactate dehydrogenase
- LL:** Lymphoblastic lymphoma
- LN:** Lymph node
- Luc:** Luciferase
- m:** monoclonal
- MCL:** Mantel cell lymphoma
- MDS:** Myelodysplastic syndromes
- MFI-R:** Median fluorescence intensity ratio
- MinT:** MabThera International Trial
- MM:** Multiple myeloma
- MOI:** Multiplicity of infection
- MRD:** Minimal residual disease

- MS:** Myelodysplastic syndrome
- MTD:** Maximum tolerated dose
- NHL:** Non-Hodgkin lymphoma
- NMC:** NUT midline carcinoma
- NSCLC:** Non-small-cell lung carcinoma
- NSG:** NOD/SCID IL2r γ null mice
- Nt:** N terminal
- ORR:** Overall response rate
- OxPhos-DLBCL:** Oxidative phosphorylation cluster
- p.o.:** oral administration
- p:** phospho
- PBMCs:** Peripheral blood mononuclear cells
- PCR:** Polymerase chain reaction
- PE:** Phycoerythrin
- PFA:** Paraformaldehyde
- PP2A:** Phosphatase 2A
- R-CHOP:** Rituximab + CHOP
- sCXCR4:** Surface CXCR4
- SD:** Standard deviation
- SDF-1 α :** Stromal derived factor 1 α
- SDM:** Site directed mutagenesis
- SDS-PAGE:** Sodium dodecyl sulfate polyacrylamide gel electrophoresis
- SEM:** Standard error of the mean
- SHM:** Somatic hypermutation
- SPF:** Specific pathogen free
- STR:** Short tandem repeat
- TF:** Transcription factor

ABBREVIATIONS

TH: "Triple hit". High-grade B-cell lymphoma with MYC and BCL2 and/or BCL6 rearrangements

TLR: Toll like receptor

TMD: Transmembrane domain

TME: Tumor microenvironment

WHO: World Health Organization

1 Introduction

Cancer is among the leading causes of death worldwide. The International Agency for Research on Cancer (IARC) of the World Health Organization (WHO) estimated, in 2012, 14.090.149 new cancer cases and a cancer mortality of 8.201.030 deaths per year worldwide (Figure 1). These figures are predicted to increase in the coming years.

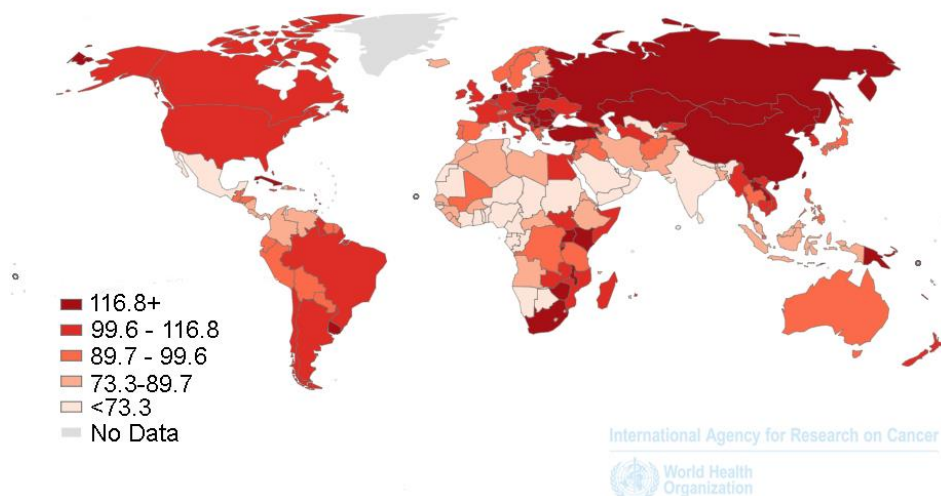


Figure 1.- Estimated cancer mortality worldwide in 2012. Age standardized rate. All cancers excluding non-melanoma skin cancer. From (GLOBOCAN, 2012), IARC.

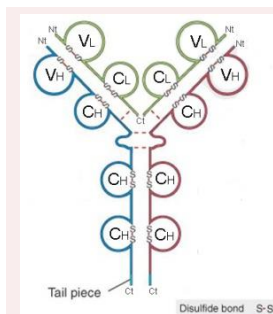
Cancer is caused by any alteration that leads to uncontrolled and continuous cell survival and proliferation. There are more than 200 pathogenically distinct cancer types, classified depending on the tissue of origin, and the type of cell from which they originate.

1.1 B-cell lymphoid neoplasms

Worldwide, 23 new cases of lymphomas are diagnosed per 100.000 people per year (National Institute of Health a). This heterogeneous group of cancers originates from lymphocytes and is estimated to account for 4% of malignant neoplasms. Ninety five percent of the lymphomas arise from B-cells, whereas the remaining 5% are T-cell malignancies (Küppers, 2005). More than 35 types of B-cell lymphomas, that rely on different oncogenic pathways, are categorized by the WHO based on the differentiation stage of the normal B-cell counterpart from which they have originated (Calinescu et al., 2017; Campo et al., 2011; Maurer et al., 2014).

1.2 Normal B-cell development

B-lymphocytes (or B-cells), are components of the humoral adaptive immune system responsible for antibody production and secretion, and immunological memory.



Structure of an Immunoglobulin.
Abbreviations: V, variable; C, constant; L, light; H, heavy.
Adapted from (Abbas et al., 2010).

Antibodies or immunoglobulins (Ig) are proteins specialized to bind to a given antigen and activate and immune response from effector cells to overcome infection. They are codified by antigen receptor genes and are composed of two heavy and two light chains with a constant region, and a variable region that matures to obtain a unique high affinity antigen-binding structure. The constant regions of the heavy chain determine their classification into 5 isotypes (IgA, IgD, IgE, IgG, and IgM). Each immunoglobulin isotype mediates different effector functions such as complement activation, phagocyte response, or mast cell degranulation among others. B-lymphocytes may also synthesise immunoglobulins, with additional hydrophobic alpha helices, that act as a membrane B-cell receptor (BCR) (also called antigen receptor) and signal through the cell with the help of two other transmembrane molecules (CD79A and CD79B).

In adults, B-cells originate from hematopoietic stem cells (HSC) in the bone marrow (BM) where they partially mature. Then, they migrate to secondary lymphoid organs (like the lymph nodes or the spleen) to encounter an antigen, complete their maturation and become an effector antibody producing cell, or a memory cell (Figure 2).

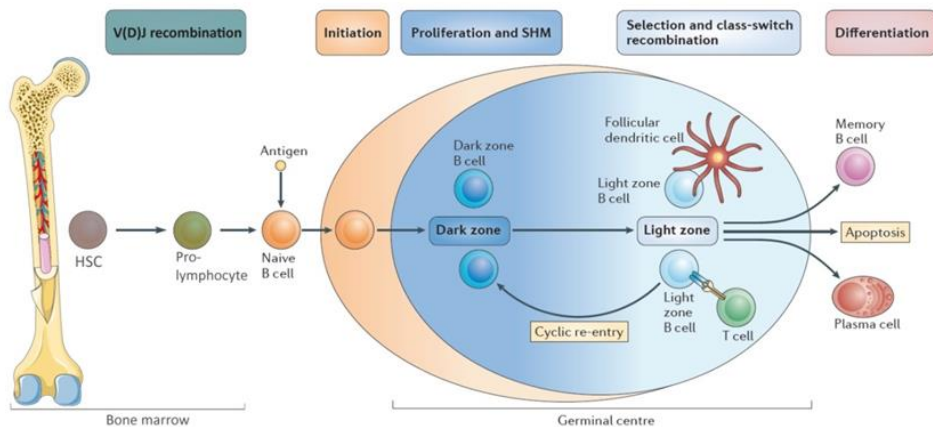


Figure 2.- Schematic representation of B-cell development. Abbreviations: HSC, hematopoietic stem cell; SHM, somatic hypermutation. Adapted from (Basso and Dalla-Favera, 2015).

The first stage of B-lymphocyte development, which takes place in the BM, is the generation of a "naive" B-cell that has not yet been in contact with an antigen. Pro-lymphocytes develop from a common lymphoid progenitor that has, in turn, originated from a pluripotent HSC committed to B-cell lineage. Pro-lymphocytes undergo DNA antigen receptor gene rearrangements in the variable regions of the heavy chain (**V(D)J recombination**) to assemble and express a pre-BCR that provides survival signals and become pre-lymphocytes. Lymphocytes that fail to express BCR or autoreact with self-antigens are negatively selected in favor of those with no auto-reactive BCR.

Naive, immature, positively selected B-lymphocytes enter the peripheral lymphoid tissues where, upon infection, become in contact with antigens and undergo two main maturation steps for antigen recognition: **affinity maturation** also called **somatic hypermutation (SHM)**, and **isotype switching** also named **class switch recombination (CSR)**. This second stage of antigen-dependent maturation takes place in the germinal centers (GC) that are formed in the follicles of secondary lymphoid organs in the context of an infection.

Naive B-cells that enter the secondary lymphoid organ through the subscapular sinus migrate towards the B cell zone in a primary follicle. After stimulation by antigens, secondary follicles with GCs histologically divided into a dark and a light zone are formed. In the dark zone, new variable regions of their antibody chains are generated through SHM and it becomes an area for enlarged, rapidly proliferating B-cells called centroblasts. Centroblasts then become smaller non dividing centrocytes that migrate to the light zone of the GC, where they interact with antigen presenting cells (APC) like T-cells, follicular dendritic cells or macrophages. This migration, and the general organization of the germinal center is mediated by chemokines and chemokine receptors such as CXCL13-CXCR5 and CXCL12-CXCR4 (Allen et al., 2004). Centrocytes

which express BCRs with low affinity for an antigen undergo apoptosis. Those centrocytes that have encountered an antigen and have bound to it with high affinity receive survival signals (i.e. via CD40, BCR...) and are positively selected. At this stage, mature B-cells may change the isotypes of their Immunoglobulin (Ig) via isotype switching to mediate distinct effector functions while they conserve the antigen high affinity of the variable region.

Finally, mature B-lymphocytes exit the GC as antibody secreting plasma cells to fight infection or as memory B-cells (Abbas et al.,2010; De Silva and Klein, 2015; Klein and Dalla-Favera, 2008) (Figure 2).

1.3 B-cell lymphomagenesis

Each type of lymphoma originates from a healthy B-cell counterpart in a particular developmental stage. This is evidenced by the similarity of the lymphoma B-cell with its normal cell of origin (COO), considering their cytological and morphological features, their common immunophenotype, and their gene expression profiling (GEP). The presence of SHM in many malignant cells indicates that most lymphoma cases originate from GC or post-GC B-cells and that malignant transformation originates in the GC (Klein and Dalla-Favera, 2008; Küppers, 2005). Depending on the developmental stage, different molecular pathways are activated and receptors are expressed on the surface of the B-cell. These characteristics are often conserved after the generation of the tumor and play an important role in its development and response to therapy.

Lymphomagenesis is driven by the cooperation between genomic aberrations and a supportive tumor microenvironment.

1.3.1 Genomic transforming events

Dysfunction of oncogenes is a crucial mechanism for tumor development. The vigorous clonal expansion accompanied by DNA breaks during SHM and isotype switching gives the developing B-cell a high genomic instability that may turn out into chromosomal translocations or SHM of proto-oncogenes. In B-cell lymphoma, oncogenic **chromosomal translocations** generally occur when immunoglobulin gene remodeling is malfunctioning and an oncogene is translocated from its chromosome to one of the immunoglobulin (Ig) loci causing an aberrant expression of this latest (Klein and Dalla-Favera, 2008).

An **oncogene** is an aberrantly expressed gene that may drive cancer development.

A **proto-oncogene** is a gene, usually related to cell death or growth control, susceptible of becoming an oncogene.

1.3.2 Tumor Microenvironment

Immunohistochemistry (IHC) of tumor biopsies reveals that the tumor mass is formed by "non-malignant" cells accompanying the transformed tumor B-cells. These cells constitute the tumor microenvironment (TME). As previously mentioned, most lymphomas originate from GC counterparts that strongly rely on adjacent APCs for selection and survival. In an analogue way, malignant cell survival and proliferation is influenced by the surrounding TME. For instance neighbor stroma cells secrete pro-survival cytokines, and immune cells like T-cells, mast cells, macrophages, and monocytes may also provide the tumor with survival and proliferation signals. A favorable microenvironment is not only necessary at the original site of a tumor to complete tumor growth and development, but also plays a crucial role in metastasis. In fact, malignant cells not only home to metastatic sites with a favorable microenvironment, but have the ability to modify and recruit more supporting cells for their own benefit (Scott and Gascoyne, 2014). In addition, TME is often responsible for environmental-mediated drug resistance by retaining tumor cells in favorable, inaccessible niches. This phenomenon is called cell adhesion mediated drug resistance (CAM-DR) (Shain et al., 2015).

1.4 Diffuse large B-cell lymphoma, NOS

1.4.1 Taxonomy

Diffuse large B-cell lymphoma (DLBCL) is an aggressive neoplasm that represents the most common subtype of non-Hodgkin lymphoma (NHL) (30-40% of all new diagnosed cases) (Campo et al., 2011; Hennessy et al., 2004). It is an entity that has, historically, included multiple clinical and biologically distinct subgroups. In 2008, the WHO updated the classification of lymphoid neoplasms with the aim to narrow this heterogeneity and refine treatment and criteria for participation in clinical trials (Swerdlow et al., 2008). The 2016 revised version of this classification identifies 23 entities constituting the aggressive mature B-cell lymphomas groups of B lymphoid neoplasms (Campo, 2017; Swerdlow et al., 2016) (Table 1).

Diffuse large B-cell lymphoma, not otherwise specified (DLBCL, NOS)
Germinal center B-cell type (GCB)
Activated B-cell type (ABC)
T-cell/histiocyte-rich large B-cell lymphoma
DLBCL, topographic site related
Primary mediastinal (thymic) large B-cell lymphoma
Primary DLBCL of the CNS
Primary cutaneous DLBCL, leg type
Intravascular large B-cell lymphoma
DLBCL, EBV-related
EBV-positive DLBCL, NOS
DLBCL associated with chronic inflammation
Lymphomatoid granulomatosis
LBCL with terminal B-cell differentiation
Plasmablastic lymphoma
ALK-positive large B-cell lymphoma
Primary effusion lymphoma
HHV8+ DLBCL, NOS
Burkitt-lymphoma
Burkitt-like lymphoma with 11q aberrations
High grade B-cell lymphoma
High-grade B-cell lymphoma, with <i>MYC</i> and <i>BCL2</i> and/or <i>BCL6</i> rearrangements
High-grade B-cell lymphoma, NOS

Table 1.- World Health Organization classification of aggressive mature B-cell lymphomas. Abbreviations: ALK, anaplastic lymphoma kinase; CNS, central nervous system; EBV, Epstein-Barr virus. Adapted from (Campo, 2017).

Among this group of aggressive B-lymphomas, **DLBCL, not otherwise specified (DLBCL, NOS)** is the predominant entity comprising about 80% of all the cases. It still presents a high clinical and biological heterogeneity, includes tumors that cannot be classified as any other entity, and is subclassified into the cell COO subgroups **germinal center B-cell type (GCB)**, and **activated B-cell type (ABC)** (Campo, 2017).

1.4.2 Clinical presentation at diagnosis

The DLBCL, NOS heterogeneous entity is slightly more common in males than females. The common age of diagnosis, is along the 70s although it may also occur in infants and younger adults. It usually arises *de novo*, but it can also originate from

transformation of indolent malignancies such as follicular lymphoma (FL) or chronic lymphocytic leukemia (CLL). Patients at diagnosis commonly present adenopathy and 60% suffer B symptoms. Although it is a mainly nodal disease, 30% of the patients present affection in extra nodal sites such as bone, gastrointestinal track, skin, thyroids or gonads. Additionally, 20-30% of the cases present BM involvement at diagnosis (Campo et al., 2011).

Morphology, immunophenotype, cytogenetics and molecular biology are used for DLBCL diagnosis and variant identification. DLBCL is diagnosed based on histopathological analysis of a biopsy of the affected area (i.e. lymph node). This biopsy is fixed and analyzed by IHC stained with antibody panels designed to confirm B-cell proliferation and lineage (CD19+, CD20+, CD79a+, CD45+, CD5-/+ , CD10-/+ , Ki67). Immunophenotypical, combined with morphological analysis are used for the definitive diagnosis.

Cluster of differentiation (CD) are lymphocyte markers. Membrane proteins that identify a particular lineage or differentiation stage. All leukocyte surface antigens whose structures are defined are given a CD designation. Classification of lymphocytes by CD antigens is widely used in the clinics and research.

It is recommended to send a fresh biopsy to the laboratory to perform flow cytometry studies that will aid a faster diagnosis prediction, and to enable high quality DNA and RNA extraction for further possible use in medical research and personalized medicine. Primary tumor cells may also be cryopreserved for functional translational research studies (Kubuschok et al., 2015; Tilly et al., 2015).

Due to the costs of GEP which requires frozen tissue often unavailable, and the difficulties in the reproducibility of distinguishing the GCB and ABC subsets by immunohistochemistry (IHC) (Colomo et al., 2003; Choi et al., 2009; Gutiérrez-García et al., 2011; Hans et al., 2004; Meyer et al., 2010; Muris et al., 2006), the WHO committee decided not to require their distinction in daily clinical practice in 2008 (Swerdlow et al., 2008). Nevertheless, as the worst prognosis impact of the ABC subtype has become clear, and new therapeutic strategies are considering the differential treatment of these subgroups, the 2016 revision requires their classification and accepts the use of IHC algorithms (Swerdlow et al., 2016).

As a consequence of this requirement, and the subjectivity and variability of IHC based strategies, an effort is being made to develop new, higher resolution assays viable to be used in the clinics. The nCounter platform of NanoString Technologies (Seattle, WA, USA) allows for gene expression detection using formalin-fixed paraffin wax-embedded (FFPE) tissues, and the Lymph2Cx assay coupled to the NanoString

platform is a promising example that has recently proven to identify COO of DLBCL and predict prognosis better than IHC algorithms (Scott et al., 2014; Yoon et al., 2017).

1.4.3 Staging and risk assessment

Staging of DLBCL is determined according to the Ann Arbor classification (Table 2). The international prognostic index (IPI) is used for patient classification with prognostic purposes and takes into account 5 predictors: age, blood levels of lactate dehydrogenase (LDH), extra nodal involvement, Eastern Cooperative Oncology Group (ECOG) performance status (Oken et al., 1982), and Ann Arbor stage (Table 3). To classify young patients with aggressive lymphomas, age adjusted IPI (aaIPI) is used (Table 4) (Kubuschok et al., 2015; Tilly et al., 2015).

Maximum bulk of the disease, a factor that is not included in the IPI, should be assessed as the MabThera International Trial (MinT) study showed a linear relationship between bulk and prognosis (Pfreundschuh et al., 2006) however it is becoming clearer that this factor may not affect current treatment strategies (Lamy et al., 2017).

Stage	
I	Involvement of a single lymphatic region (I) or localized involvement of single extralymphatic organ or site (IE)
II	Involvement of two or more lymphatic regions on the same side of the diaphragm (II) or localized involvement of a single extralymphatic organ or site and of one or more lymphatic regions on the same site of the diaphragm (IIE)
III	Involvement of lymphatic regions on both sides of the diaphragm
IV	Diffuse or disseminated involvement of one or more extralymphatic organs with or without lymphatic involvement

Table 2.- Ann Arbor staging classification. Adapted from (Tilly et al., 2015).

International prognostic Index		
Risk factors		
Age >60 years		
Serum LDH>normal		
Stage III-IV		
Performance status 2-4		
Extranodal sites>1		
Risk categories	Number of risk factors	Estimated 3-year overall survival (95% CI)
Low	0-1	91 (89-94)
Low intermediate	2	81 (73-86)
High intermediate	3	65 (58-73)
High	4-5	59 (49-69)

Table 3.- International prognostic index. Abbreviations: LDH, lactat dehydrogenase; CI, confidence interval. Adapted from (Tilly et al., 2015).

Age adjusted international prognostic index (aalPI) in patients ≤60 years		
Risk factors		
Serum LDH>normal		
Stage III-IV		
Performance status 2-4		
Risk categories	Number of risk factors	Estimated 3-year overall survival (95% CI)
Low	0-1	91 (89-94)
Low intermediate	2	81 (73-86)
High intermediate	3	65 (58-73)
High	4-5	59 (49-69)

Table 4.- Age adjusted international prognostic index (aalPI) in patients ≤60 years. Abbreviations: LDH, lactate dehydrogenase; CI, confidence interval. Adapted from (Tilly et al., 2015).

As detailed in the next chapter of this introduction, biological factors such as COO subtype and TME also affect prognosis and response to treatment.

1.4.4 Pathobiology

GEP studies have confirmed the heterogeneity of DLBCL, NOS, and have recognized two major subtypes according to the putative COO from which they develop: GCB and ABC (Figure 3). GCB-DLBCL and ABC-DLBCL rely on different

oncogenic pathways and differ on prognostic impact, being ABC the most aggressive subgroup (Figure 4) (Alizadeh et al., 2000; Bea et al., 2005; Rosenwald et al., 2002; Staudt and Dave, 2005).

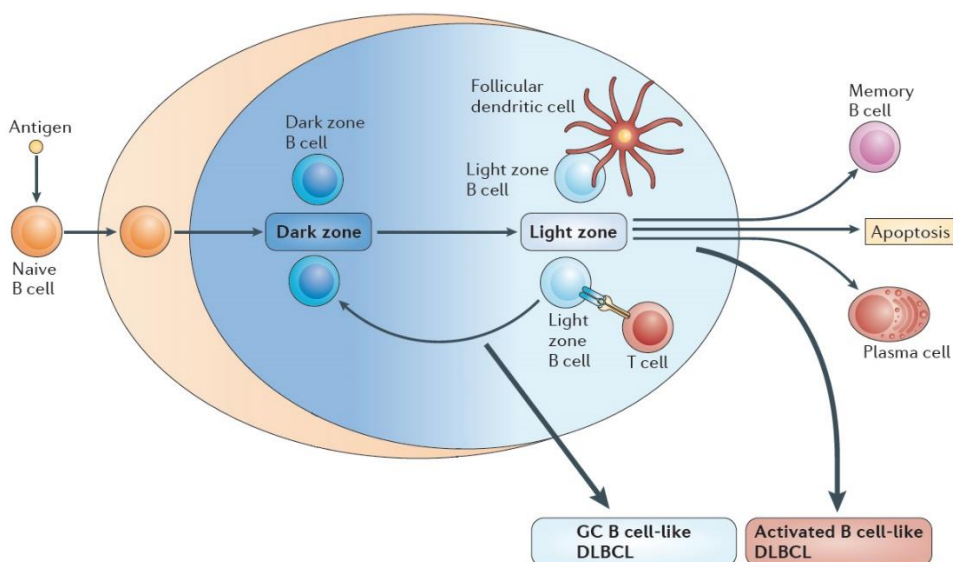


Figure 3.- Origin of GCB and ABC DLBCL. Adapted from (Basso and Dalla-Favera, 2015).

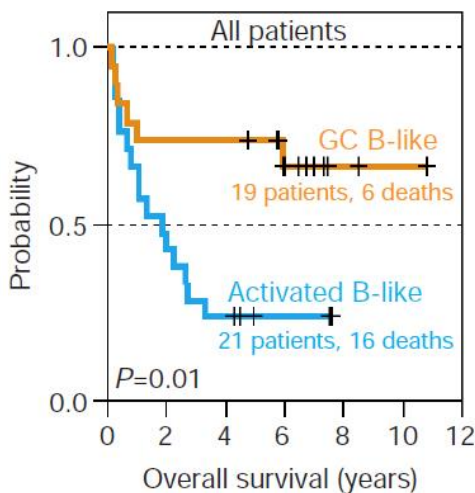


Figure 4.- Kaplan Mayer plot of overall survival of GCB and ABC DLBCL subgroups. ABC patients present a poorer outcome than GCB patients. From (Alizadeh et al., 2000).

Another sub-classification that considers other aspects of DLBCL biology and that is gaining increased importance is the consensus clustering classification (CCC). It includes 3 groups that capture tumor-intrinsic characteristics: the BCR/proliferation cluster (**BCR-DLBCL**) characterized by up-regulation of component genes of the BCR, the OxPhos cluster (**OxPhos-DLBCL**) that presents an increase in mitochondrial oxidative

phosphorylation, and the host response (**HR**) group that is characterized by an inflammatory immune infiltrate (Scott et al., 2014).

Both genetic alterations in the tumor cells and TME play an important role in DLBCL, NOS development and progression.

1.4.4.1 Genetic alterations

With a high number of point mutations, copy number aberrations, and chromosomal translocations, DLBCL, NOS shows significantly higher genomic instability than other B-cell neoplasms (Pasqualucci and Dalla-Favera, 2014). Many tumor cells present genomic instability that leads to aberrant chromosomal structures that may be due to three forms of chromosomal alterations: **translocations, duplications** and **deletions**. A translocation takes place when a proto-oncogene, is translocated into a different chromosome and, under control of a different promoter, becomes aberrantly expressed. The rapid proliferation rate, and immunoglobulin mutations and rearrangements that the CG B-cells are exposed to, is the main reason for the high genomic instability found in post GC lymphomas like DLBCL, NOS where insertions of protooncogenes in immunoglobulin *loci* of chromosome 14 are often detected. Translocations of *MYC* t(8;14), *BCL2* t(14;18) or *BCL6* t(3;14) are found in DLBCL, NOS with a frequency of 20%, 40% and 40% respectively (Testoni et al., 2015).

Below are the common oncogenic alterations found in DLBCL depending on the COO subgroup also summarized in [Table 5](#).

GCB-DLBCL

GCB-DLBCL derives from GC B-cells and presents SHM in Ig genes accordingly. The following alterations are characteristic of GCB-DLBCL:

The **EZH2** methyltransferase is a component of the polycomb repressive complex and acts as a gene silencer through methylation of histone 3 (H3). It is targeted by gain of function SHM that are a hallmark of GCB-DLBCL and have been reported in 20% of the cases. These mutations lead to EZH2 overexpression and enhanced activity linked to aberrant repression of tumor suppressor genes (Béguelin et al., 2013; McCabe et al., 2012a). Recurrent mutations of the **GNA13** gene that codifies for a Gα13 protein involved in several cellular processes and dynamics such as cell-cycle, and actin polymerization are also found in 30% of the cases of this subtype of DLBCL (Lenz et al., 2008a). Given the variability that characterize DLBCL, other recurrent mutations or genomic rearrangements of oncogenes or tumor suppressor genes such as **PTEN**, **CREBB**, **TNFRSF14**, **MLL2**, and members of the **PI3K** pathway may also be detected in a

percentage of GCB-DLBCL (Basso and Dalla-Favera, 2015; Pasqualucci, 2013; Pasqualucci and Dalla-Favera, 2014; Pasqualucci and Dalla-Favera, 2015) (Table 5).

ABC-DLBCL

ABC-DLBCL seems to derive from plasmablasts, from GC cells arrested during the early stages of post-GC plasma cell differentiation. Therefore this subtype expresses genes that are upregulated in B-cells with activated BCRs such as *IRF4* and *XBP1*. Genetic alterations that repress *BLIMP1* and therefore block differentiation into final stage of plasma cells are also found in ABC-DLBCL.

Constitutive activation of the **NF- κ B** pathway through different mechanisms distinguishes the ABC subtype. For instance, *MYD88*, and adaptor protein of toll like receptors (TLR), is found to be mutated in 30% of the cases and it constitutively activates its downstream target NF- κ B (Ngo et al., 2011). Recurrent mutations in *CD79B*, *CD79A* (20%) and *CARD11* (10%) lead to an aberrant constitutive activation of the **BCR** and consequent tumorigenic survival signals and NF- κ B activation. In addition, the *TNFAIP3* which encodes the negative regulator of NF- κ B, A20, is genetically inactivated in 30% of the cases (Basso and Dalla-Favera, 2015; Pasqualucci and Dalla-Favera, 2014; Pasqualucci and Dalla-Favera, 2015) (Table 5).

GENETIC ALTERATIONS SHARED ACROSS SUBTYPES

In addition, several alterations are common in both GCB-DLBCL and ABC-DLBCL.

Ectopic expression of the transcription factor and oncogene **MYC** consequent to chromosomal translocations is detected in 20% of GCB- and 5% of ABC-DLBCL cases. **BCL-2** translocations, which occur in 40% of the cases lead to the consequent overexpression of the antiapoptotic BCL-2 protein that drives tumorigenesis (Basso and Dalla-Favera, 2015). Genetic lesions that result in a deregulation of **BCL-6** are common in DLBCL. BCL-6, is a transcription factor required for GC formation, and is responsible for 1) allowing cells to sustain rapid proliferation rates and the genotoxic stress of SHM, 2) preventing activation of immature B-cells by T-cells, and 3) blocking B-cell differentiation into plasma cells (Basso and Dalla-Favera, 2012; Basso and Dalla-Favera, 2015; Pasqualucci, 2013). Deregulation of *BCL-6* expression plays an important role in lymphomagenesis and may be given through chromosomal translocations (40%), point mutations of the gene (15%), or through mutations or deletions in the *BCL6* negative regulators *CREBBP* and *EP300* (40%). Mutations or deletion of *FBXO11* (13%) (Duan et al., 2012), which controls protein degradation, and *MEF2B* (11%) (Ying et al., 2013), which inactivates *BCL-6*, also lead to its overexpression.

Escape of the immune response is a crucial mechanism for tumorigenesis. In DLBCL it may be due to lack of human leukocyte antigen I (HLA-I) expression consequent to the loss of *B2M* (60%), the escape from Cytotoxic T lymphocytes, or to a lack of *CD58* (21%) expression allowing B-cells to escape from natural killer cells (Challa-Malladi et al., 2011; Pasqualucci and Dalla-Favera, 2014; Pasqualucci and Dalla-Favera, 2015) (Table 5).

Altered gene	Product	Function in tumorigenesis
GCB-DLBCL		
<i>EZH2</i>	Enhancer of zeste homologue 2 (methyltransferase of the PRC)	Aberrant suppression of tumor suppressor genes
<i>GNA13</i>	Gα13 protein	Modulator of migration and PI3K signaling
<i>PTEN</i>	Phosphatase and tensin homolog	(loss of function) Constitutive activation of PI3K signaling pathway
<i>TNFRSF14</i>	Tumor necrosis factor receptor superfamily, member 14,	(loss of function) Tumor-suppressor. It negatively regulates BCR signaling. Activated by BTLA
ABC-DLBCL		
<i>MYD88</i>	Myeloid differentiation primary response 88	Constitutive NF-κB activation through enhance of the TLR signaling
<i>CD79A & CD79B</i>	Components of the BCR	Constitutive activation of the BCR and consequent tumorigenic signaling, NF-κB activation
<i>CARD11</i>	Caspase recruitment domain-containing protein 11	Acts as a scaffold downstream of BCR and is a positive regulator of NF-κB activation
<i>TNFAIP3</i>	A20	(loss of function) NF-κB negative regulator
Shared across subtypes		
<i>MYC</i>	BHLH transcription factor	Transcription of multiple oncogenes
<i>BCL6</i>	Zinc finger transcription factor	Multiple functions (see text)
<i>BCL2</i>	Anti-apoptotic protein	Inhibition of apoptosis
<i>MEF2B</i>	Myocyte enhancer factor 2B	(loss of function) Negative regulator of BCL6
<i>CREBBP</i>	CREB-binding protein (histone acetyltransferase)	(loss of function) Negative regulator of BCL6
<i>EP300</i>	(chromatin modifier) E1A-binding protein p300	(loss of function) Negative regulator of BCL6
<i>FBXO11</i>	F-box only protein 11	(loss of function) Negative regulator of BCL6
<i>B2M</i>	β2 microglobulin	(loss of function) Immune escape from cytotoxic T-cells
<i>CD58</i>	CD recognized by NKs	Escape from natural killers due to loss of CD58 expression

Table 5.- Genetic alterations in DLBCL. Refer to text for more details. Abbreviations: PRC, polycomb repressive complex; BCR, B-cell receptor; BTLA, B- and T-lymphocyte attenuator; TLR, toll like receptor; BHLH, basic-helix-loop-helix.

1.4.4.2 DLBCL microenvironment

The sub-classification of DLBCL, NOS in the GCB and ABC pathogenically distinct subgroups narrows the variability of this entity and is expected to lead to higher therapeutic success, but fails to provide information on the particular role of the microenvironment in this disease. GEP studies have evidenced the role of the stromal microenvironment in environment-mediated resistance to chemotherapeutics and in the pathogenesis of DLBCL (Alizadeh et al., 2000; Lenz et al., 2008b; Monti et al., 2005; Rosenwald et al., 2002), and so has the CCC. In both CHOP and R-CHOP pre-treated biopsies of 233 and 181 patients respectively, Lenz *et al.* found two differentiated stromal signatures of genes expressed by the stromal cells that conferred prognostic factor. They showed that the "stromal signature 2" significantly correlated with blood-vessel density, a parameter associated with bad prognosis in DLBCL (Cardesa-Salzman et al., 2011; Lenz et al., 2008b). Not surprisingly, among the genes included in this signature are endothelial markers, key angiogenesis regulators, and the chemokine CXCL12 that is secreted by stromal cells that may promote angiogenesis.

It seems therefore clear that microenvironment biomarkers would be potential predictors of patients outcome and response to treatment. However, the determination of relevant biomarkers that could be easily studied in the context of a clinical laboratory remains a challenge (Coutinho et al., 2015).

1.4.5 Treatment

Treatment of DLBCL has undergone notable advances in the last 50 years. As a consequence, what was considered a fatal disease in many patients is now curable in a higher proportion.

The use polychemotherapy was established in the 70s, and a study in 1993 revealed that the chemotherapeutic regime CHOP (cyclophosphamide, doxorubicin, vincristine and prednisone) obtained similar complete remission results than other more complex and toxic regimens (Fisher et al., 1993). CHOP was therefore established as the standard treatment for DLBCL patients.

CHOP is a combination of chemotherapeutic agents with a complex mechanism of action composed of cyclophosphamide, doxorubicin, vincristine and prednisone. **Cyclophosphamide** acts when it is metabolized to phosphoramidate mustard. This alkylating agent, transfers an alkyl group to the guanine bases of the DNA which impedes replication (Colvin et al., 1976). **Doxorubicin** is from the family of anthracyclines and exerts an antitumor effect mainly by DNA intercalation and blockage of topoisomerase II which leads to inhibition of macromolecule biosynthesis and

replication. **Vincristine** binds to tubulin and prevents cell replication, and **prednisone** is a corticosteroid that reduces inflammation, suppresses immune response, and has the ability to decrease normal and malignant lymphoid tissue (Moreno et al., 2000).

Altogether, these agents inhibit tumor cell proliferation and induce cancer cell death with a 3-years complete response of approximately 50%.

1.4.5.1 Immunochemotherapy

CD20 is a transmembrane receptor, with no known ligand, expressed in normal and malignant B-cells. **Rituximab** is an anti-CD20 monoclonal (m) antibody. It is formed by human kappa and IgG1 constant regions and murine light and heavy chain variable regions making it a human/murine chimeric IgG1- κ mAb. It exerts its antitumor properties upon binding to the CD20 antigen by activation of the immune system through induction of complement dependent cytotoxicity (CDC), antibody dependent cell-mediated cytotoxicity (ADCC), and apoptosis (Salles et al., 2017). In 1997, Rituximab was approved for treatment of low-grade NHL (Maloney et al., 1997) and was soon applied for the treatment of DLBCL.

In 2002, the Groupe d'Etude des Lymphomes de l'Adulte (GELA) published the results of the first clinical trial (LNH98-5) comparing CHOP vs Rituximab + CHOP (R-CHOP) in DLBCL patients aged 60-80 years. The complete response was higher in those patients treated with R-CHOP (76% vs 63%) (Coiffier et al., 2002; Coiffier et al., 2010). The CALGB 9793/ECOG-SWOG 4494 clinical trial in 2006 further confirmed the benefit of R-CHOP over CHOP and that the maintenance with rituximab after R-CHOP infusion does not offer any therapeutic benefit (Habermann et al., 2006). With these studies, R-CHOP was established as the standard therapy for DLBCL patients over 60 years. Regarding young patients, a study by the Mab Thera International Trial (MINT), revealed a complete remission of 85% in the R-CHOP group compared to the 68% in the CHOP group in a cohort of young patients with good prognosis (Pfreundschuh et al., 2006); (Pfreundschuh et al., 2011). It was therefore concluded that the benefit of Rituximab is age independent and that treatment with immunochemotherapy significantly improved the outcome of DLBCL patients. Nevertheless a proportion of 1/3 of the patients still did not respond to treatment.

In an attempt to improve the results in these higher risk patients, the clinical trials UK NCRI and LNH-03-6B compared the general R-CHOP administration (every 21 days, R-CHOP21) with intense chemotherapy (every 14 days, R-CHOP14). The results showed that R-CHOP-14 was not superior to R-CHOP-21 administration and R-CHOP-21 remained the standard first-line treatment (Cunningham et al., 2013; Delarue et al., 2013). Another attempt, which only provided therapeutic benefit for patients with high

risk aalPI, was following R-CHOP with **autologous hematopoietic stem cell transplantation** (AHSCT) (Greb et al., 2008; Stiff et al., 2013). **Radiotherapy** seemed to show a significant better outcome in localized DLBCL in the pre-Rituximab era, nevertheless, the long term outcome was statistically similar in both groups (Miller et al., 1998). Whether radiotherapy is beneficial in combination with R-CHOP remains controversial (Grande, 2011; Miyazaki, 2016).

In summary, at the present time, the treatment algorithms for DLBCL are based on the state of the malignancy, differing between patients with local (Ann Arbor I and II) or with advanced disease (Ann Arbor III and IV). R-CHOP is the standard of care for all DLBCL patients. It may be combined with field radiation in patients with localized, low stage DLBCL or, followed by transplantation in patients with advanced disease (National Comprehensive Cancer Network, 2014)

Still, refractory patients, and those that relapse after treatment with Rituximab have a dismal outcome and new therapies need to be developed for these high risk patients.

1.4.5.2 Cell-of-origin based therapies

The current clinical approach does not take into account the distinct biology of the DLBCL molecular subtypes. Nevertheless, ABC and GCB are two defined entities (with ABC presenting a worse prognostic) and new therapeutic strategies are being designed to treat them differentially (Camicia et al., 2015; Campo et al., 2011; Grande, 2011; Miyazaki, 2016).

PROTEASOME INHIBITORS

ABC-DLBCL presents an elevated expression and activity of the NF- κ B pathway with a known role in inflammation and cancer (Lenz et al., 2008a). **Bortezomib** is a proteasome inhibitor with antitumor activity and is approved for treatment of haematological neoplasia like mantle cell lymphoma (MCL) (Moros et al., 2014a) and multiple myeloma (MM) (Bueno et al.). It prevents the degradation of the NF- κ B physiological inhibitor I κ B after its phosphorylation and, in a relapse/refractory cohort it improves response of ABC-DLBCL patients in combination with chemotherapy compared to GCB-DLBCL patients (complete remission: 42% vs 6%) (Dunleavy et al., 2009). In addition, with the introduction of bortezomib, Ruan *et al.* did not observe the classical survival differences between GCB and non-GCB following R-CHOP in subjects with untreated DLBCL (Ruan et al., 2010). In summary, bortezomib seems like a valid strategy for the treatment of ABC-DLBCL.

IMMUNOMODULATORY DRUGS

Lenalidomide is an immunomodulatory drug approved for treatment of MM, myelodysplastic syndrome (MS) and MCL. It is known to inhibit angiogenesis, tumor secreted cytokines and to induce apoptosis. Although its mechanism of action is not fully understood, it inhibits NF- κ B in vitro providing a rationale for ABC-DLBCL treatment. A retrospective clinical trial compared relapsed/refractory ABC vs GCB treated with lenalidomide as a single agent and obtained a significant complete remission of 29.4% vs 4.3% (Hernandez-Ilizaliturri et al., 2011). In addition, the worst prognosis of the ABC subtype observed with the current standard of care was unnoticed when R-CHOP was combined with lenalidomide (Nowakowski et al., 2016). These studies suggest that lenalidomide mitigates the negative prognosis of the ABC subtype.

BTK INHIBITORS

Somatic mutations affecting the ITAM signaling modules of CD79B and CD79A are found frequently in ABC-DLBCL and result in an over activation of the BCR signaling and a consequent NF- κ B activation (Davis et al., 2010). Inhibitors of signaling molecules downstream of the BCR have been suggested as potential drugs for ABC-DLBCL treatment. The Bruton's tyrosine kinase (BTK) inhibitor **ibrutinib** as a single agent has shown a response rate of 37% in ABC subjects compared to a 5% in GCB. Wild type CD79 ABC subjects in the study also benefited from the treatment indicating that future ibrutinib-based clinical trials should also enroll ABC-DLBCLs with CD79A or CD79B wild type tumors (Wilson et al., 2015). Encouraging clinical trial results are being published on ibrutinib in combination with R-CHOP in relapsed/refractory non-GCB DLBCL (Goy et al., 2016; Younes et al., 2014). Besides the above, several ongoing clinical trials with ibrutinib are currently registered and if treatment with ibrutinib is a safe and successful strategy for ABC-DLBCL will be confirmed in the near future.

EZH2 INHIBITORS

Twenty percent of GCB-DLBCL cases present gain of function point mutations in *EZH2* which confer a worst prognosis due to an over activation of the polycomb repressive complex that causes aberrant histone methylation. The EZH2 inhibitor EPZ-6438 is currently being evaluated in phase II clinical trials for the treatment of NHL (Brach et al., 2017; Garapaty-Rao et al., 2013; McCabe et al., 2012b; Qi et al., 2012; Van Aller et al., 2013).

1.4.5.3 Other novel therapies

Targeted therapies against COO independent clue molecules are also being currently developed and clinically and preclinically evaluated.

PI3K INHIBITORS

The PI3K pathway plays a major role in cell survival and proliferation. Although it is altered by through different mechanisms depending on the COO subtype, it is found to be overactivated in DLBCL. Targeting the PI3K pathway with the PI3K δ inhibitor **idelalisib** was successful in CLL and aggressive lymphomas (Brown et al., 2014; Kahl et al., 2014). However it has not been fully evaluated in DLBCL. A phase II clinical trial with the pan-PI3K inhibitor **copanlisib** in heavily pre-treated patients with relapsed or refractory, indolent or aggressive malignant lymphoma demonstrated promising efficacy. However, DLBCL was not included in the subtype specific posterior trials (Dreyling et al., 2017). The next generation PI3K δ inhibitor, **umbralisib** which overcomes the toxicity of idelalisib, has an overall response rate (ORR) of 100% in several aggressive and indolent NHLs. However it only showed an effectivity of 17% ORR in DLBCL although a promising 66% ORR was obtained in combination with the anti-CD20 ublituximab, and the chemotherapeutic agent bendamustine (Lunning et al., 2017). Even though the results of PI3K targeting in DLBCL are disappointing in the clinics, this axis seems like a promising target, and efforts are being made to overcome the toxicity of the first generation inhibitors, to understand the resistances of inhibition of this axis, and to optimize combinatory strategies (Lampson and Brown, 2017).

BCL2 INHIBITORS

The pro-apoptotic protein BCL2 is up regulated in both ABC and GCB subtypes, and its inhibition through the selective inhibitor **venetoclax** was FDA-approved as a monotherapy in a subgroup of CLL patients (Deeks, 2016). A phase I study with venetoclax has led to an underway phase II trial in DLBCL (NCT02987400).

BCL6 INHIBITORS

BCL6 is crucial for the formation of GCs upon infection and plays an important role in lymphomagenesis. DLBCL *in vitro* and *in vivo* models respond to treatment with peptidomimetics or small molecule BCL6 inhibitors (Cardenas et al., 2017).

CAR-T CELLS

Chimeric antigen receptor T-cells (CAR T-cells) are the culmination of immunotherapy. It is the first and only type of adoptive cell transfer (ACT) (infusion of cells to a patient) FDA-approved. In 2017 it was approved for treatment of children with ALL. In October 2018, the FDA approved the use of axicabtagene ciloleucel (axi-cel) (Yescarta) for patients with relapsed/refractory DLBCL, among other NHLs, after a clinical trial where approximately half of the patients presented a complete remission and nearly 30% of patients a partial response (Neelapu et al., 2017). The CAR T-cell

therapy consists of an autologous transplantation of genetically modified T-cells that express, in the case of axi-cel, a CD19-directed CAR to generate a B-cell specific cytotoxic immune response. The results of this therapy are being highly successful, but common and severe side effects is an issue that needs to be addressed and CAR T-cells therapy is still waiting for approval by the European Medicines Agency (EMA) (National Institute of Health, 2017a; National insitute of Health, 2017b).

This thesis focuses on CXCR4 and MYC targeting and therefore therapeutic inhibition strategies for these molecules are widely described below.

1.5 CXCR4

Chemokines are small signaling peptides secreted by cells involved in several cellular processes such as survival and chemotaxis. As mentioned earlier in this introduction (section 1.3.2) they play an important role in tumorigenesis as they are secreted by accompanying cells of the TME.

CXCR4 (formally known as fusin or CD184) is a membrane bound chemokine G-protein coupled receptor (GPCR). As a GPCR, it contains 7 α -helix transmembrane domains (TMD) interconnected by extra membrane loops (Figure 5A and B). It is expressed in several tissues particularly in B and T-lymphocytes. Its role as a co-receptor in CD4+ T-cell human immunodeficiency virus (HIV) infection owes its discovery in 1996 (Feng et al., 1996).

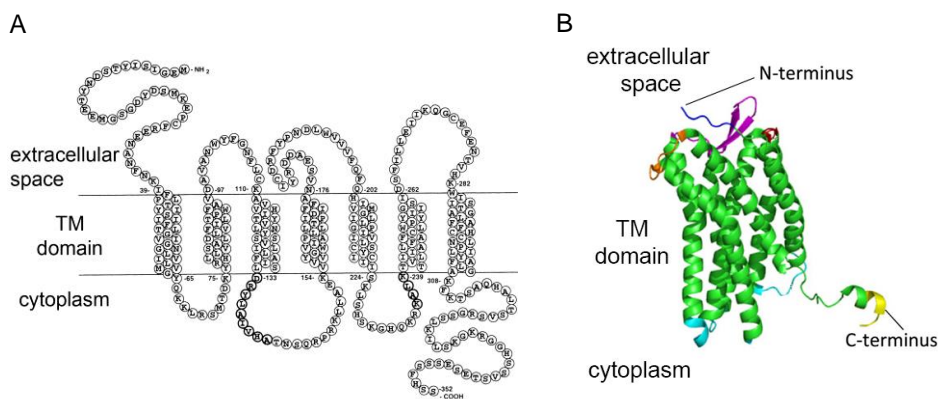


Figure 5.- CXCR4 structure. A) CXCR4 primary structure. Adapted from (Berson et al., 1996). B) CXCR4 tertiary structure. Adapted from (Pawig et al., 2015).

Chemokines are a family of **chemostatic** cytokines. These small secreted signaling peptides (8-12 KDa) function as chemoattractants and are involved in cell trafficking, survival, differentiation, and proliferation. They signal through GPCRs, have 4

conserved cysteines, and are classified in subfamilies according to the spacing of their first 2 N-terminal Cys. **CXCL12** (formally called stromal cell-derived factor (SDF-1 α)) is a homeostatic chemokine of the CXC subfamily that signals through CXCR4. It was first discovered as a stroma secreted pre-B-cell proliferation stimulating factor in the early 90s (Nagasawa et al., 1994; Tashiro et al., 1993), and in 1996 CXCL12 was described as a highly efficacious lymphocyte chemoattractant produced by bone marrow stromal cell lines (Bleul et al., 1996).

1.5.1 The CXCL12 - CXCR4 pathway

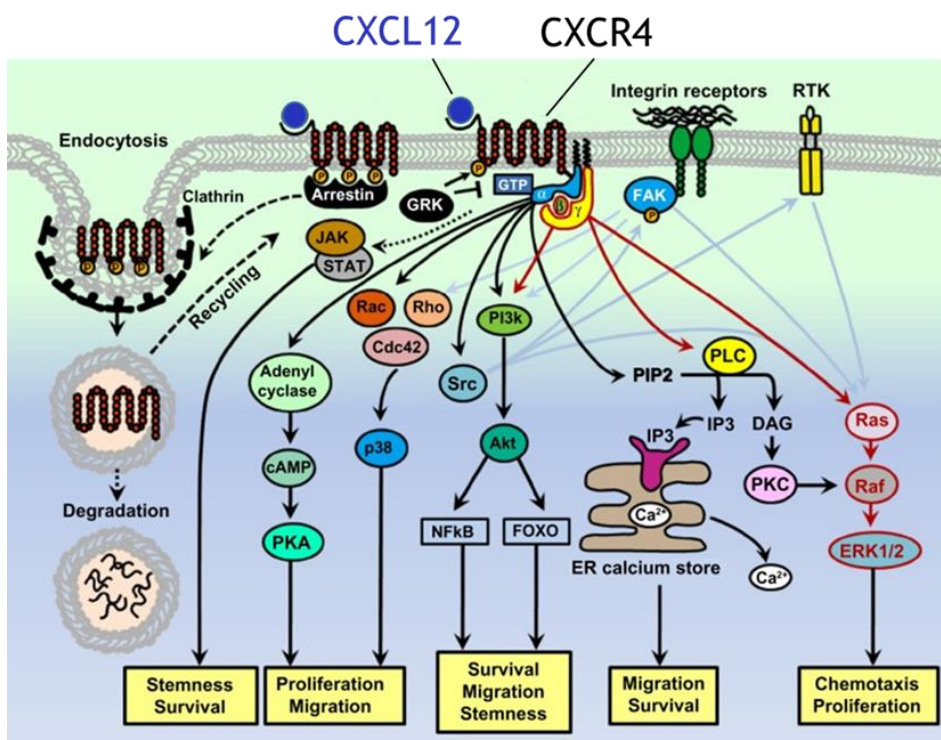


Figure 6.- CXCR4 signaling pathway. Abbreviations: ER, endoplasmic reticulum; GTP, Guanosine-5'-triphosphate; RTK, receptor tyrosine kinase; CXCL, chemokine (C-X-C motif) ligand; CXCR, C-X-C chemokine receptor; cAMP, cyclic adenosine monophosphate; PKA, protein kinase A; JAK, Janus kinase; STAT, signal transducer and activator of transcription; Cdc42, Cell division control protein 42 homolog; Rac, Ras-related C3 botulinum toxin substrate; Rho, Ras homolog gene family; GRK, G protein-coupled receptor kinase; FOXO, Forkhead box protein; NFκB, nuclear factor kappa-light-chain-enhancer of activated B cells; PIP2, phosphatidylinositol bisphosphate; FAK, focal adhesion kinase; PLC, phospholipase C; PKC, protein kinase C; Ras, Rat sarcoma protein family; ERK, extracellular-signal-regulated kinase. Adapted from (Cojoc et al., 2013).

Upon activation by its only ligand, CXCL12, the CXCR4 GPCR activates its heterotrimeric G-protein composed of the G α i, G β and G γ subunits that initiate different pathways culminating in chemotaxis, survival, and proliferation (Figure 6).

Activation of the MAPK pathway leads to **ERK1/2** phosphorylation at Thr202/Tyr204 and consequent triggering of cell chemotaxis and transcription of a number NF- κ B dependent genes involved in cell survival.

PI3K activation phosphorylates **AKT** (Ser473) and provides the cell with survival signals by inhibiting apoptosis through phosphorylation of proapoptotic BAD. AKT may also activate NF- κ B and consequent gene transcription. Moreover, PI3K may induce chemotaxis and angiogenesis through activation of FAK and so does the intracellular calcium mobilization induced by activation of PLC.

The MAPK, p38, which is also a downstream target of CXCR4, is known to be implicated in cell survival.

CXCR4 activates mTOR and consequent cell growth and proliferation. CXCR4 has also been reported to activate BTK phosphorylation evidencing a crosstalk between CXCR4 and the BCR.

Finally, β -arrestin is responsible for the antagonist induced internalization of CXCR4 by clathrin induced vesicles for a posterior lysosomal degradation of the receptor and signal finalization. CXCL12 may also bind to CXCR7 that is believed to sequester CXCL12 and attenuate CXCR4 activation (Busillo and Benovic, 2007; Marchese, 2014; Scala, 2015; Sun et al., 2010; Teicher and Fricker, 2010).

1.5.2 The role of CXCL12 - CXCR4 in healthy biological processes

After they discovered CXCL12 (Nagasawa et al., 1994), Nagasawa *et al.* reported that CXCL12 was essential for mice development and BM hematopoiesis as mice with CXCL12 disruption died before birth and presented reduced myeloid progenitors in the BM (Nagasawa et al., 1996). Later, other studies continued to evidence the role of the CXCL12-CXCR4 axis in heart, brain, and vascular development and lymphopoiesis (Tachibana et al., 1998; Zou et al., 1998), while hematopoietic stem cells (HSC) engraftment in the BM was found to be CXCR4-dependent (Peled et al., 1999).

In the present, the function of CXCR4-CXCL12 in normal B-cell development is well known. In adults, this axis is mainly specific to homing of HSCs to the bone marrow, lymphocyte homing, lymphoid hematopoiesis, leukocyte trafficking, survival and proliferation. CXCR4 expression is higher in GC B-cells compared to follicular B-cells and is more abundant in the centroblasts localized in the CXCL12 rich dark zone in comparison to light zone centrocytes. CXCR4 and CXCL12 differential expression is therefore responsible for positioning of B cells in the dark or light zone of the GC during antigen driven immune response (Allen et al., 2004; Bannard et al., 2013).

Apart from HSC, T-lymphocytes and B-lymphocytes, CXCR4 is also expressed in a variety of other cells including monocytes, macrophages, eosinophils, endothelial and epithelial cells, and tissue-committed stem-cells. These CXCR4 expressing cells migrate along CXCL12 gradients and home to CXCL12-expressing sites to execute their site-specific biological function. If damaged, brain, heart, kidney, bone, skin and BM upregulate CXCL12 to promote migration of CXCR4+ stem cell progenitors that participate in repair and regeneration of the injured tissues (Anders et al., 2014).

In summary, the CXCL12-CXCR4 axis plays a fundamental role in embryonic development, hematopoiesis, lymphoid trafficking and tissue repair by positioning and retaining specific CXCR4-expressing cells to the correct CXCL12-expressing site.

1.5.3 The role of CXCL12 - CXCR4 in cancer

As normal B-cells harbor a strong dependence on stroma-secreted cytokines for their development and throughout their whole life, it is not surprising that lymphoma cells exploit their microenvironment interaction properties for their own selective advantage. As a chemokine receptor, CXCR4 interacts with the chemokines secreted by the TME. In the last years, a large number of studies have evidenced the role of the TME, CXCL12, and CXCR4 in tumor progression and in DLBCL pathogenesis.

CXCR4 was first connected to cancer in 1999, in a study in CLL by Burger *et al.* where they demonstrated that CLL cells displayed CXCR4, and chemotaxis towards CXCL12-expressing BM stromal cells, that could be blocked by CXCR4 inhibition (Burger et al., 1999). Since then, CXCR4 has been shown to be expressed or overexpressed and linked to organ-specific metastasis in several cancers including breast, kidney, brain, prostate, ovarian, lung and melanomas (Zlotnik et al., 2011). CXCR4 overexpression may be induced by hypoxia, growth factors such as FGF, VEGF, EGF or NRF, and NF- κ B, YY1, or MYC (Hatano et al., 2013).

Metastasis is defined as the capacity of localized tumors to invade and spread to other parts of the body. To accomplish this, cancer cells need to acquire metastatic potential and have the ability to leave the primary tumor, extravasate to the blood or lymph torrent, and colonize and proliferate in a secondary site. The CXCR4-CXCL12 axis has been found to play a crucial role in this process. CXCL12 is highest expressed in brain, bone marrow, lungs and liver, common sites of metastasis and, in mouse models, abrogation of this axis reduces metastasis. In addition, high expression levels of CXCR4 have been linked to increased metastatic activity (Moreno et al., 2015).

As schematized in [figure 7](#), CXCL12 retains tumor cells in their tumor site and, together with other cytokines secreted by cells of the TME, it provides the tumor with

pro-survival signals. CXCL12 attracts metastatic CXCR4-expressing neoplastic cells and retains them in favorable niches for tumor growth and survival, such as the BM, which protect tumor cells from chemotherapy through CAM-DR (Burger and Kipps, 2006). These niches are therefore a reservoir for minimal residual disease (MRD) and play an important role in relapses. If local levels of CXCL12 become low, CXCR4 expressing tumor cells may follow a CXCL12 cue and migrate, along a positive concentration gradient, towards sites of metastasis with high CXCL12 expression. Once they reach the secondary site, again, the chemokine ligand retains the tumor cells and encourages survival and growth (Balkwill, 2004). In addition, CXCR4-expressing endothelial progenitors are also recruited to the tumor and angiogenesis takes place (Figure 7).

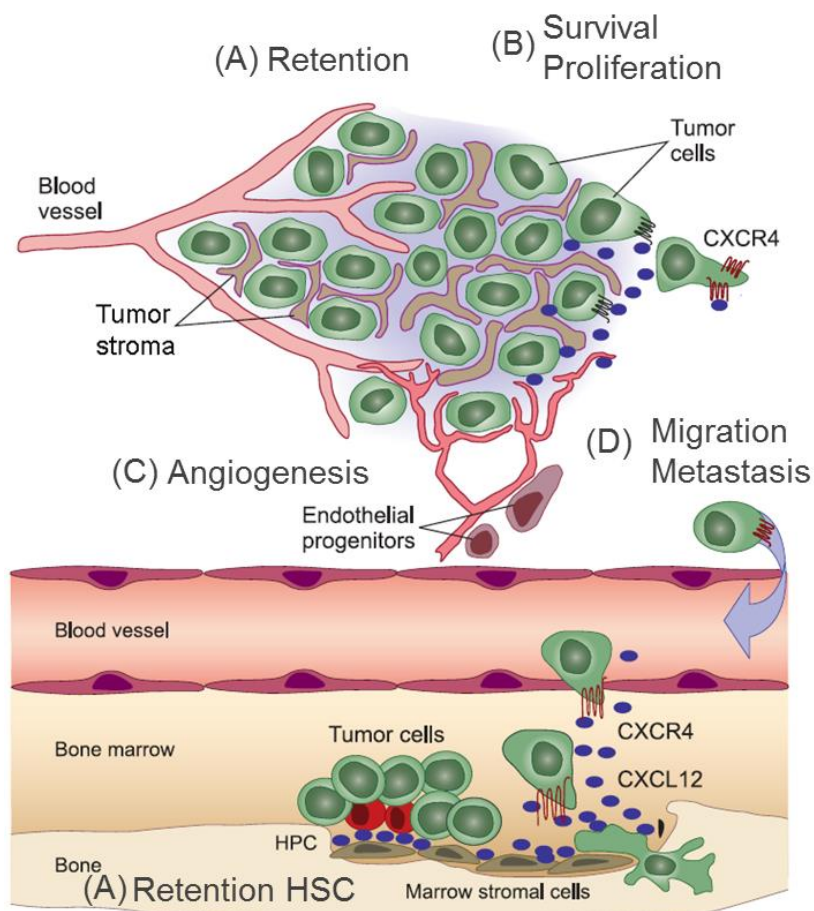


Figure 7.- Role of the CXCL12 - CXCR4 axis in cancer. Bone marrow (BM) stromal cells secrete CXCL12 and retain CXCR4 HSC cells in the BM. In the same way, tumor stromal cells also secrete CXCL12 and retain CXCR4 expressing tumor cells (A). Activation of the receptor induces survival and proliferation of the malignant cells (B). High levels of CXCL12 in the tumor also recruit endothelial progenitors and favor angiogenesis (C). If for some reason, CXCL12 at the tumor site becomes low, tumor cells will migrate towards a secondary site with higher levels of the chemokine (D). Abbreviations: HSC and HPC, hematopoietic stem cells. Adapted from (Burger and Kipps, 2006).

1.5.4 The role of CXCL12 - CXCR4 in DLBCL

High CXCR4 levels have been recently identified as an adverse prognostic factor in DLBCL. Moreno *et al.* correlated CXCR4 expression of DLBCL cell lines with increased migration capacity *in vitro* and tumor dissemination *in vivo*. They also described CXCR4 as an independent predictor of worst prognosis in DLBCL patients (Moreno et al., 2015). In addition, a study by Chen *et al.* also correlated CXCR4 expression with worst prognosis in *de novo* DLBCL patients treated with R-CHOP. They found that CXCR4 expression was associated with MYC overexpression in DLBCL, while GEP pointed out an immunosuppressive, proliferative and anti-apoptotic CXCR4 signature both in GCB and ABC subtypes (Chen et al., 2015). Accordingly, in a recent publication by Xu *et al.*, in DLBCL, CXCR4 was also significantly linked to worst prognosis and to the expression of mTOR, an essential regulator of cell growth, proliferation, survival, and motility (Xu et al., 2017).

Additionally, the CXCR4 ligand, CXCL12, is among the genes included in the proangiogenic “stromal 2 signature” which is associated with an unfavorable outcome in DLBCL (Lenz et al., 2008b). Accordingly previous work in the lab had shown that CXCL12 protein levels in tumor biopsies correlated with BM involvement and with highly vascularized tumors (factors associated to worst prognosis) (Recasens-Zorzo et al., 2017).

The above studies have uncovered the CXCR4-CXCL12 axis as a new prognostic marker in cancer and DLBCL. They have also evidenced the role of this axis in drug resistance.

1.5.5 CXCR4 inhibition

CXCR4 plays a role in tumor progression, metastasis and drug resistance and thus represents a potential pharmacological anti-cancer target. Various ongoing clinical trials and preclinical studies are evaluating the benefit of targeting the CXCL12-CXCR4 axis (see section 1.5.6).

Four main putative **mechanisms of action** are to be considered prior the evaluation of new anti-CXCR4 approaches:

- I. The CXCR4 signaling pathway leads to survival and proliferation. Therefore, CXCR4 inhibition should stop cell proliferation and induce apoptosis in the targeted CXCR4 expressing tumor cells.

- II. CXCL12, the CXCR4 ligand, is a major inducer of cell chemotaxis and this axis is known to play a crucial role in tumor metastasis. Therefore treatment with CXCR4 inhibitors should influence the high capacity of CXCR4 to mobilize cells. In this regard, inhibition of CXCR4 should reduce engraftment of tumor cells to CXCL12-expressing sites and inhibit metastasis.
- III. The CXCL12-CXCR4 axis also plays an important role in homing of CXCR4 expressing cells, retention and CAM-DR. Disruption of the interaction between CXCL12-secreting stromal cells and CXCR4-expressing tumor cells may lead to the mobilization of these malignant cells that are trapped in a protected niche inaccessible to chemotherapy into the blood flow, and to a consequent sensitization to treatment.
- IV. CXCL12 attracts CXCR4-expressing endothelial cells. As a consequence the CXCL12-CXCR4 axis induces angiogenesis. CXCR4 inhibition may therefore induce blockade of blood flow to the tumor.

The therapeutic benefits of targeting this axis as well as its biological relevance in DLBCL, and what effect would CXCR4 inhibition exert in this pathology have just started to be investigated and remain largely unexplored. Moreno *et al.* first reported in 2015 that CXCR4 inhibition reduced CXCL12-induced migration of DLBCL cell lines *in vitro*, and dissemination in a xenograft mouse model of DLBCL (Moreno *et al.*, 2015). Another study has shown that CXCR4 inhibition enhances the growth-inhibitory and apoptotic effect of Rituximab in two DLBCL cell lines *in vitro* (Reinholdt *et al.*, 2016). Finally, CXCR4 inhibition in combination with the mTOR inhibitor everolimus had a synergistic effect in inhibiting proliferation of DLBCL cell lines (Xu *et al.*, 2017).

1.5.6 CXCR4 inhibitors in the clinic or in development

Except for the study by Xu *et al.*, which uses the CXCR4 inhibitor WZ811, the previous studies of CXCR4 inhibition in DLBCL, use the first in class CXCR4 inhibitor AMD3100 (Figure 8). Due to the patent role of CXCR4 in cancer and other pathologies, and the pharmacological limitations of AMD3100, several new CXCR4 inhibitors are

being synthesized and tested. In this section, AMD3100, the standard CXCR4 inhibitor, as well as IQS-01.01, the CXCR4 inhibitor studied in this thesis, are described in detail. Additionally, the CXCR4 inhibitors that are currently in clinical trials are also outlined.

1.5.6.1 AMD3100

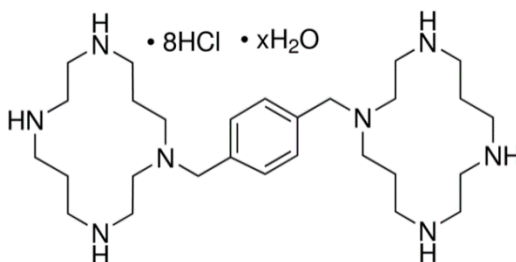


Figure 8.- Molecular structure of AMD3100. Presented as a chlorohydrate salt, AMD3100 is composed of two cyclam rings attached by an aromatic bridge.

AMD3100 (Plerixafor, Mozobil) is the only CXCR4 inhibitor approved by the FDA and the EMA for clinical use. Synthesized by Johnson Matthey (AnorMED) in collaboration with the Rega Institute of Leuven, Belgium, it is characterized as a bicyclam with the bicyclam rings bound by an aromatic bridge and presented as a chloride salt (Figure 8). It was developed as an anti-HIV drug in 1994 and in 1997 bicyclams were demonstrated to target only CD4+ T-cell tropic X4 HIV strains which use CXCR4 as a co-receptor for infection (De Clercq, 2009). After proofing that AMD3100 was a highly specific CXCR4 inhibitor with no cross-reactivity with other chemokine receptors, a phase I clinical trial in healthy volunteers, prior anti-HIV activity evaluation, exhibited an increase in leukocyte blood count as an unexpected side effect (Hendrix et al., 2000). Further studies demonstrated that the mobilized cells were predominantly HSC (Liles et al., 2003). These findings lead to the investigation of AMD3100 as an HSC mobilizing agent for HSC collection and transplantation. In 2005 it was concluded that addition of AMD3100 to healthy volunteers treated with granulocyte-colony stimulating factor (G-CSF), the HSC mobilizing therapy used at that time, had a synergistic effect (Liles et al., 2005). Further studies showed that AMD3100 in combination with G-CSF mobilized HSC in patients affected by NHL and MM.

In 2008, AMD3100 was authorized in the USA by the FDA (De Clercq, 2009) and approved one year later by the European Medicines Agency (EMA) (European Medicines Agency). AMD3100 is authorized to treat the condition of myelosuppression caused by chemotherapy treatment of malignant disorders, which requires an AHST. It is indicated in combination with granulocyte colony stimulating factor (G-CSF) to

enhance mobilization of hematopoietic stem cells to the peripheral blood for collection and subsequent AHST in patients with lymphoma and MM whose cells mobilize poorly.

Around 30 clinical trials with Plerixafor are documented by the U. S. National Library of Medicine (National Institute of Health b). Most of the trials aim at evaluating and improving AMD3100 HSC mobilization capacity in leukemia and lymphoma such as acute myeloid leukemia (AML), MM, and NHL for AHST. Additionally, the following clinical trials are based in the hypothesis that CXCR4 inhibition by AMD3100 might be an anticancer pharmacological strategy (Table 6):

Combined with chemotherapy and radiation therapy, AMD3100 is being evaluated in glioma patients in a Phase I/II study (NCT01977677).

Clinical trials in adult patients with relapsed AML have demonstrated promising results when combining AMD3100 with cytotoxic chemotherapy. A Phase I study is testing the safety of AMD3100 together with chemotherapy in pediatric patients with relapsed or refractory acute lymphoblastic leukemia (ALL), AML and myelodysplastic syndromes (MDS) with the purpose of mobilizing leukemia cells from their protective stromal environment and chemosensitizing them (NCT01319864).

Another phase I study in elderly AML patients is also assessing if AMD3100 will improve treatment outcomes via mobilization of leukemia stem cells in combination with chemotherapy (NCT01352650).

The NCT01236144 trial also aims at establishing the feasibility of combining AMD3100 with chemotherapy in older patients with AML and high risk MDS.

A phase I study in patients with advanced pancreatic, high grade serous ovarian and colorectal adenocarcinomas is recruiting to assess the impact of treatment with AMD3100 on the TME modulation (NCT02179970).

Malignancy	Combined with	Phase	Reference
Glioma	Chemotherapy, radiation	Phase I/II	NCT01977677
Pediatric relapsed or refractory ALL, AML and MDS	Chemotherapy	Phase I	NCT01319864
Elderly AML	Chemotherapy	Phase I	NCT01352650
Elderly AML and high risk MDS	Chemotherapy	Phase I/II	NCT01236144
Advanced pancreatic, high grade serous ovarian, and colorectal adenocarcinomas	-	Phase I	NCT02179970

Table 6.- Ongoing clinical trials with AMD3100 as an antitumor drug. Abbreviations: ALL, acute lymphoblastic leukemia; AML, acute myeloid leukemia; MDS, myelodysplastic syndromes.

In summary, the antitumor effect of CXCR4 inhibition by means of AMD3100 has, and is being investigated in the clinics in glioma, AML, MM, MDS, and ovarian, colorectal, and pancreatic cancer. There are currently no ongoing trials in other malignancies such as DLBCL (European Medicines Agency; National Institute of Health b).

LIMITATIONS OF AMD3100

Anti-HIV studies were precluded because, in clinical trials, treatment with AMD3100 had poor anti-HIV efficacy and resulted in serious side effects. In fact, in a phase I/II clinical trial in HIV, out of 40 enrolled patients, 8 subjects discontinued drug study due to serious adverse events or adverse events including cardiac toxicity such as ventricular ectopy and bigeminy, thrombocytopenia and paresthesias. Other adverse events such as gastrointestinal disorders, abdominal pain, hypertension and tachycardia were frequent (Hendrix et al., 2004). This dose escalation study administered AMD3100 as a 10 day continuous effusion at doses ranging from 2.5µg/kg/h to 160µg/kg/h.

The authorized route of administration for AMD3100 is subcutaneous injection and it should be administered 6 to 11 hours prior to initiation of each apheresis following 4 day pre-treatment with G-CSF. AMD3100, has been commonly used for 2 to 4 consecutive days as a single dose in clinical trials. It may be used for up to seven consecutive days being suitable for the short-term setting regimens required for AHSCT. In this treatment context, the most common side effects (which may affect more than 1 patient in 10) are diarrhea, nausea and reactions at the site of injection (European Medicines Agency, 2017).

To enable a continuous CXCR4 inhibition needed to obtain an antitumor effect, an orally available, more stable, and adequate for long-term administration inhibitor would be required.

1.5.6.2 Other CXCR4 inhibitors in clinical trials

CXCR4 inhibitors with better pharmacological properties than AMD3100 for use in the treatment of different tumors are being explored in several clinical trials (Table 7).

BL-8040/BKT-140 is an orally available peptidic CXCR4 inhibitor developed by Biokine and licensed to BioLineLX. It is currently in phase II clinical trials for anticancer treatment of ALL or lymphoblastic lymphoma (LL), unresectable or metastatic gastric cancer, AML, pancreatic cancer, and mobilization for AHSCT. And in phase I in metastatic non-small cell lung cancer (NSCLC).

PF-06747143 is a CXCR4 antagonist IgG1 antibody developed by Pfizer for the treatment of hematological malignancies. Promising results have been obtained in preclinical studies (Liu et al., 2017) and its safety is currently being evaluated in a phase I clinical study administered intravenously (NCT02954653).

Ulocuplumab (BMS-936564) (MDX-1338) is a Bristol-Myers Squibb fully human IgG4 anti-CXCR4 with antitumor properties *in vitro* and *in vivo* in preclinical models of haematological malignancies (Kuhne et al., 2011). Administered intravenously, its safety is being tested in phase Ib clinical trials in MM, AML, CLL and FL (Amaya-Chanaga et al., 2013).

Originated and developed by Proximagen (Upsher-Smith Laboratories), **USL311** is an orally available small molecule that is under a phase I/II clinical trial for advanced solid tumors and glioblastoma (NCT02765165).

LY2510924 is a small peptide developed by Lilly that is subcutaneously administered in phase I studies for advanced refractory solid tumors (NCT02737072, NCT01391130, NCT01439568).

Drug	Type	Administration route	Company
BL-8040/ BKT-140	Peptidic	Oral	BioLineLX
PF-06747143	IgG1 Antibody	Intravenous	Pfizer
Ulocuplumab (BMS-936564) (MDX-1338)	IgG4 Antibody	Intravenous	Bristol-Myers Squibb
USL311	Small molecule	Oral	Proximagen (Upsher-Smith Laboratories)
LY2510924	Small peptide	Subcutaneous	Lilly

Table 7.- CXCR4 inhibitors in clinical trials other than AMD3100.

1.5.6.3 IQS-01.01

With the aim to find a CXCR4 inhibitor with improved pharmacological properties, in this thesis we have analyzed the preclinical activity of the new CXCR4 inhibitor **IQS-01.01**. Like the reference CXCR4 inhibitor AMD3100, IQS-01.01 is a symmetric molecule with a central p-phenylene group. Nitrogen atoms on each site are intercalated in carbon chains (Figure 8 and 9).

It was designed by the Molecular Engineering Group (GEM) at Institut Químic de Sarrià (IQS) School of Engineering as an **anti-HIV drug**. IQS-01.01 (referred as **1** {8,8} in the original study) was the best lead candidate of a library of 53 compounds designed to improve AMD3100. Structurally, it preserves the main features of AMD3100; symmetry, a central p-phenylene group, and nitrogen atoms on each site at a similar

distance than those of the cyclam in AMD3100. By computational calculations, it has been determined that at physiological pH, these nitrogens become positive and interact electrostatically with the lateral chains of acidic amino acids of CXCR4. A methyl group is attached to the chiral carbon of each of the two piperidine rings on each site of the molecule. The spatial orientation of these methyl groups is responsible for the different stereoisomers (RR, SS, and RS) (Pettersson et al., 2008) (Figure 9).

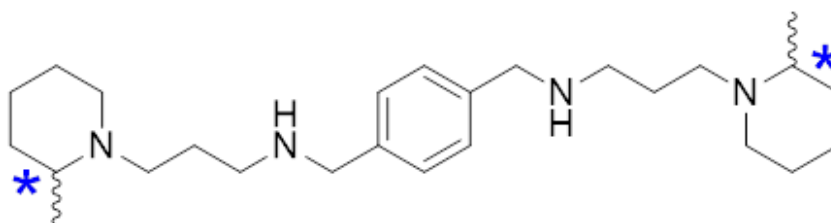


Figure 9.- Molecular structure of IQS-01.01. Skeletal structure of IQS-01.01. *chiral carbons.

As AMD3100, IQS-01.01 was originally designed as an anti-HIV drug. CXCR4 residues that are crucial for HIV binding and consequent cell infection have been determined by site-directed mutagenesis (SDM) (Brelot et al., 2000). *In silico* docking studies predicted IQS-01.01 to bind to this CXCR4 SDM-defined binding pocket through electrostatic interactions between the positively charged nitrogen atoms of the drug and the negatively charged lateral chains of Asp262 and Glu288. *In vitro* experiments showed that, among the 53 tested compounds, IQS-01.01 presented the higher antiviral activity with an EC₅₀ of 0.008 µg/ml that was comparable to the EC₅₀ of 0.001 µg/ml of AMD3100, without cytotoxicity at the tested concentrations. Additionally, time-of-drug addition experiments revealed that IQS-01.01 presented a similar time and site of interaction than AMD3100. Finally, an occupancy assay demonstrated that IQS-01.01 efficiently prevented the binding of an anti-CXCR4 antibody, but failed to block the binding of anti-CD4, CCR5, or CD45 antibodies, pointing out the specificity of the compound toward CXCR4, but not other lymphoid receptors (Pettersson et al., 2008).

As a new CXCR4 inhibitor with comparable activity to the reference compound AMD3100, IQS-01.01's **antitumor activity** has been investigated in a preclinical model of glioma. The tetrachlorohydrate of **1** {8,8} (referred as compound **11** in their study) and its 3 stereoisomers (SS, RR and RS) were evaluated and compared using AMD3100 as a reference. With the lowest K_b, the stereoisomer IQS-01.01RS was the compound with the highest CXCR4 binding activity. IQS-01.01RS could also inhibit AKT phosphorylation in patient-derived neutrospheres suggesting that it is a more potent CXCR4 inhibitor than AMD3100 and the other stereoisomers. Although none of the compounds had a major effect on cell proliferation or viability, the four CXCR4 inhibitors decreased the

amount of glioma initiating cells of the neurospheres. This translated into a decrease in tumor number and mass in an orthotropic human glioma mouse model generated from IQS-01.01 or AMD3100 pre-treated glioma cells (Ros-Blanco et al., 2012).

According to the published results detailed above, IQS-01.01 seems like a promising lead CXCR4 inhibitor and therefore, further testing should be carried out in other to understand and improve its limitations and potentiate its strengths. This thesis aims at the evaluation of the anti-tumor activity of this new CXCR4 inhibitor in preclinical models of DLBCL.

1.6 MYC

1.6.1 The role of MYC in healthy biological processes

Located in chromosome 8q24, *MYC* was first described in 1978 as an homolog of the avian retroviral oncogene *v-myc* (Hayward et al., 1981; Sheiness et al., 1978). It is an essential transcription factor (TF), member of the basic-helix-loop-helix-leucine zipper (bHLH-LZ) family, that by recruiting histone-modifying and chromatin-remodeling enzymes, regulates genes related to basic cellular processes such as cell growth and proliferation, metabolism, and apoptosis. MYC requires the dimerization with its partner MAX (another bHLH-LZ TF) to bind to DNA enhancer box sequences (E-boxes) (Figure 10). In healthy adults, MYC expression is generally low and restricted to cells with proliferative and regenerative potential. B-cells are rapid proliferating cells that rely on MYC for their normal development and maturation (Adhikary and Eilers, 2005; Karube and Campo, 2015; Kress et al., 2015).

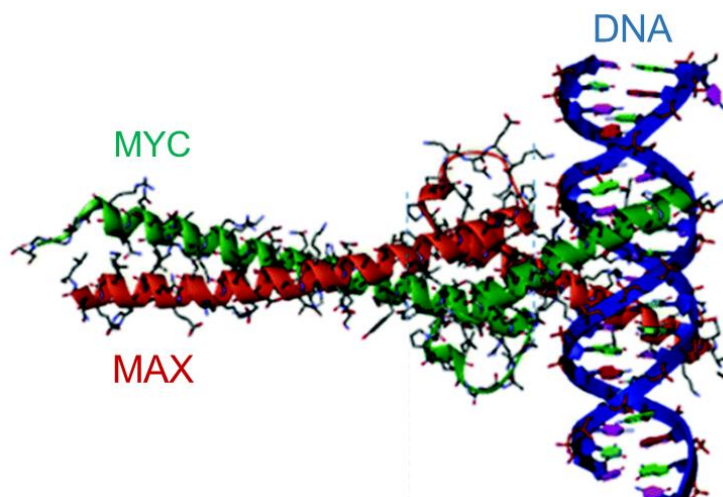


Figure 10.- MYC-MAX heterodimer and DNA binding. Adapted from (García et al., 2017).

1.6.2 The role of MYC in cancer and DLBCL

The normal function of MYC in cell growth and proliferation makes MYC a potent proto-oncogene implicated in the generation of several different tumors.

The discovery of the translocation of MYC into the Ig heavy chain locus in Burkitt lymphoma (BL) was the first evidence of the involvement of MYC in human neoplasia (Dalla-Favera et al., 1982). Considering the power of MYC as an oncogene and the important role it plays in B-cell development, the relevance of MYC in lymphomas is not surprising

Between 30 and 50% of DLBCLs aberrantly overexpress MYC and around 20% present MYC chromosomal translocations. The presence of MYC rearrangements is an independent predictor of poor outcome in DLBCL patients treated with standard therapy. MYC overexpression is associated with shorter survival in DLBCL patients while Valera *et al.* have correlated high MYC protein levels with poorer overall survival (Karube and Campo, 2015; Valera et al., 2013).

1.6.3 MYC inhibition

MYC had been historically considered an undruggable oncogene mainly due to its nuclear localization, lack of a defined ligand binding site, and physiological function essential to the maintenance of normal tissues. At the present, several direct and indirect MYC inhibitory strategies are being evaluated (Whitfield et al., 2017).

An exciting first approach in the 90s was the use of antisense oligonucleotides that interacted with MYC mRNA to impair the expression of the gene, a strategy that in spite of improving overall survival in a neointimal hyperplasia phase I/II study in 2007, hasn't been further developed (Kipshidze et al., 2007). Small molecules to inhibit the MYC-MAX dimerization have also been investigated and shown to be effective *in vitro*, however no specific druggable domain is involved in this interaction, and poor bioavailability and lack of selectivity characterize this strategy (Whitfield et al., 2017). Omomyc is a miniprotein that acts as a dominant negative of MYC. It displaces MYC by binding to MAX and generates DNA-bound inactive dimers. Based on promising preclinical results, the Vall d'Hebron Instituto de Oncología (VHIO) spinoff Peptomyc S.L. is planning the initiation of clinical trials (Annibali et al., 2014; Soucek et al., 2008; Soucek et al., 2013).

1.6.3.1 BET inhibitors

BRD4 is a member of the subfamily bromodomain and extra-terminal (BET) which belongs to the bromodomain (BD) family. The BD family is constituted by a group

of proteins that contain BDs. BDs recognize acetylated lysines (Ac-Lys) in the N-terminal (Nt) histone tails and attach to them through easily druggable, specific, hydrophobic binding pockets (Filippakopoulos et al., 2012). The BET subfamily is characterized by containing 2 BDs plus an extra-terminal (ET) domain responsible of protein-protein interactions. This ET domain confers BET proteins the capacity to act as scaffolds for transcription factors (TF) and form active transcription complexes. BRD4 was identified as a component of a recurrent t(15;19) chromosomal translocation in the aggressive NUT midline carcinoma (NMC) (French et al., 2008). As a BET family member, BRD4 is a global regulator of gene transcription that selectively recognizes and binds to Ac-Lys residues in histones to activate transcription and mitosis. It preferentially localizes in super-enhancers associated with key transcription factors implicated in lymphomagenesis such as MYC that are, therefore, specifically sensitive to BRD4 inhibition. This explains the selective anti-tumor effect of BRD4 inhibitors (Whitfield et al., 2017) (Figure 11).

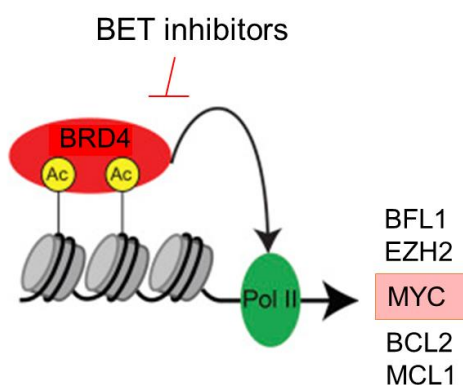


Figure 11.- BET inhibition. Schematic representation of the mechanism of action of BET inhibitors. Histones represented in gray and DNA string in black. Abbreviations: Ac, acetyl group; Pol II, polymerase II. Adapted from (Zhu et al., 2016).

The development of the first BRD4 inhibitor **JQ1** in 2010 by Filippakopoulos *et al.* was a promising indirect strategy to target MYC. They showed that JQ1 displaced BRD4 from nuclear chromatin in cells and that it was antitumoral in NMC mice xenografts (Filippakopoulos et al., 2010). This highly potent, selective and cell permeable inhibitor of BRD4 also showed preclinical antitumor activity in several tumor types including MM, ALL, AML and DH lymphoma among others (Filippakopoulos and Knapp, 2014; Whitfield et al., 2017). Several other BRD4 inhibitors have been synthesized with the aim to improve JQ1 pharmacological properties and further studies have validated BET-bromodomain targeting as a promising therapeutic strategy in different subtypes of aggressive B-cell lymphoma, including DLBCL (Boi et al., 2015; Esteve-Arenys et al., 2018). **GSK525762 (I-BET762)** is in a phase I/II study in subjects with

relapsed, refractory hematologic malignancies (Borthakur et al., 2016) and is also being evaluated in solid tumors. **BI-894999** is under a clinical trial for solid malignancies and DLBCL (NCT02516553). A phase I/II trial in DLBCL and other haematological malignancies using the BET-inhibitor **OTX015 (MK-8628)** is being executed (NCT01713582). **FT-1101**, **GS-5829** and **INCB054329** are also under evaluation in clinical trials of hematologic malignancies (NCT02543879, NCT02392611 and NCT02431260).

Promising results are arising from this trials, however, resistances due to rebound increase in protein levels of BRD4 target genes or other mechanisms have been reported (Kumar et al., 2015) and besides, an atypical kinase activity has been associated to BRD4 (Devaiah et al., 2012). To address this, combination of BET-bromodomain inhibitors with classic kinase inhibitors screened by their ability to bind to the Ac-Lys binding pockets is being evaluated and so is a new generation of dual-activity BET-kinase inhibitors (Ember et al., 2014). Moreover, proteolysis targeting chimeras (PROTACs) of BET-inhibitors with a linked E3 ligase have appeared with the aim of simultaneously targeting BET-BD and degrading them showing promising activity (Saenz et al., 2017).

CPI203

CPI203 is a BRD4 inhibitor developed by Constellation Pharmaceuticals (Figure 12) with improved bioavailability in mice compared to JQ1 that has proved antitumor activity through MYC down regulation in neuroendocrine tumors, MCL and MM (Díaz et al., 2017; Moros et al., 2014b; Siegel et al., 2015; Wong et al., 2014). CPI0610 is a CPI 203 analogue that is currently in three separate phase I clinical studies in progressive lymphoma, MM and AML (NCT01949883, NCT02157636 and NCT02158858).

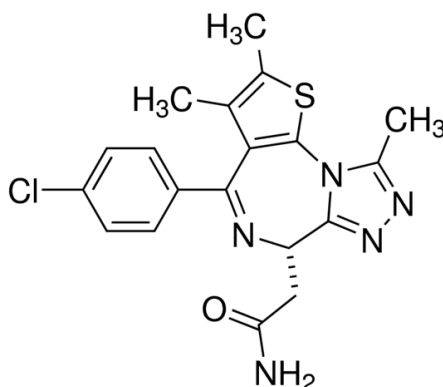


Figure 12.- Molecular structure of the BRD4 inhibitor CPI203.

It is worth pointing out that BET inhibition downregulates other tumor related genes apart from *MYC*. Nevertheless, in this work, we focused on the capacity of CPI203 to inhibit *MYC*.

1.7 CXCR4 and MYC

Association between CXCR4 and *MYC* has been observed in DLBCL. Chen *et al.* reported that CXCR4 positive patients presented a higher *MYC* expression compared to CXCR4 negative patients regardless the ABC/GCB subtype (Chen *et al.*, 2015).

1.7.1 MYC stability

MYC protein is highly unstable with a half-life of between 20 and 30 minutes (Gregory and Hann, 2000). This rapid turnover is caused by regulation of *MYC* mRNA stability (Dani *et al.*, 1984; Herrick and Ross, 1994), translational and posttranslational modifications (Kress *et al.*, 2015).

MYC proteolysis is mediated by the ubiquitin-proteasome pathway (Gregory and Hann, 2000) and its poly-ubiquitination is regulated by two evolutionally conserved phosphorylation sites, Ser62 and Thr58. When Ser62 is phosphorylated by phospho (p) ERK1/2, *MYC* is stabilized. P-Ser62 may then be recognized by glycogen synthase kinase 3 β (GSK-3 β) which phosphorylates *MYC* at Thr58. Only when Thr58 is phosphorylated, the phosphatase PP2A is able to remove the phosphate from Ser62 and the E3 ubiquitin ligase may bind to *MYC* p-Thr58 and proceed to its N-terminal ubiquitination. Ubiquitinated *MYC* undergoes proteolysis through proteasomal degradation (Hann, 2006; Jóźwiak *et al.*, 2014; Sears *et al.*, 2000). P-AKT, may also induce *MYC* protein stability because it has the ability to phosphorylate GSK-3 β at Ser9 and inhibit its activity (Vervoorts *et al.*, 2006) (Figure 13). As a GPCR, activation of CXCR4 leads to the activation of ERK1/2 and the PI3K/AKT pathway (Figure 6) which may stabilize *MYC*.

Deregulation of any of the components of these regulatory pathways may lead to the aberrant overexpression of the *MYC* oncogene and add up to the tumor effects of any possible genetic aberration. In fact, stabilization of *MYC* through ERK or AKT has been related to resistance to chemotherapy and aggressiveness in melanoma (Tsai *et al.*, 2012) and prostate cancer (Hatano *et al.*, 2013).

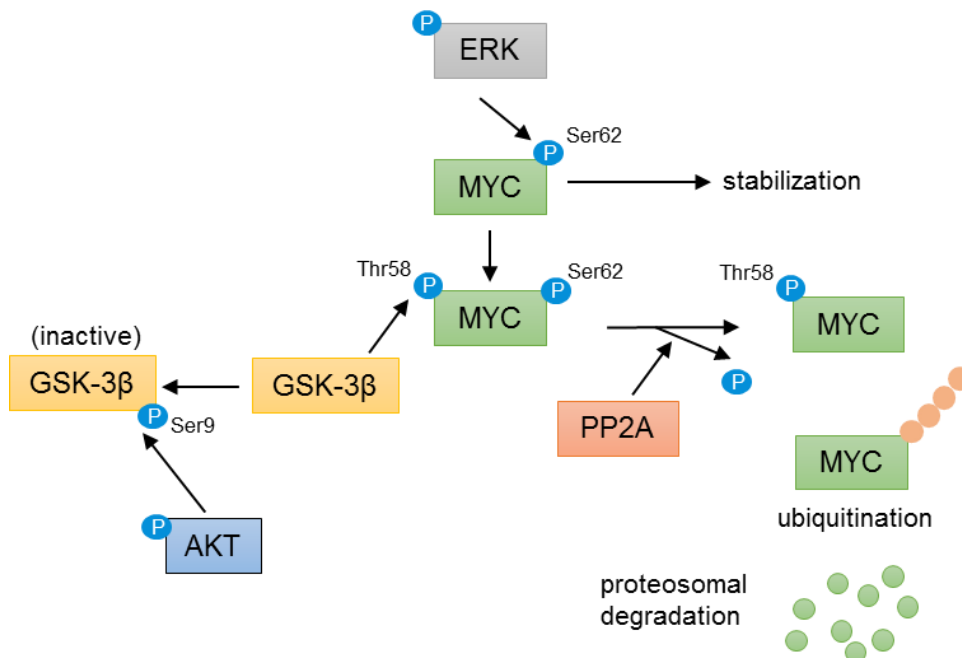


Figure 13.- Regulation of MYC protein stability. Adapted from (Jóźwiak et al., 2014). Abbreviations: PP2A, phosphatase 2A.

1.7.2 The CXCR4 - ERK1/2 - MYC signaling loop

As ERK1/2 and AKT are downstream targets of CXCR4, activation of the receptor should lead to the stabilization of MYC. In this sense, Moriuchi *et al.* reported that not only MYC is regulated by CXCR4, but that CXCR4 is among the MYC target genes. In a study published in 1999, they showed that MYC enhanced the promoter activity of CXCR4. They identified an E-box in the promoter of CXCR4 (at -260 relative to CXCR4 transcription start site) and confirmed that, as a bHLH-LZ transcription factor, MYC was able to bind to this E-box. They further showed that PBMCs transfected with MYC, up-regulated the expression of CXCR4 promoter-luciferase reporter constructs. In addition, they showed that when the E-box was mutated, CXCR4 promoter activity ceased to be upregulated (Moriuchi et al., 1999).

Hatano *et al.* have also investigated the link between CXCR4 and MYC in prostate cancer (Hatano et al., 2013). In their attempt to understand the mechanism of resistance to chemotherapy, they found constitutive activation of CXCR4, ERK1/2, and MYC signaling in tissue samples from therapy-resistant patients. After confirming that chemotherapy-resistant residual prostate cancer cells had a higher tumorigenic potential than primary cancer cells, they aimed to understand the mechanisms underlying this increase in aggressiveness. They found an over-activation of ERK1/2 in resistant cells that was linked to posttranslational MYC stabilization. They also found

that CXCR4 transcript levels were upregulated in resistant cells and that the observed over-activation of ERK1/2 and consequent MYC stabilization was induced by the CXCL12-CXCR4 pathway. Chemotherapy also upregulated CXCR4 in primary cancer cells, a phenomenon that was inhibited by MYC knock-down, suggesting that, as in the study by Moriuchi *et al.* (Moriuchi et al., 1999), MYC was enhancing the transcription of CXCR4 that, in turn, stabilized MYC through ERK1/2 activation (Figure 14). They therefore concluded that residual prostate cancer cells after chemotherapy increased their tumorigenic potential via a CXCR4-ERK1/2-MYC positive feedback loop and that the activation of this loop conferred, to the tumor cells, a more aggressive phenotype.

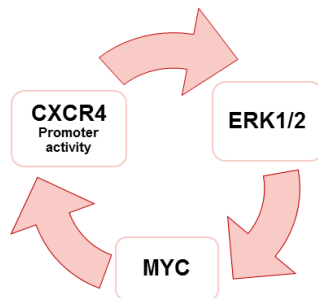


Figure 14.- CXCR4 - ERK1/2 - MYC signaling loop. Schematic representation of the CXCR4, ERK1/2 and MYC positive feedback loop described by Hatano *et al.* (Hatano et al., 2013).

2 Hypothesis & Aims

2.1 Hypothesis

There is increased awareness of the pivotal role of tumor-TME crosstalk in the outcome of many types of cancer, including lymphoid malignancies. Consequently, the disruption of this communication has become a source of new targeted therapies.

In the model of study of this doctoral thesis, DLBCL, a correlation between the expression of the chemokine receptor CXCR4 and the patient outcome has been recently acknowledged. Hence we hypothesized that CXCR4 inhibition might be a promising anti-tumor strategy to treat this disease.

In the context of cancer, CXCR4 has been previously associated to MYC expression. Based on this, the second hypothesis of this thesis is that inhibition of MYC is a rational therapeutic strategy of combination that could potentiate the antitumor effect of CXCR4 targeting.

2.2 General aim and specific objectives

The general aim of this thesis is to investigate the therapeutic potential of targeting CXCR4 in DLBCL as well as to improve the current pharmacological intervention toward this receptor for the translation into the clinics of an effective and safe therapy.

In the context of this general aim, we established the following specific objectives:

1. To evaluate the antitumor effects of the new CXCR4 inhibitor IQS-01.01 in preclinical models of DLBCL.
 - 1.1. To determine the most potent stereoisomer of IQS-01.01.
 - 1.2. To compare the selected stereoisomer with the first-in-class CXCR4 inhibitor, AMD3100.

2. To study the therapeutic effects of simultaneous CXCR4 and MYC inhibition in preclinical models of DLBCL by combining IQS-01.01 with the BET bromodomain inhibitor CPI203.
 - 2.1. To determine the combinational effect of CXCR4 and MYC targeting *in vitro*.
 - 2.2. To validate this therapeutic combination *in vivo* using a DLBCL mouse xenograft model.

3 Methods

3.1 Cell lines, cell culture and patient samples

3.1.1 DLBCL cell lines

The following DLBCL cell lines from GCB and ABC subtypes were used in this study (Table 8). SUDHL4, SUDHL6, SUDHL8, SUDHL16, NUDHL1 and U2932 cell lines were purchased at DSMZ. SUDHL2 and WSU-DLCL2 were obtained from ATCC cell bank (LGC Standards). OCI-Ly8 and Toledo were kindly provided by Dr. M. Raffeld (National Cancer Institute Bethesda, MD, USA) and Dr. MA. Piris (Fundación Jiménez Díaz, Madrid, Spain). OCI-Ly3 and OCI-Ly10 cells were provided by Dr. A. Staiger (Dr. Margarete Fischer-Bosch Institute of Clinical Pharmacology, Stuttgart, Germany). HBL1 was provided by Dr. E. Valls (Transcriptional regulation of gene expression group, IDIBAPS, Barcelona, Spain).

All cell lines were routinely cultured at 37°C in a humidified atmosphere with 5% carbon dioxide in RPMI 1640 or IMDM medium supplemented with 10% to 20% heat-inactivated fetal bovine serum (FBS), 2 mM glutamine and 50 µg/ml penicillin-streptomycin (Thermo Fisher) (Table 8). Mycoplasma infection was routinely tested by PCR. Cell line authentication was performed upon reception by short tandem repeat (STR) profiling, using AmpFISTR identifier kit (Thermo Fisher Scientific), and based on available STR profiles.

The following table shows the culture medium and main characteristics and genetic alterations of each cell line.

Subtype	Cell line	Culture media	Gender	Age	Ethnicity	Year	MYC	BCL2	BCL6	Relevant karyotype
GCB	OCI-Ly8	IMDM, 20% FBS	-	-	-	-	trans	trans	trans	t(8;14), t(14;18), t(3;14;8)
	SUDHL4	RPMI, 10% FBS	M	38	Caucasian	1975	-	trans	trans Non-IG	t(14;18) t(1;3)
	SUDHL6	RPMI, 20% FBS	M	43	Caucasian	1977	trans Non-IG	trans	-	t(8;19;9), t(14;18)
	SUDHL16	RPMI, 20% FBS	M	-	-	1980	-	trans	-	t(14;18)
	WSU-DLCL2	RPMI, 10% FBS	M	41	Caucasian	1990	-	trans	-	t(14;18)
	Toledo	RPMI, 10% FBS	F	Adult	Caucasian	1990	trans	trans	-	t(8;14), t(14;18)
	SUDHL8	RPMI, 20% FBS	M	59	Caucasian	-	trans	-	-	t(8;22)
	NUDHL1	RPMI, 20% FBS	M	73	Caucasian	1982	trans Non-IG	trans	-	t(3;8), t(14;18)
ABC	OCI-Ly3	IMDM, 10% FBS	M	57	-	1983	-	trans	-	t(4;18)
	OCI-Ly10	RPMI, 20% FBS, 10 mM HEPES, 0.9 mM β-mercaptoethanol	-	-	-	-	-	-	-	-
	SUDHL2	RPMI, 10% FBS	F	73	Caucasian	1974	-	-	-	-
	U2932	RPMI, 10% FBS	F	29	-	1996	-	amp	amp	amp(18q21), amp(3q27)
	HBL1	RPMI, 10% FBS	M	65	Asian	1984	-	-	-	-

Table 8.- Main characteristics of the DLBCL cell lines used in this study. Abbreviations: FBS, fetal bovine serum; M, male; F, female; IG, immunoglobulin; trans, translocation; amp, amplification.

3.1.2 Generation of SUDHL6-GFP+/Luc+

The generation of stable green fluorescence protein (GFP) and luciferase (Luc) expressing SUDHL6 cells (SUDHL6-GFP+/Luc+) through lentiviral infection was performed as previously described (Bosch et al., 2011) at the Institute of Biomedical Research (IIB Sant Pau), Hospital de la Santa Creu i Sant Pau, in Barcelona, in the group headed by Dr. Ramon Mangues and under the supervision of Dr. Isolda Casanova.

Briefly, the following steps were followed:

3.1.2.1 Plasmid amplification

To obtain the necessary plasmids for the generation of the lentivirus, the competent strain of *Escherichia Coli* DH5 α transformed with the following plasmids was amplified in LB with the corresponding selection antibiotic.

- pVSV-G contains the genes of the virus envelope
- p8.91 contains the capsid genes
- pSIN-DUAL-GFP-Luc contains the genes of interest (GFP and Luc)

Plasmids were purified using the maxi kit (Qiagen), and confirmed by enzyme restriction digestion and agarose gel analysis of the molecular weight of the fragments.

3.1.2.2 Lentivirus generation

293-T cells were grown in poly-lysine coated plates and transfected in lipofectamine (Thermo Fisher) with the 3 plasmids above. Supernatant containing the virus was collected after 3 days and virus titration was determined using 293T cells.

3.1.2.3 Infection of SUDHL6 and sorting of GFP+ cells

Virus supernatant was added to the SUDHL6 cell line using different multiplicity of infection (MOI). The optimum MOI of 0.5 was determined through GFP positivity detected by flow cytometry. GFP positive cells were gradually sorted using a FACSAria cell sorter (BD Biosciences) until the recovery of > 90% GFP+ cells. Luc expression was confirmed *in vitro* using the luciferase assay system with reporter lysis buffer (Promega).

3.1.3 StromaNKtert

The mesenchymal stromal cell line StromaNKtert is an immortalized cell line generated by isolation of adherent cells from human bone marrow transduced with *hTERT* to maintain the length of the telomeres (Kawano et al., 2003). It prevents *ex vivo* cultured primary cells from dying. This cell line was obtained from Riken Cell Bank

(Tsukuba, Ibaraki, Japan) and cultured in MEM α , no nucleosides media (Gibco) supplemented with 2 mM glutamine and 50 μ g/ml penicillin-streptomycin, 12.5% heat-inactivated FBS, 12.5% horse serum, 100 μ M β -mercaptoethanol (Sigma), and 1 μ M Hydrocortisone solution (Sigma).

3.1.4 Isolation and culture of DLBCL primary cells

DLBCL patients were diagnosed according to the WHO classification criteria (see clinical characteristics in Table 9). Primary cells were obtained from lymph nodes (LN), spleen or peritoneal biopsies through aspiration using a fine needle, with RPMI 1640 (Thermo Fisher) culture medium. Samples were stored within the Hematopathology collection of our institution registered at the Biobank from Hospital Clínic-IDIBAPS (R121004-094). The ethical approval for this project including the informed consent of the patients was granted following the guidelines of the Hospital Clínic Ethics Committee (IRB, reg. num. 2012/7498).

Cells were thawed at 37°C, DMSO was removed by washing with RPMI 10% FBS, and cells were resuspended in complete RPMI 1640 medium as above and cocultured with StromaNKtert at a proportion of 5:1 (DLBCL:StromaNKtert) to prevent spontaneous *ex vivo* apoptosis and used for functional studies. Percentage of tumor cells was determined by staining with a fluorescent-conjugated anti-CD19 or anti-CD20 antibodies (BD biosciences) followed by analysis on an Attune acoustic cytometer. CXCR4 surface expression was determined in CD20 or CD19 positive cells as explained in 3.7.1.

Patient	Source	Gender	Date of diagnosis	Age at diagnosis	Previous treatment	Response to treatment	Stage	LDH	IPI	% tumor cells	CXCR4 expression
DLBCL #1	Peritoneal effusion	M	-	-	-	-	-	-	-	92%	ND
DLBCL #2	Spleen	M	1992	63	-	-	-	-	-	20%	2.8
DLBCL #3	Tonsil	F	2016	78	R-CHOP	CR	IIIA	Normal	2	6%	ND
DLBCL #4	LN	M	2000	78	CHOP	Refractory	IIIA	Abnormal	3	70%	12.1
DLBCL #5	Spleen	F	2010	80	No treatment	-	IA	Normal	1	34%	8.7

Table 9.- Patients characteristics. Abbreviations: LN; lymph node; ND, non-determined; R-CHOP, Rituximab CHOP; CR, complete remission.

3.1.5 Isolation and culture of PBMCs

Peripheral blood mononuclear cells (PBMCs) were isolated by gradient centrifugation on ficoll (GE Healthcare, Little Chalfont, UK) from buffy coats of healthy donors and cultured freshly in RPMI 1640 supplemented with 10% FBS, 2 mM glutamine and 50 μ g/ml penicillin-streptomycin (Thermo Fisher).

3.2 Drugs

The following drugs were used in this study:

The CXCR4 inhibitors IQS-01.01 (racemic mixture), IQS-01.01SS, IQS-01.01RR, IQS-01.01RS and IQS-01.01RS tetrahydrochloride hydrate were synthesized by the Molecular Engineering group (GEM) at IQS School of Engineering (Pettersson et al., 2008). The first-in-class CXCR4 inhibitor AMD3100 octahydrochloride hydrate was purchased from Sigma-Aldrich. CPI203 was kindly provided by Constellation Pharmaceuticals (Cambridge, MA, USA).

For *in vitro* studies, racemic IQS-01.01 and the individual stereoisomers were reconstituted in DMSO, aliquoted, and stored at -20°C . AMD3100 was reconstituted in ddH₂O, aliquoted, and kept frozen at -20°C . CPI203 was reconstituted in DMSO, aliquoted and stored at -80°C . Immediately prior the experiment every drug was diluted in culture media to obtain the indicated concentration for the treatment. A dose of 100 μM for IQS-01.01 and AMD3100, and 100 and 500 nM for CPI203 was used throughout the study unless otherwise specified.

For *in vivo* studies, IQS-01.01RS tetrahydrochloride hydrate was reconstituted in physiological serum (B.Braun) immediately prior treatment. AMD3100 was reconstituted in physiological serum (B.Braun) at the indicated concentration, aliquoted and stored at -20°C . An aliquot was defrosted immediately prior treatment. CPI203 was weekly reconstituted in DMSO and diluted in a 20% solution of 2-hydroxypropyl- β -cyclodextrin (Sigma- Aldrich) to obtain the indicated concentration prior i.p. inoculation. Vehicles were prepared the same way excluding the drug. See section 3.11.2 for more information on doses and administration details.

3.3 cAMP-based CXCR4 activity assay

CXCR4-dependent modulation of intracellular cAMP by the racemic IQS-01.01, the stereoisomers SS, RR and RS, and AMD3100 was evaluated at DiscoverX (Fremont, CA, USA). The cAMP Hunter™ CHO-K1 CXCR4 Gi cell line was stimulated with recombinant CXCL12 + forskolin to determine the EC₈₀ of the receptor's physiological ligand. Forskolin is a cAMP activator. Cells were then exposed for 1 hour to CXCL12 at the EC₈₀ dose (0.004 μM), with or without a 30 minutes pre-treatment with the different compounds (10 μM), and intracellular cAMP was quantified with the HitHunter cAMP XS+ assay. Incubation with forskolin alone was used as a positive

control (Figure 15). Chemiluminescent signal was detected on a Perkin Elmer Envision instrument. Percentage inhibition was calculated using the following formula:

$$\%inhibition = 100\% \frac{\text{mean RLU of test sample} - \text{mean RLU of EC80 control}}{\text{mean RLU of forskolin positive control} - \text{mean RLU of EC80 control}}$$

where: RLU stands for relative luminescence unit; test sample refers to the condition treated with forskolin and an EC₈₀ concentration of CXCL12 plus the compound of interest; forskolin positive control refers to the condition treated with forskolin; and EC₈₀ control refers to the condition treated with an EC₈₀ concentration of CXCL12 plus forskolin.

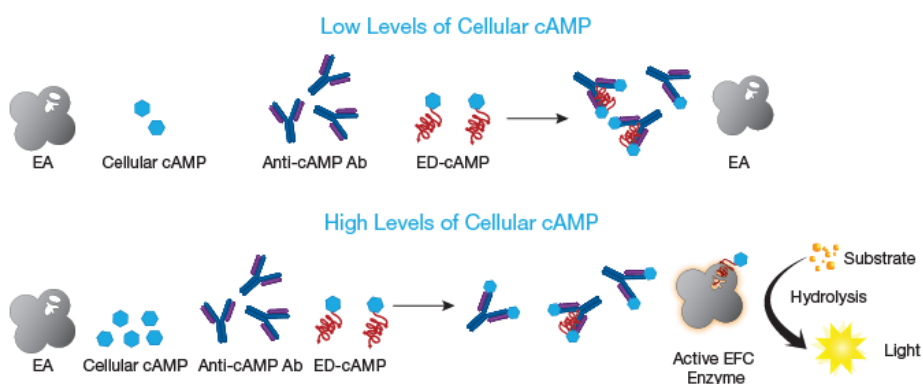


Figure 15.- Schematic representation of the HitHunter cAMP Assay Principle. This assay uses a technology called Enzyme Fragment Complementation that relies on the capacity of the enzyme β -galactosidase to hydrolyze a substrate and produce detectable luminescence. The enzyme is split into two complementary portions, the enzyme acceptor (EA), and the enzyme donor that is covalently bound to exogenous cAMP (ED-cAMP). In addition, anti-cAMP antibodies are added to the reaction. When cellular cAMP is low, the ED-cAMP is arrested by the antibody and no luminescence reaction takes place. In contrast, when cellular cAMP levels are high, it competes for binding to the antibody and, free ED-cAMP together with the EA become active and generate luminescence. Therefore, luminescence intensity is proportional to levels of cAMP. Abbreviations: EA, enzyme acceptor; ED, enzyme donor; Ab, antibody; EFC, Enzyme Fragment Complementation. From (Discoverex SL).

3.4 MTT assay

PBMCs and cell lines were seeded in 96 well plates (5×10^4 cells per well) and incubated for 24-48 hours with racemic IQS-01.01, IQS-01.01RR, SS or RS, AMD3100 and/or CPI203 at the indicated doses. MTT (3-(4,5-dimethylthiazolyl-2)-2,5-diphenyltetrazolium bromide) reagent (Sigma-Aldrich) was added 1-5 hours before formazan dissolution with acidified isopropanol and posterior spectrophotometric measurement with a Synergy HT (BioTeck). Each measurement was made in triplicate. Values were represented using untreated control cells as reference. Combination indexes (CIs) were calculated using the Calcsyn software version 2.0 (Biosoft). The interaction between two drugs was considered synergistic when CI < 0.8.

3.5 Chemotaxis assay

DLBCL cells (5×10^6 cells/ml) were cultured for 1 hour in FBS-free culture medium supplemented with 0.5% bovine serum albumin (Sigma-Aldrich), in the presence or absence of AMD3100 or IQS-01.01RS 100 μ M. CXCL12-induced migration was evaluated using 24-well chemotaxis chambers containing 8 μ m or 5 μ m pore size inserts (Corning Life Science, Tewksbury, MA, USA). Treated or untreated cells (5×10^5) were placed in the upper chamber of the inserts and incubated for 5 hours. The number of cells that migrated towards the CXCL12-containing medium in the lower chamber was counted on an Attune acoustic focusing cytometer (Thermo Fisher) (Figure 16). In parallel, all the conditions were also placed in a well without CXCL12 in order to determine the basal, CXCL12-independent chemotaxis. Migration Index was calculated as the number of cells having migrated to lower chamber containing CXCL12, divided by the number of cells present in the lower chamber without CXCL12.

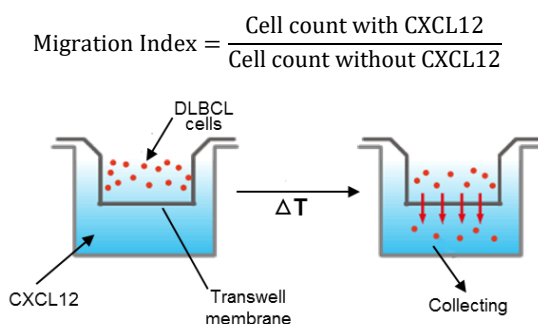


Figure 16.- Schematic representation of the transwell chemotaxis assay system. 1) Media with 200ng/ml of recombinant CXCL12 was added to a 24 well plate. 2) A membrane with pore inserts and an upper chamber was placed over the well. 3) $5 \cdot 10^5$ pre-treated or control DLBCL cell lines were placed in the upper chamber and plates were kept in the incubator for 5 hours for the cells to migrate towards CXCL12. 4) Media from the lower chamber was collected and the number of cells counted.

3.6 Docking study

The interaction of the small molecule CXCR4 inhibitors with CXCR4 was predicted by molecular docking using Autodock software. IQS-01.01RS, SS and RR, and AMD3100 molecular structures were generated and geometry optimized with the MOE software (Chemical Computing Group). CXCL12 and CXCR4 structures were obtained from the Protein Data Bank (accession numbers 2N55 and 3OE6). Blind docking was conducted including the whole receptor into the grid box. The best interaction conformation was found in the binding pocket.

3.7 Flow cytometry analysis

3.7.1 CXCR4 staining

For the detection of surface (sCXCR4) and intracellular (iCXCR4) CXCR4, either fresh, or paraformaldehyde (PFA)-fixed and saponin-permeabilized cells (2×10^5) were stained with a phycoerythrin (PE)-labeled anti-CXCR4 or isotype control antibody (BD Biosciences) for 20 minutes and washed. A total of 10,000 events were acquired and analyzed on an Attune cytometer. Median fluorescence intensity ratio (MFI-R) was calculated as the ratio between median fluorescence intensity (MFI) of the CXCR4-labeled sample and the MFI of the isotype.

3.7.2 Occupancy assay

Cells were pre-treated for 1 hour with IQS-01.01RS, AMD3100 (Sigma-Aldrich) or an anti-human CXCR4 blocking antibody (30 $\mu\text{g}/\text{ml}$, R&D Systems) followed by sCXCR4 staining as above.

3.7.3 Annexin V staining

For apoptosis quantification, cells lines treated for 48 hours were labelled with Pacific Blue-conjugated Annexin V (Thermo Fisher). Patient derived samples cocultured with StromaNKtert were co-stained with anti-CD20 or anti-CD19 antibodies (BD Biosciences) and Pacific Blue-conjugated Annexin V (Thermo Fisher). To determine the percentage of apoptotic cells, 10,000 events were acquired and analyzed on an Attune acoustic cytometer.

3.8 Protein isolation and Western blot

Proteins were extracted from 10^7 DLBCL cells lysed using RIPA buffer (Sigma-Aldrich) or Triton buffer (20 mM TrisH-HCl pH7.6, 0.15 M NaCl, 1 M EDTA, 1% TritonX-100 (Sigma-Aldrich)) complemented with Halt™ Protease and Phosphatase Inhibitor Cocktail (Invitrogen). Protein extracts were quantified using the Bradford reagent (BioRad), and 30-50 $\mu\text{g}/\text{lane}$ were subjected to 10% sodium dodecyl sulfate polyacrylamide gel electrophoresis (SDS-PAGE), and transferred onto PVDF membranes (Immobilon-P; Millipore), or nitrocellulose membranes (Amersham Biosciences). Membranes were then incubated with primary and secondary antibodies (Table 10 and see below) and visualized on a mini-LAS4000 device (Fujifilm) by enhanced chemiluminescence (ECL, Amersham Life Science).

WESTERN BLOT ANTIBODIES

PVDF membranes were incubated with anti-p-ERK1/2 (T202/Y204), anti-p-AKT (S473), anti-AKT, anti-p-MYC (S62), anti-MYC, anti-p-GSK-3 β (S9) (Cell Signaling Technology), anti-ERK 1/2 (Santa Cruz), anti- α -tubulin and anti- β -actin (Sigma-Aldrich) antibodies, and nitrocellulose membranes with anti-CXCR4 (ProSci Incorporated) antibody, followed by species-matched secondary horseradish peroxidase (HRP)-labelled antibodies (Cell Signaling Technology) (Table 10).

Antibody against	Concentration	Diluent (in TBS-T)	Incubation time	Company	Reference
p-ERK (T202/Y204)	1/1000	2.5 % p-blocker	O/N	Cell Signaling Technology	#4377
p-AKT (S473)	1/1000	5% non-fat milk	O/N	Cell Signaling Technology	#4060S
p-MYC (S62)	1/1000	5% BSA	O/N	Cell Signaling Technology	#13748S
p-GSK-3 β (S9)	1/1000	5% BSA	O/N	Cell Signaling Technology	#5558
CXCR4	1.5 μ m/ml	5% non-fat milk	O/N	ProSci Incorporated	1009
ERK	1/500	5% BSA	2h	Santa Cruz	sc-94
AKT	1/1000	5% BSA	O/N	Cell Signaling Technology	#9272
MYC	1/1000	5% BSA	O/N	Cell Signaling Technology	#5605
α -tubulin	1/5000	5% non-fat milk	1h	Sigma-Aldrich	T6074
β -actin	1/5000	5% non-fat milk	1h	Sigma-Aldrich	A5441

Table 10.- Description of primary antibodies used for western blotting. Abbreviations: p, phospho; TBS-T, tris-buffered saline-Tween 20; BSA, bovine serum albumin; O/N, overnight; h, hour.

BLOTS QUANTIFICATION

Densitometry of western blot bands was quantified using the Image J software. Mean grey value was determined for each band and normalized to the mean value of its corresponding loading control post subtraction of the blank value. Data was then represented using the control condition as a reference.

3.9 Protein stability assay

SUDHL6 cells were treated with 50 ng/ml of the protein translation blocker cycloheximide (CHX; Sigma) in the presence or absence of 100 μ M IQS-01.01RS for 0 to 30 minutes and then harvested. Time-dependent MYC protein levels were determined by SDS-PAGE as previously. β -actin was used as a loading control.

3.10 RNA isolation and real-time PCR

Total RNA was extracted using TRIZOL (Thermo Fisher) following manufacturer's instructions. To avoid amplification of genomic DNA, purified RNA was subjected to DNase treatment using the DNA-free™ Kit (Ambion) following manufacturer's instructions. Concentration of RNA was quantified with a Nanodrop (Thermo Fisher) and one microgram of RNA was retrotranscribed to complementary DNA using moloney murine leukemia virus reverse transcriptase (M-MLV-RT) (Thermo Fisher) and random hexamer primers (Roche). mRNA expression was analyzed in duplicate by quantitative real-time PCR on the Step One system by using predesigned Assay-on-Demand primers and probes (Thermo Fisher): *MYC* (Hs00153408m1), *CXCR4* (Hs00607978s1). The relative expression of *MYC* and *CXCR4* was quantified by the comparative cycle threshold method ($\Delta\Delta C_t$). β -*ACTIN* was used as an endogenous control.

3.11 *In vivo* experiments

Mice were housed and bred in the specific pathogen free (SPF) animal facility of the University of Barcelona, under a 12/12 hour light/dark cycle at 22°C, where they received a standard diet and acidified water ad libitum. Animal handling was performed following protocols approved by the Animal Ethics Committee of the University of Barcelona (protocol #154/16).

3.11.1 NOD/SCID-IL2rynull strain

NOD/SCID-IL2rynull (NSG) mice have been used in this study for the subcutaneous and systemic model of DLBCL. Deletion of multiple genes in this mouse strain causes severe impairment in T and B-cell development and absence of NK cells. This defective immune system increases human tissue engraftment. Table 11 presents the status of immune cells in NSG.

Mature B-cells	Absent
Mature T-cells	Absent
Macrophages	Defective
Natural Killers	Absent
Complement	Absent

Table 11.- Characteristics of the immune system of NSG mice.

3.11.2 Drug administration

3.11.2.1 Toxicity assay

To establish the dosages and route of administration for our DLBCL *in vivo* model, an acute toxicity assay was conducted in NSG mice exposed to IQS-01.01RS tetrahydrochloride or AMD3100 prior efficacy testing. Animals (2 adult males and 2 adult females per dose) received a single administration of vehicle, IQS-01.01RS (p.o.) or Plerixafor (i.p.) at doses ranging from 2 to 10 mg/kg, and were monitored during the first 4 hours after administration, and daily for 2 weeks for viability/mortality, and vital parameters. This toxicity test defined a maximum tolerated dose (MTD) of 5 mg/kg for AMD3100. The MTD dose for orally administered IQS-01.01RS was not reached and is therefore greater than 10mg/kg. CPI203 *in vivo* administration had been previously established (Moros et al., 2014b).

3.11.2.2 Doses

The administration route and *in vivo* doses of the studied compounds are gathered in Table 12.

Compound	Route of administration	Dose	
		Systemic model	Subcutaneous model
IQS-01.01RS	Oral (gavage)	10 mg/kg	2 mg/kg
AMD3100	Intraperitoneal (syringe)	5 mg/kg	-
CPI203	Intraperitoneal (syringe)	-	1.5 mg/kg

Table 12.- *In vivo* route of administration and doses.

3.11.3 Systemic model

For the systemic DLBCL model, 8-week old NSG female mice were inoculated intravenously with 10^7 SUDHL6-GFP+/Luc+ cells, randomly assigned into 3 equivalent cohorts of four mice, and treated daily on a 5 on/2 off schedule with 5 mg/kg AMD3100 (i.p.), 10 mg/kg IQS-01.01RS salt (p.o.) or vehicle.

After 27 days, animals were sacrificed and peripheral blood was collected by submandibular puncture. Erythrocytes were lysed using ACK buffer (Quality Biological). Brains and ovaries were homogenized and filtered through 70 μ m nylon sieves (Becton Dickinson). Percentage of SUDHL6-GFP+/Luc+ cells was evaluated by the detection of GFP signal on an Attune acoustic cytometer.

3.11.4 Subcutaneous model

For the subcutaneous DLBCL model, 10^7 SUDHL6-GFP+/Luc+ cells were inoculated subcutaneously in 8-week old NSG female mice into their lower dorsum in matrigel basement membrane matrix (Becton Dickinson). When tumors were palpable, mice were randomized into 4 cohorts of 4 mice each, receiving a twice daily dose of 1.5 mg/kg CPI203 (i.p.), a daily dose of 2 mg/kg IQS-01.01RS (p.o.), both agents, or an equal volume of vehicle on a 5 on/2 off schedule. Tumor engraftment was determined weekly following mice injection with 75 mg/kg of D-luciferin (AnaSpec) and bioluminescence imaging (BLI) using an Aequoria Luxiflux device equipped with an ORCA-ER camera (Hamamatsu). Color maps were generated with Matlab and BLI signal was quantified using Image J software. The shortest and longest diameters of the tumors were measured with external calipers twice a week, up to 28 days, and tumor volume was calculated with the use of the standard formula $\pi \frac{1}{2} \times L \times W^2$ where L= length (longest diameter), and W= width (shortest diameter) (Tomayko and Reynolds, 1989). Animals were then sacrificed and tumors were weighted and harvested, and formalin-fixed before paraffin embedding on silane-coated slides in a fully automated immunostainer (Bond Max; Vision Biosystems).

3.12 IHC

Xenograft tumor samples were subjected to immunohistochemical staining using primary antibodies against p-histone H3 (1:1000; Epitomics), cleaved caspase-3 (1:1000; Cell Signaling Technology), MYC (1/100; Cell Signaling Technology), p-AKT-Ser473 (1/50; Cell Signaling Technology), and CD20 (DAKO) (Table 13). Paraffin sections on silane-coated slides were developed in a fully automated immunostainer (Bond Max, Vision Biosystems, Mount Waverley, Australia). Low or high pH (Table 13) retrieval was done in a Bond ER1 Buffer solution (Vision Biosystems) for 20 minutes followed by the incubation with primary antibody at room temperature and 30 minutes of Bond Refine Polymer (Vision Biosystems). 5,3-diaminobenzidine was used for 10 minutes as a chromogen. Preparations were evaluated on a DP70 or a BX51 microscope using the Cell B Basic Imaging Software (Olympus).

Antibody	Reference	dilution	pH	Company
Cleaved caspase-3 (5A1E)	#9664	1/100	high	Cell Signaling Technology
MYC	#5605	1/100	high	Cell Signaling Technology
p-AKT (Ser473) (D9E) XP	#4060S	1/50	high	Cell Signaling Technology
p-histone H3	#1173-1	1/100	high	Epitomics
CD20	#IS604	Ready to use	high	DAKO

Table 13.- Description of the antibodies used for IHC. Abbreviations: p, phospho.

3.13 Statistics

Unpaired t-tests were employed to obtain the statistical significance. Non-parametric Wilcoxon signed rank test was used to compare the median of a set of samples against a hypothetical median. All results are expressed as mean±SD except *in vivo* results where SEM is used. Results were considered statistically significant when $p < 0.05$ (* $p \leq 0.05$, ** $p \leq 0.01$, *** $p \leq 0.001$).

For the correlation studies, the software SPSS Statistics was used for the determination of Spearman's rank correlation coefficient (ρ). To test the null hypothesis that the slope of the regression line equaled 0 and that there was therefore no linear dependence between the tested variables, the t-Student's t-distribution was used (Scheaffer and McClave, 1993).

4 Results

4.1 Description of IQS-01.01 and its stereoisomers

4.1.1 IQS-01.01RS stereoisomer is the most potent CXCR4 inhibitor

As stated in the introduction (section 1.5.6.3), IQS-01.01 is a racemic mixture of 3 stereoisomers (IQS-01.01RR, IQS-01.01SS and IQS-01.01RS). A previous study suggested that IQS-01.01RS (Figure 17A) had a slightly higher CXCR4 inhibitory activity than the racemic mixture, the other two stereoisomers (RR and SS), and AMD3100 in glioma models (Ros-Blanco et al., 2012). To compare the racemic mixture with its 3 individually purified stereoisomers, we performed a cAMP-based antagonist screening using AMD3100 as a reference CXCR4 antagonist. Figure 17B shows that all the stereoisomers harbored an improved inhibitory activity when compared to AMD3100, and that IQS-01.01RS was the most potent agent with a 181% efficacy of inhibition. An effect of a 100% corresponds to the inhibition of the activation of the CXCR4 receptor with an EC_{80} dose of CXCL12 down to the basal activity of the GPCR. When a compound, like IQS-01.01RS, inhibits greater than 100% some inverse agonist activity is suspected (see section 3.3 for detailed methodology). We then analyzed the antitumor activity of this highly active stereoisomer, together with the racemic mixture in 6 representative DLBCL cell lines from both GCB and ABC subtypes. As shown in Figure 19C, IQS-01.01RS was significantly more active than the racemic mixture at all the doses tested, with a major effect observed at the 100 μ M dose (mean cytotoxicity: 44%, range 42-49%). In agreement with this observation, migration experiments against a CXCL12 gradient, further demonstrated that IQS-01.01RS was a more potent inhibitor of cell chemotaxis than the racemic mixture with a 2-fold improvement of cell migration blockade (Figure 17D).

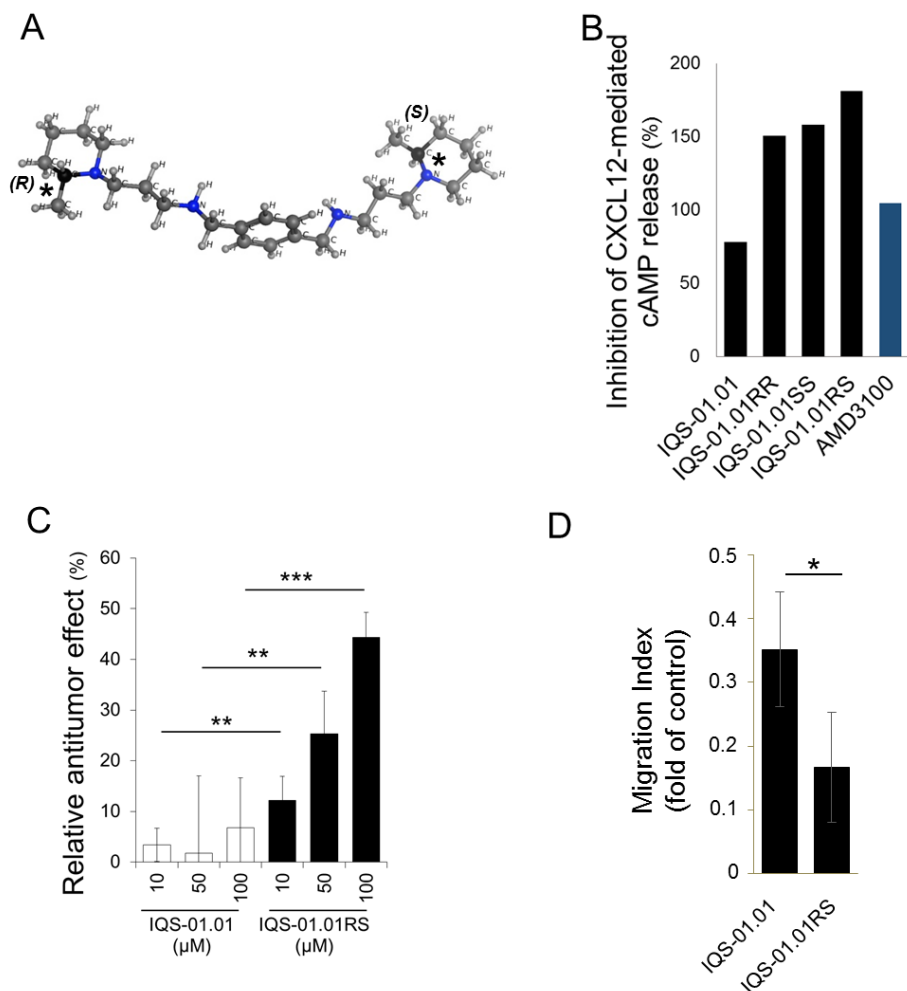


Figure 17.- Design of a new potent CXCR4 inhibitor. A) Ball-and-stick representation of IQS-01.01RS. *chiral carbons. B) Inhibition of CXCL12-mediated intracellular cAMP release was determined in presence of 10 μM of IQS-01.01 racemic mixture or its 3 individually purified stereoisomers, using AMD3100 blocking activity as a reference control. C) MTT assay shows superior antitumor effect of IQS-01.01RS when compared to IQS-01.01 racemic mixture after 48 hours. Shown are the mean values obtained from $n=3$ GCB-DLBCL cell lines (SUDHL6, SUDHL16, WSU-DLCL2) and $n=3$ ABC-DLBCL cell lines (OCI-Ly3, OCI-Ly10 and SUDHL2). D) Inhibition of CXCL12-induced migration upon DLBCL cell treatment with a 100 μM dose of IQS-01.01 racemic mixture or IQS-01.01RS. Shown are mean values from SUDHL6 and OCI-Ly3 cell lines.

4.1.2 Differential CXCR4 binding properties of IQS-01.01RS over other stereoisomers

In order to understand the differences in activity between the different IQS-01.01 stereoisomers, a comparative docking model was generated. Figure 18 shows the predicted position of IQS-01.01RS and IQS-01.01SS within the binding pocket of CXCR4.

Due to the difference in the spatial conformation caused by the chiral carbons, the stereoisomer RS adopts a more internal binding position compared to the RS. The same was observed when RS was compared to the RR stereoisomer (data not shown). The fact that each methyl group bound to the chiral carbons faces opposite each other in the stereoisomer RS confers the molecule a higher flexibility that could reduce some allosteric impediments and facilitate its binding to a deeper CXCR4 domain. This might localize IQS-01.01RS closer to the negatively charged lateral chain of Glu288 and explain its higher activity.

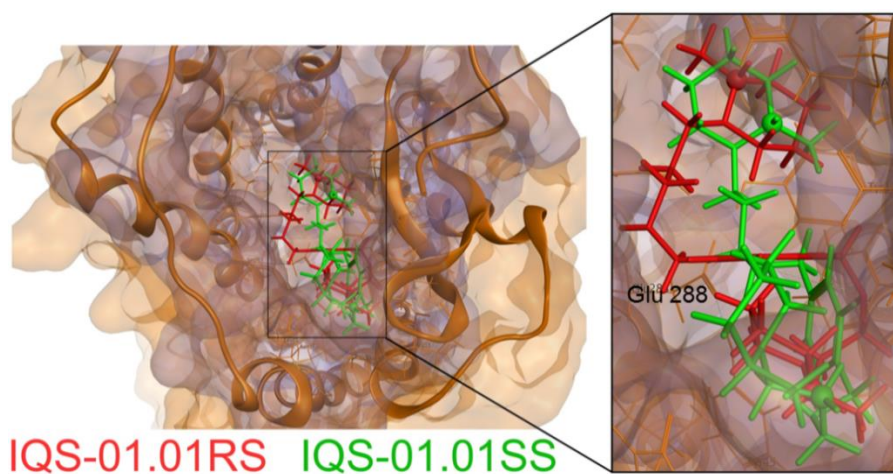


Figure 18.- Docking model. Predicted docking of IQS-01.01RS (red) and IQS-01.01SS (green) on their target, CXCR4 (orange) from an overhead shot perspective. The binding pocket is shaded in blue.

Based on these results, we proceeded to fully characterize the stereoisomer of choice, IQS-01.01RS, in comparison with the first in class CXCR4 inhibitor AMD3100.

4.2 IQS-01.01RS holds better pharmacological properties than AMD3100

4.2.1 IQS-01.01RS binds to a deeper area in CXCR4 than AMD3100

As above described, IQS-01.01RS is the most active stereoisomer of the compound and it inhibits CXCL12-induced CXCR4 activation more potently than AMD3100 (Figure 17B). In an attempt to understand this difference, we generated another predictive docking model that showed that IQS-01.01RS was able to bind to a more internal area of the binding pocket of CXCR4 than AMD3100 (Figure 19A). According to this model, while the binding site of AMD3100 overlaps almost completely with that of the physiological ligand, CXCL12, IQS-01.01RS shares its binding site with

CXCL12 only partially (see zoomed image in Figure 19A). This suggests that, when CXCL12 is absent, both IQS-01.01RS and AMD3100 are able to bind the receptor, but that only IQS-01.01RS has the ability to bind CXCR4 in the presence of the ligand.

To validate this predictive informatics model, we performed a CXCR4 occupancy assay by fluorescent labeling of the receptor and flow cytometry analysis, in the representative cell line SUDHL6 that presents average to high levels of surface CXCR4 (Table 14). When compared to a control CXCR4 blocking antibody, IQS-01.01RS showed a similar occupancy of the receptor, as demonstrated by an equivalent decrease in CXCR4 labelling, thus confirming the specificity of the compound towards CXCR4 (Figure 21B). In addition, according to the previous *in silico* docking model, IQS-01.01RS showed slightly lower CXCR4 occupancy activity than AMD3100 (Figure 19B).

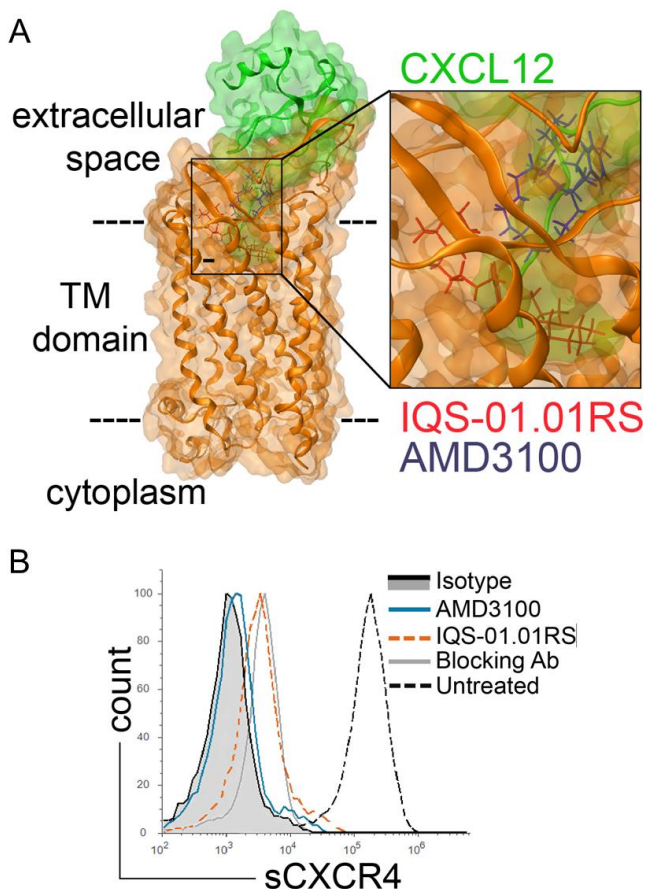


Figure 19.- Docking model. A) Predicted docking of IQS-01.01RS (red) and AMD3100 (blue) on their target, CXCR4 (orange). The physiological ligand CXCL12 is represented in green. In the amplification green shade represents space occupied by CXCL12. B) CXCR4 occupancy assay shows the competition between IQS-01.01RS or AMD3100 (100 μ M) with a PE-labeled anti-CXCR4 antibody for the binding to the receptor. A control blocking antibody (30 μ g/ml, R&D Systems) was used as a control. Abbreviations: Ab, antibody; sCXCR4, surface CXCR4.

Based on these results, IQS-01.01RS stands as a novel promising CXCR4 inhibitor. We therefore proceeded to analyze the antitumor activity of this small molecule compared side-by-side with the standard CXCR4 inhibitor AMD3100.

4.2.2 IQS-01.01RS blocks migration of DLBCL tumor cells

To compare the anti-migratory capacity of both drugs, we performed a CXCL12-induced transwell chemotaxis assay. We found that in ABC and GCB DLBCL cell lines, both IQS-01.01RS and AMD3100 harbored comparable anti-migratory properties against a CXCL12 gradient (Figure 20).

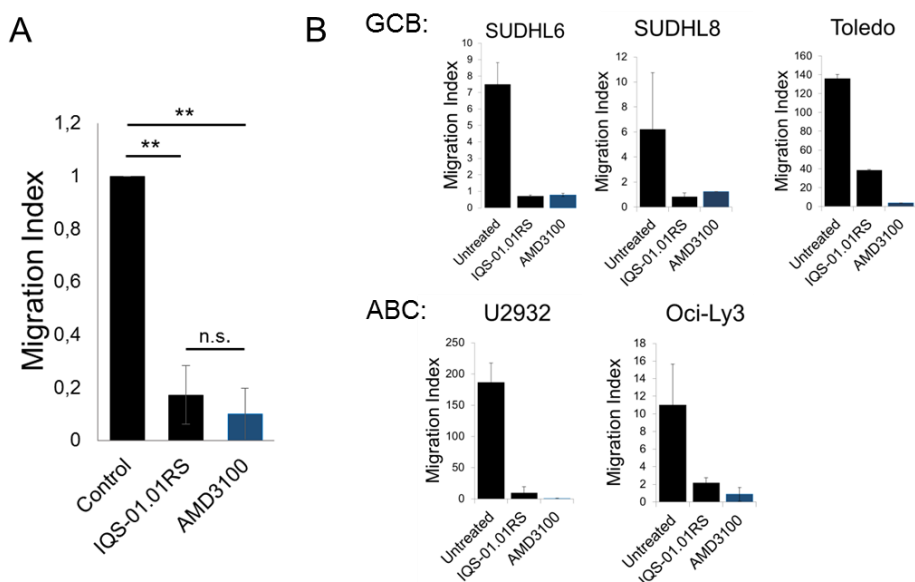


Figure 20.- Anti-CXCL12-induced chemotaxis activity of IQS-01.01RS and AMD3100. A) Inhibition of CXCL12-induced migration upon DLBCL cell treatment with IQS-01.01RS (100 μ M) and AMD3100 (100 μ M). Shown are the mean values from n=3 GCB-DLBCL cell lines (SUDHL6, Toledo and SUDHL8) and n=2 ABC-DLBCL cell lines (U2932 and OCI-Ly3). Data are representative of at least three independent experiments. B) Shown is the individual migration index of each line and the effect of IQS-01.01RS and AMD3100. GCB cell lines are in the upper panel and ABC in the lower panel.

4.2.3 IQS-01.01RS increases mobilization of DLBCL tumor cells

A protein-protein blast revealed a 93% of homology between the query murine CXCL12 and human CXCL12 (National Center for Biotechnology Information) (Figure 21). This makes the mouse an excellent model to understand CXCL12-CXCR4 dependent tumor cell recruitment and metastasis, as well as the effect of targeting this axis in tumor cell mobilization and inhibition of metastasis.

stromal cell-derived factor 1 isoform alpha precursor [Homo sapiens]

Sequence ID: [NP_954637.1](#) Length: 89 Number of Matches: 1

[▶ See 7 more title\(s\)](#)

Range 1: 1 to 89		GenPept	Graphics			▼ Next Match	▲ Previous
Score	Expect	Method	Identities	Positives	Gaps		
159 bits(403)	7e-52	Compositional matrix adjust.	83/89(93%)	86/89(96%)	0/89(0%)		
Query	1	MDAKVVAVLALVLAALCISDGKPVLSYRCPFRFFESHIRANVKHLKILNTPNCALQIV	60				
Sbjct	1	.N....V..V...T...L.....V.....	60				
Query	61	ARLKNNNRQVCIDPKLKIQEQYLEKALNK	89				
Sbjct	61	89				

Figure 21.- Protein-protein blast using *Mus musculus* CXCL12 protein sequence (accession number: CAJ18596.1) as a query shows 93% of amino acid identities with human CXCL12. Dots indicate identities; red indicates unmatched amino acids.

To evaluate the capacity of IQS-01.01RS to inhibit CXCL12 induced chemotaxis in comparison with AMD3100, we generated a systemic mouse model of DLBCL mimicking the physiological dissemination pattern of the disease. The SUDHL6 DLBCL cell line was genetically modified to express GFP and luciferase (SUDHL6-GFP+/Luc+) (see materials and methods, section 3.1.2), and injected intravenously in the tail vein of immunocompromised NSG mice.

In this systemic model of DLBCL, both SUDHL6 and SUDHL6-GFP+/Luc+ circulating tumor cells migrated and were retained in the brain and the ovaries, as shown by IHC detection of CD20 positive cells and confirmed by bioluminescence signal recording and GFP cytometric detection (Figure 22).

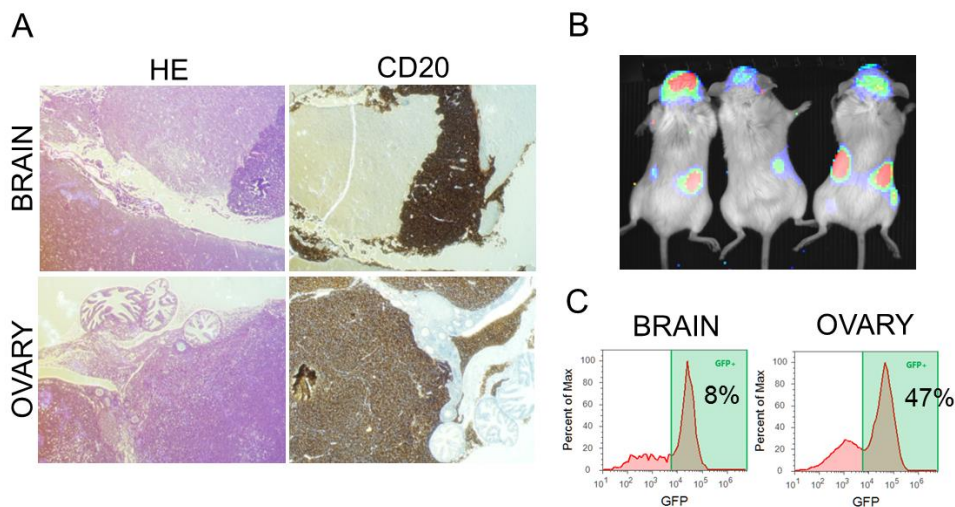


Figure 22.-Homing of SUDHL6 and SUDHL6-GFP+/Luc+ injected intravenously in NSG mice. A) Detection of SUDHL6 cells on the infiltrated organs by CD20 IHC 27 days after inoculation. B) *In vivo* bioluminescence detected on day 22 after SUDHL6-GFP+/Luc+ injection. C) Percentage of GFP+ cells assessed by flow cytometry 27 days post inoculation. Abbreviations: EH, hematoxylin and eosin stain; GFP, green fluorescent protein.

Treatment of mice with both IQS-01.01RS and AMD3100 impaired tumor cell infiltration into the brain, as observed by a decreased cytofluorimetric detection of GFP positive cells in this organ (Figure 23A). In addition, IQS-01.01RS triggered superior mobilization of DLBCL cells into the circulating blood of these animals 12 hours after the last administration of the compound (Figure 23B). No difference in the tumor load between the vehicle and the treatment groups was observed in the ovaries (data not shown).

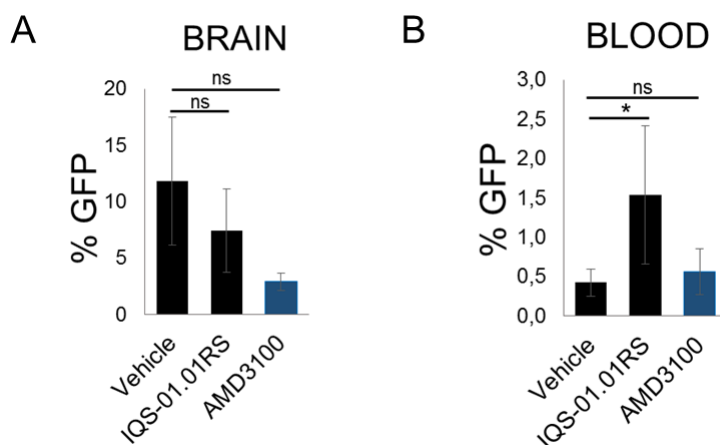


Figure 23.- Comparison of IQS-01.01RS vs AMD3100 in a systemic mouse model. Mean percentage of GFP positive tumor B-cells detected in brain (A) and blood (B) samples of NSG mice injected intravenously with SUDHL6-GFP+/-Luc+ cells and treated for 27 days with IQS-01.01RS, AMD3100, or vehicle (n=4 animals/group).

4.2.4 IQS-01.01RS inhibits DLBCL tumor growth

CXCR4 has a major role in CXCL12-mediated chemotaxis, but its activation also leads to survival and proliferation. It is reported that AMD3100 has a minor effect in tumor cell proliferation and that it is not able to induce apoptosis in DLBCL cell lines (Reinholdt et al., 2016). Nevertheless, considering the improved pharmacological properties of IQS-01.01RS over AMD3100, we investigated the capacity of the compound to impair tumor cell proliferation beside its inhibitory effect towards CXCL12-induced chemotaxis. In a panel of 13 DLBCL cell lines, we observed that IQS-01.01RS was able to block cell proliferation, in a time- and dose-dependent manner, contrasting with the moderate antitumor activity of AMD3100 (40% versus 12% mean cell growth inhibition at 48 hours) (Figure 24A and B, and Table 14).

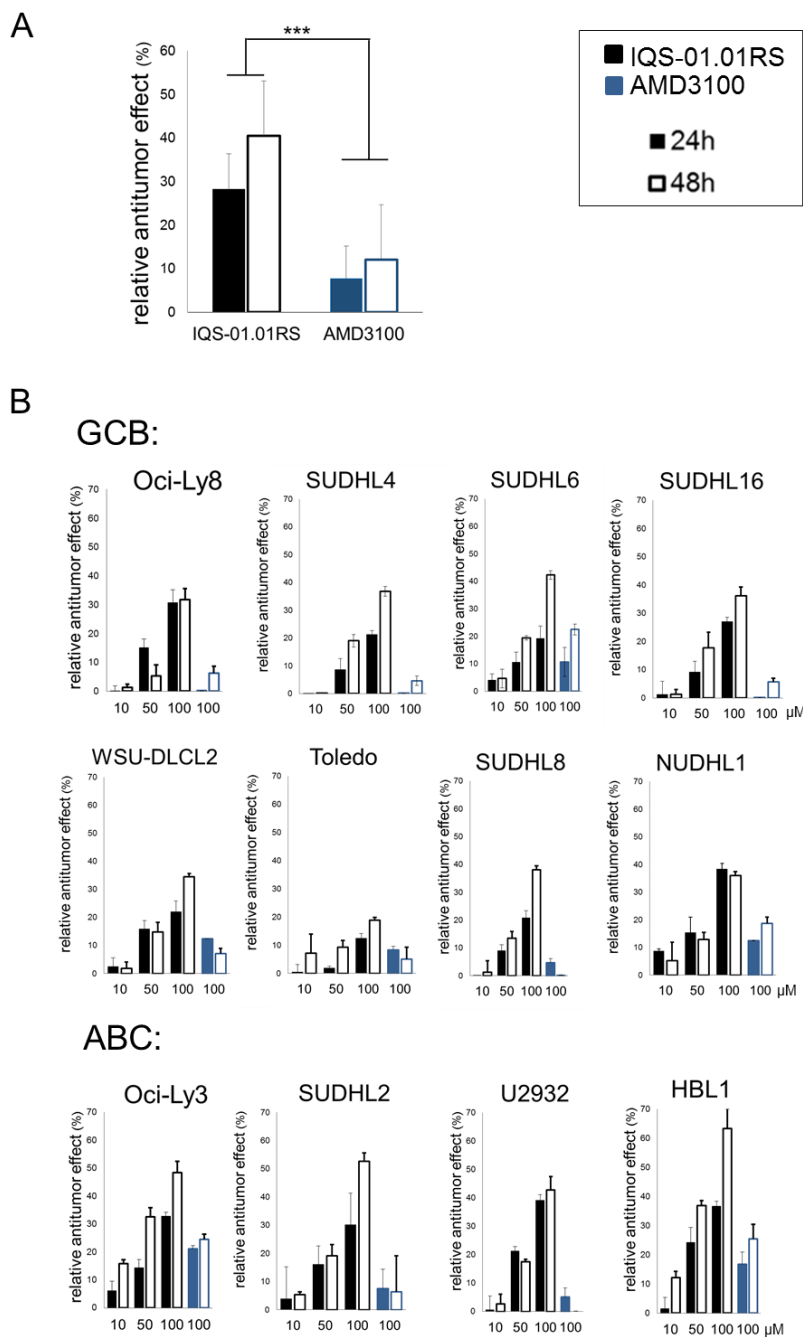


Figure 24.- Anti-tumor effect of IQS-01.01RS. A) Mean values of the time dependent effect of IQS-01.01RS and AMD3100 of the 13 DLBCL cell lines in B. B) Time and dose dependent antitumor effect of IQS-01.01RS and AMD3100 in the indicated cell lines, as determined by MTT assay at the indicated times and μM concentrations. Shown are representative results from at least $n=3$ independent experiments.

Subtype	Cell line	sCXCR4 expression (MFI-R)	IQS-01.01RS cytotoxic effect (100 μ M)	CPI203 cytotoxic effect (0.5 μ M)	Combination Index
GCB	OCI-Ly8	36	32%	38%	1.1
	SUDHL4	25	37%	59%	0.6
	SUDHL6	41	42%	47%	0.4
	SUDHL16	1	36%	86%	0.5
	WSU-DLCL2	3	35%	55%	0.4
	Toledo	52	9%	43%	0.5
	SUDHL8	91	38%	14%	1.1
	NUDHL1	1	36%	60%	0.8
ABC	OCI-Ly3	4	48%	75%	0.7
	OCI-Ly10	1	40%	40%	0.8
	SUDHL2	1	53%	95%	0.8
	U2932	46	43%	31%	0.9
	HBL1	1	63%	39%	0.6

Table 14.- Sensitivity of DLBCL cell lines to CXCR4 and BET bromodomain inhibition. Abbreviations: sCXCR4, surface CXCR4; MFI-R, median fluorescence intensity ratio.

To further analyze the antitumor effect of IQS-01.01RS, we evaluated the level of apoptosis induction after a 48 hours treatment with IQS-01.01RS by standard Annexin V assay and flow cytometry analysis. As shown in [figure 25A](#), a marginal induction of apoptosis (< 5%) could be detected in cells exposed to the compound. This confirmed that the effect seen in [figure 24](#) was mainly due to proliferation blockade. However, in a set of 5 DLBCL primary cultures ([Table 9](#)), a dose-dependent apoptosis induction of an $18\pm 7\%$ was observed in tumor B-cells, contrasting with the reported inability of AMD3100 to induce cell death in DLBCL (Reinholdt et al., 2016) ([Figure 25B](#)).

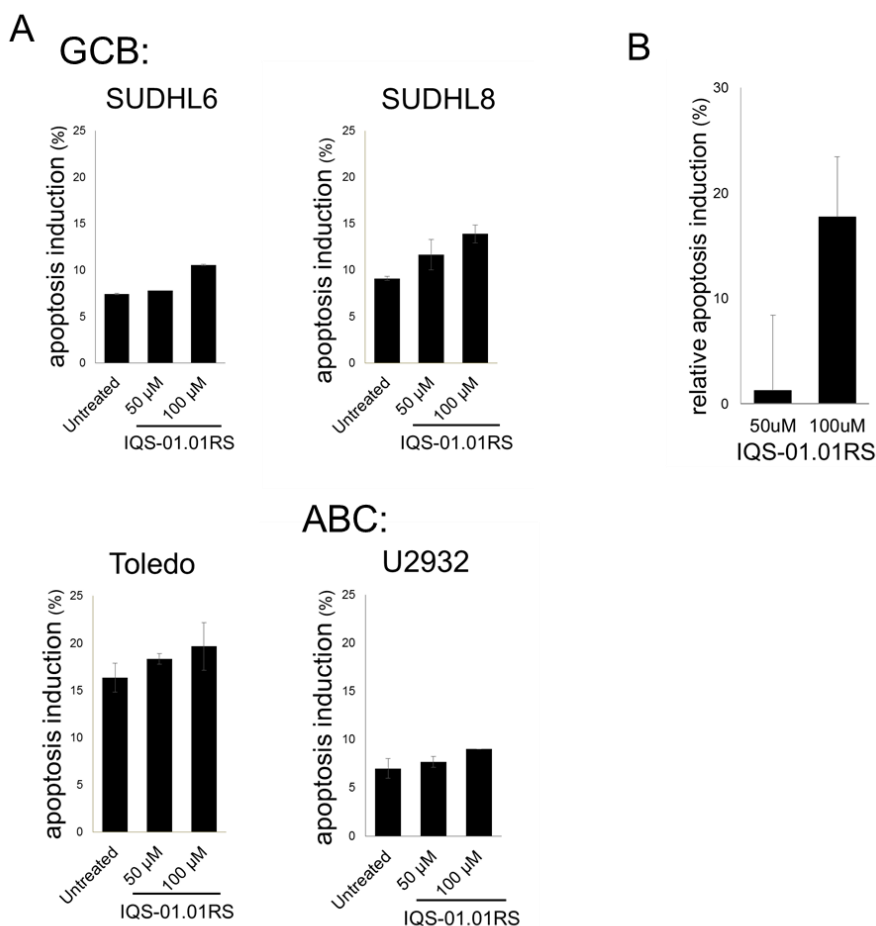


Figure 25.- Apoptosis induction by IQS-01.01RS. A) Percentage of apoptosis induction calculated by means of Annexin V staining in SUDHL6, SUDHL8, Toledo and U2932 upon 48 hours of treatment with IQS-01.01RS. B) Relative apoptosis induction in CD19 or CD20 positive tumor B-cells after a 48 hour treatment of primary DLBCL biopsies (n=5) with the indicated doses of IQS-01.01RS. Mean viability of untreated primary cells was 79±8%.

4.2.4.1 IQS-01.01RS anti-proliferative activity does not correlate with CXCR4 expression levels

To investigate whether IQS-01.01RS anti-proliferative activity correlated with CXCR4 expression levels, we proceeded to characterize the levels of sCXCR4 in our panel of DLBCL cell lines (Table 14). For each cell line, we plotted the IQS-01.01RS antitumor activity *versus* sCXCR4 and, using a lineal regression the null hypothesis that IQS-01.01RS antitumor effect was not affected by CXCR4 levels could not be refuted indicating that the antiproliferative activity of the molecule was not significantly affected by sCXCR4 levels linearly (Figure 26). This result was confirmed by a Spearman's correlation of $\rho = -0.26$ and $p = 0.38$, which indicated that no other

monotonic relationship exists (Figure 26A). Similarly, no relation was found between IQS-01.01RS antitumor effect and levels of iCXCR4 protein by either t-Student or Spearman's correlation (Figure 26B). Neither it correlated with CXCR4 RNA levels (data not shown).

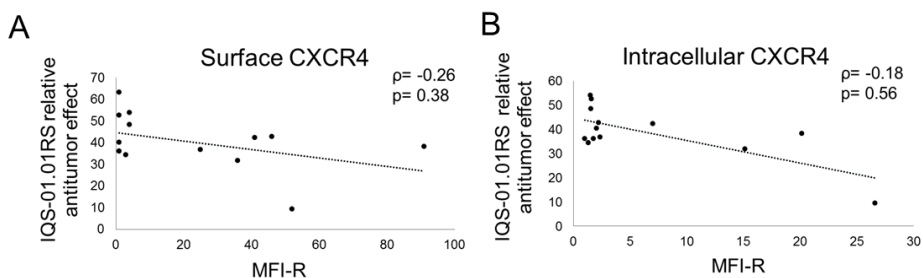


Figure 26.- IQS-01.01RS antitumor effect vs CXCR4 expression dot plot in DLBCL cell lines. Spearman's correlation (ρ) in the right top corner of each dot plot. A) IQS-01.01RS antiproliferative effect vs sCXCR4 in 13 DLBCL cell lines. B) IQS-01.01RS antiproliferative effect vs iCXCR4 in 13 DLBCL cell lines. Abbreviations: MFI-R, median fluorescence intensity ratio; sCXCR4, surface CXCR4; iCXCR4, intracellular CXCR4.

4.2.4.2 IQS-01.01RS presents selectivity towards tumor cells

We investigated the selectivity of IQS-01.01RS by treating peripheral blood mononuclear cells (PBMCs) from healthy donors with 100 μ M of the compound or of AMD3100 for 24 or 48 hours. Then we compared the effect with that in DLBCL cell lines. A significant difference was observed in the antitumor effect of IQS-01.01RS at 24 and 48 hours between normal PBMCs and DLBCL cells, indicating that the compounds may exert selective cytotoxic effect in malignant B cells. Of note, AMD3100 did not show significant activity either in normal or DLBCL cell culture (Figure 27).

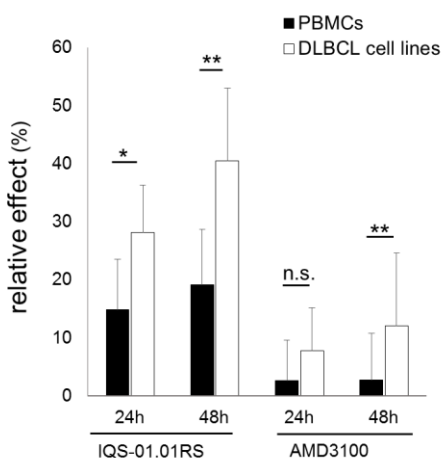


Figure 27.- IQS-01.01RS selectivity. Time-dependent mean effect of IQS-01.01RS (100 μ M) and AMD3100 (100 μ M) was compared between PBMCs from healthy donors (n=5) and DLBCL cell lines (n=13) determined by MTT assay.

4.2.5 IQS-01.01RS potently inhibits CXCR4 downstream signaling

We further proceeded to investigate the different capacity of IQS-01.01RS and AMD3100 to disrupt CXCR4 downstream signaling. For this aim, SUDHL6 and U2932 cells were starved and pretreated with IQS-01.01RS or AMD3100 for 1 hour. Post stimulation with CXCL12 for 1 minute, they were subjected to western blot analysis of different CXCR4 downstream effectors. As shown on [figure 28](#), IQS-01.01RS presented a superior capacity to inhibit CXCL12-induced phosphorylation of ERK1/2 and AKT at Thr202/Tyr204 and Ser473 residues, respectively. Of special interest, we observed that IQS-01.01RS treatment led to an efficient down-regulation of the potent proto-oncogene MYC known to have an important role in the pathogenesis of DLBCL (see introduction).

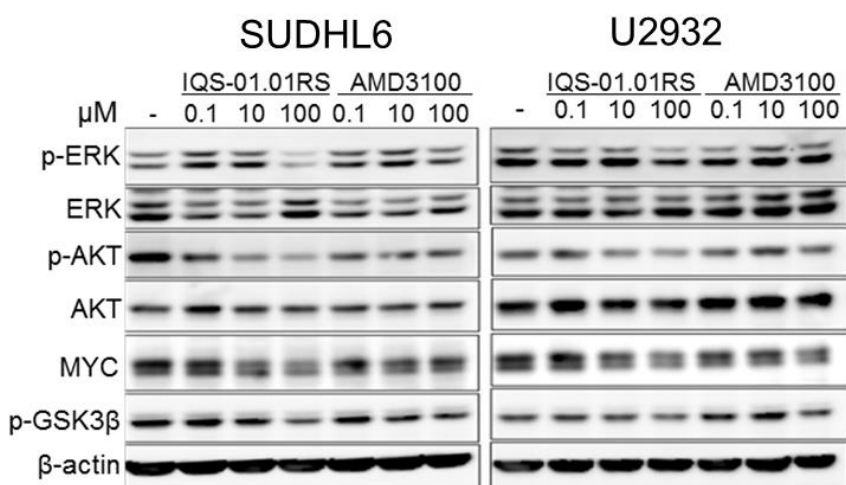


Figure 28.- Effect of IQS-01.01RS and AMD3100 on CXCR4 signaling. Western blot analysis of CXCR4 downstream signaling in SUDHL6 (GCB) and U2932 (ABC) cells upon 2 hour-starvation, followed by a 1 minute exposure to recombinant CXCL12, with or without 1 hour pretreatment with indicated doses of IQS-01.01RS or AMD3100. β-actin was used as a loading control.

ALTOGETHER, THESE RESULTS SHOW that the orally available CXCR4 inhibitor IQS-01.01RS inhibits *in vitro* CXCL12-induced chemotaxis and presents improved mobilizing properties *in vivo* compared to AMD3100. It also inhibits the proliferation of DLBCL cell lines independently of CXCR4 expression levels and shows pro-apoptotic activity in DLBCL patient samples. At a molecular level, IQS-01.01RS inhibits CXCR4 downstream signaling more efficiently than AMD3100 and is capable of reducing MYC protein levels. As the blockade of MYC oncogenic signature remains a challenge in DLBCL, this specific feature makes IQS-01.01RS a potent relevant agent for the treatment of MYC-overexpressing tumors.

4.3 IQS-01.01RS destabilizes MYC protein

4.3.1 CXCL12 mediates MYC upregulation

Following the above results, we observed that in the representative DLBCL cell line, SUDHL6, MYC protein levels were not only affected by CXCR4 inhibition, but also by CXCL12-mediated triggering of the receptor (Figure 30A). As this upregulation was observed after only 1 minute of CXCL12 stimulation, we discarded a transcriptional regulation of these phenomena, a hypothesis that was experimentally confirmed by the analysis of MYC mRNA levels by qPCR (Figure 29).

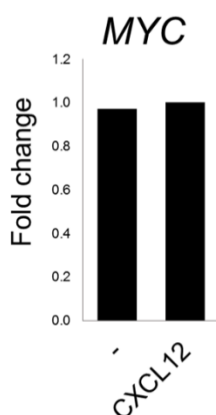


Figure 29.- Relative MYC transcript levels in SUDHL6 cells upon stimulation with CXCL12. β -ACTIN was used as a housekeeping gene.

4.3.2 IQS-01.01RS sustainably downregulates MYC

Together with MYC, p-ERK and p-AKT protein levels were upregulated as soon as 1 min after CXCL12-mediated activation of CXCR4 in cells previously starved (Figure 30A). This effect was maintained up to 30 minutes and over 3 hours following the stimulation (Figure 30A and data not shown). The addition of IQS-01.01RS almost completely abrogated basal and CXCL12-induced ERK1/2 and AKT phosphorylation. This was accompanied by the downregulation of MYC protein, which could be maintained for at least 3 hours (Figure 30A and data not shown). These results suggest that IQS-01.01RS offers a strong and sustained blockade of CXCR4 signaling, with the consequent downregulation of MYC.

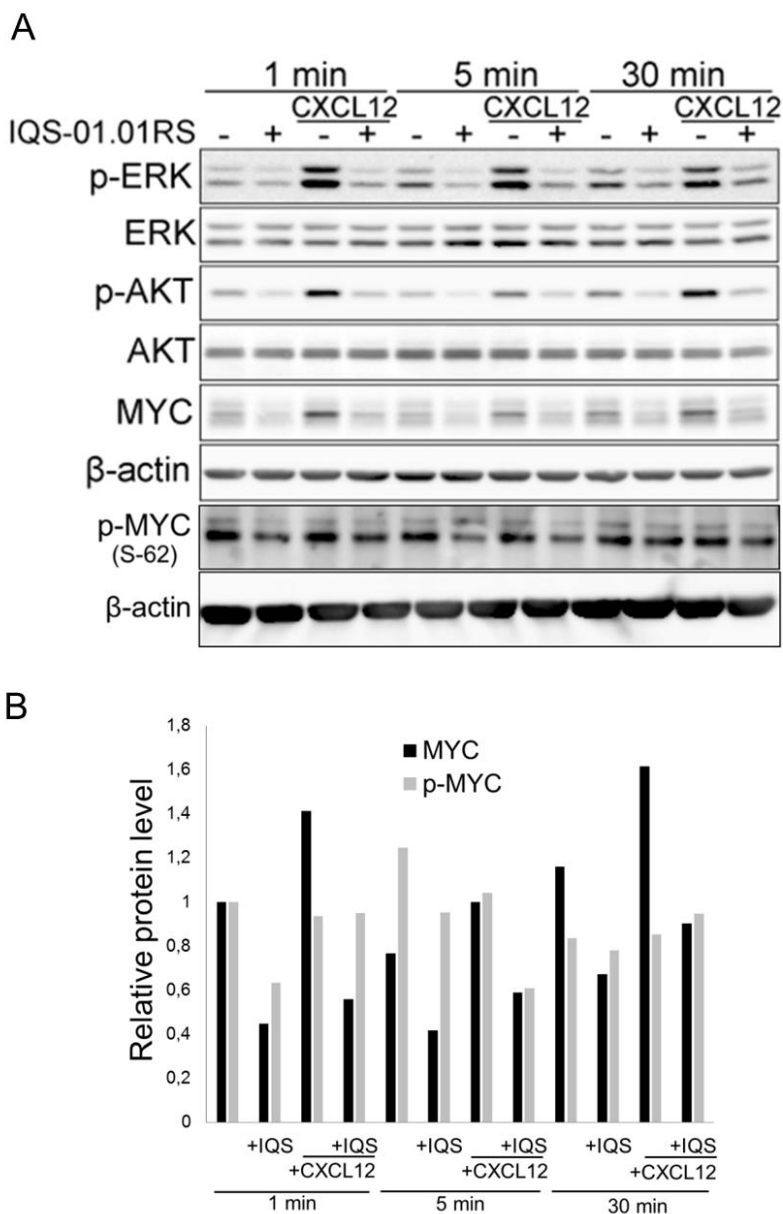


Figure 30.- Modulation of CXCR4 signaling. A) CXCR4 downstream signaling and MYC modulation in SUDHL6 cells at different time points, after a 2 hour starvation followed by receptor triggering in the presence or absence of 100 μ M IQS-01.01RS was used as a loading control. B) Quantification of MYC and p-MYC levels in A normalized to β -actin and relative to the 1 minute untreated basal condition.

Based on these observations, we further investigated the mechanism underlying the observed effect of IQS-01.01RS on MYC protein expression in DLBCL cells.

4.3.3 IQS-01.01RS destabilizes MYC protein via AKT

We first evaluated the possible existence in DLBCL cells of a CXCR4-ERK1/2-MYC positive feedback loop, as described by Hatano *et al.* in prostate cancer cells (Hatano *et al.*, 2013) (see section 1.7.2). To this end, we analyzed the ERK-dependent stabilizing phosphorylation of MYC at Ser62. No correlation was found between total MYC and p-MYC levels upon CXCR4 stimulation by CXCL12 or inhibition by IQS-01.01RS (Figure 30A and B). This suggested that, at least in our model, ERK1/2 was not involved in the control of MYC stability and that the destabilization of MYC by IQS-01.01RS must be linked to an alternative pathway. We then investigated a possible role for the AKT-GSK-3 β axis in MYC stabilization, by checking GSK-3 β phosphorylation levels at Ser9 residue. Supporting the hypothesis that the downregulation of MYC may be consequent to the inhibition of the CXCR4-AKT axis in IQS-01.01RS-treated cells, GSK-3 β phosphorylation levels correlated well with p-AKT and MYC protein levels in CXCR4-inhibited cells (Figure 28). To confirm that IQS-01.01RS was downregulating MYC at a post-translational level, we performed a MYC protein stability assay using the inhibitor of protein biosynthesis, cycloheximide (CHX). With this assay we confirmed that the half-life of MYC in DLBCL was between 5 and 30 minutes, according to published data (Gregory and Hann, 2000), and that IQS-01.01RS treatment accelerated the MYC degradation process (Figure 31). Accordingly, figure 34 confirmed that IQS-01.01RS did not affect MYC transcription.

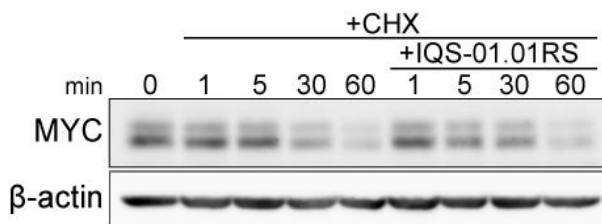


Figure 31.- MYC protein stability assay. Time-dependent determination of MYC protein levels in SUDHL6 cells treated with the translational blocker cycloheximide (CHX) as previously described (Moros *et al.*, 2014 b), in the presence or absence of 100 μ M IQS-01.01RS. β -actin was used as a loading control.

These results indicate that CXCR4 activation regulates MYC at a posttranslational level by modulation of an AKT-GSK-3 β -mediated degradation machinery in DLBCL cells, and that IQS-01.01RS efficiently disrupts this signaling axis.

4.4 IQS-01.01RS cooperates with BET bromodomain inhibition *in vitro*

Based on our observation that IQS-01.01RS had the capacity to downregulate MYC, we further investigated in our 13 DLBCL cell lines whether the compound could cooperate with the BET bromodomain antagonist, CPI203, the main effect of which relies on the disruption of MYC oncogenic signaling through repression of its transcription (see section 1.6.3 of the introduction).

4.4.1 CPI203 enhances IQS-01.01RS toxicity in DLBCL

To evaluate if CPI203 could enhance the anti-tumor activity of IQS-01.01RS, we analyzed the combination of different doses of each agent by MTT assay. The combination induced a 78% cytotoxicity at the optimal doses of 100 μ M IQS-01.01RS and 500 nM CPI203, with a mean CI of 0.67, indicative of a synergistic drug interaction in both GCB and ABC DLBCL cells (Figure 32 and Table 14). We noted that if the GCB and ABC subgroups were analyzed separately, even though the differences were not statistically significant, the first group presented a slightly more synergistic profile with a CI value of 0.59 ± 0.33 , whereas the ABC subgroup appeared slightly less synergistic with a CI value of 0.77 ± 0.1 .

While CPI203 and IQS-01.01RS alone failed to trigger apoptosis in these cell lines, the cell death rates observed upon exposure to the combination ranged from a 5% increase in U2932 cells to a 37% in SUDHL8 cells, when compared to the untreated control (Figure 32B).

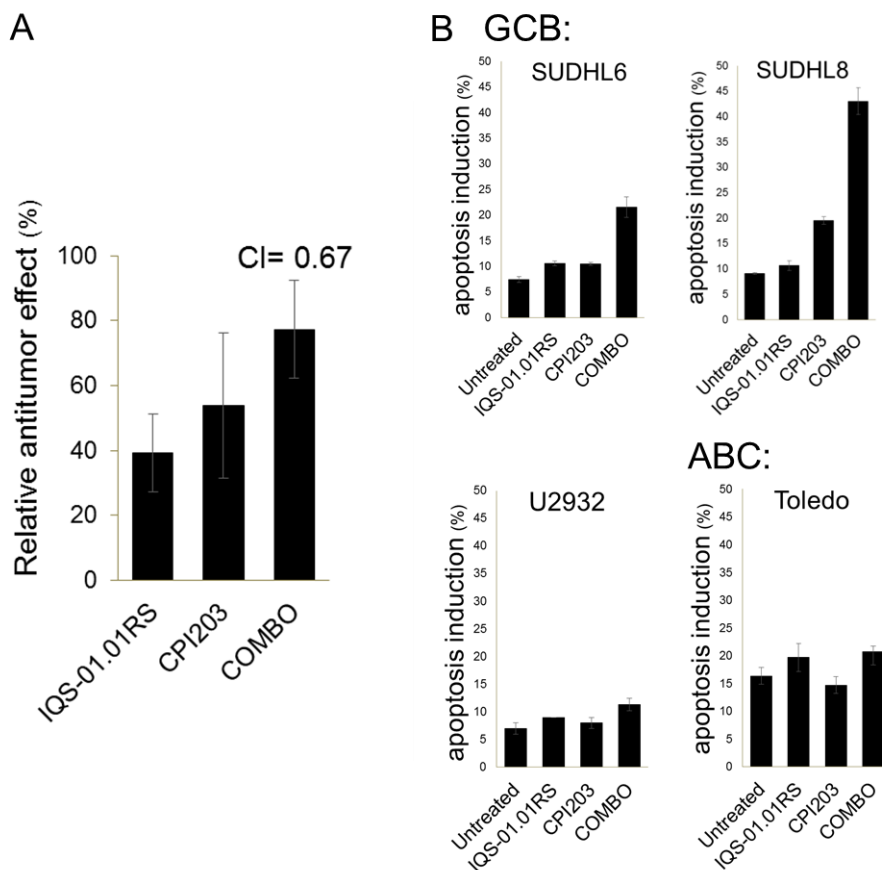


Figure 32.- Antitumor effect of the combination of IQS-01.01RS and CPI203 in DLBCL cell lines. A) Relative antitumor effect of IQS-01.01RS, CPI203, and the combination of both was determined by MTT assay, after 48 hours. Data shown are the mean results of the 13 DLBCL cell lines. B) Percentage of apoptosis induction by Annexin V staining and flow cytometer analysis in the indicated cell lines.

These results pointed out that the addition of CPI203 to IQS-01.01RS showed a promising synergistic activity in DLBCL, regardless the subtype.

4.4.2 IQS-01.01RS and CPI203 cooperate by reducing MYC protein expression

We then proceeded to analyze if the combination of IQS-01.01RS with CPI203 further reduced MYC protein levels. A dramatic downregulation in MYC protein expression was seen in cells treated with the combination when compared to untreated cells or cells exposed to single agents (Figure 33).

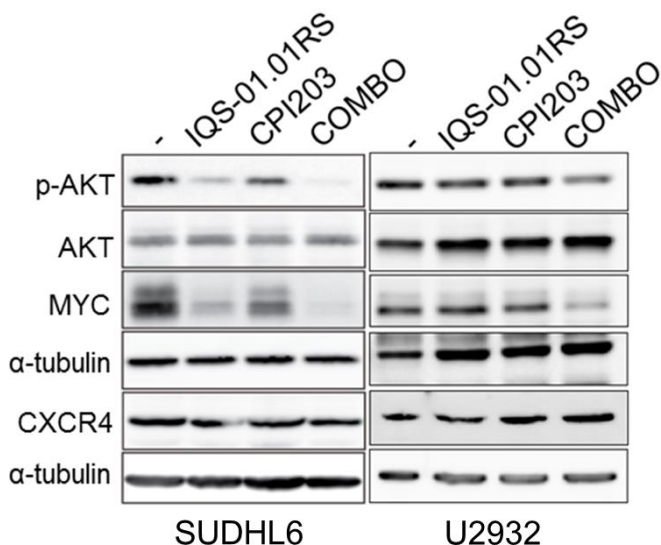


Figure 33.- Effects of the IQS-01.01RS and CPI203 combination on signaling. Cooperation between IQS-01.01RS and CPI203 in the inhibition of CXCR4 downstream signaling, as assessed by western blot analysis of p-AKT and MYC. SUDHL6 cells were treated for 6 hours with 100 μ M IQS-01.01RS and/or CPI203 (0.5 μ M) and starved for 2 hours, prior a 1 minute stimulation with 200 ng/ml of recombinant CXCL12. α -tubulin was used as a loading control.

As expected, **figure 34** shows that CPI203 treatment led to the transcriptional repression of *MYC*, strongly suggesting that the synergistic downregulation of *MYC* seen in cells exposed to the drug combination in **figure 35** is the consequence of a simultaneous CPI203-induced transcriptional repression of *MYC* and IQS-01.01RS-mediated *MYC* protein destabilization.

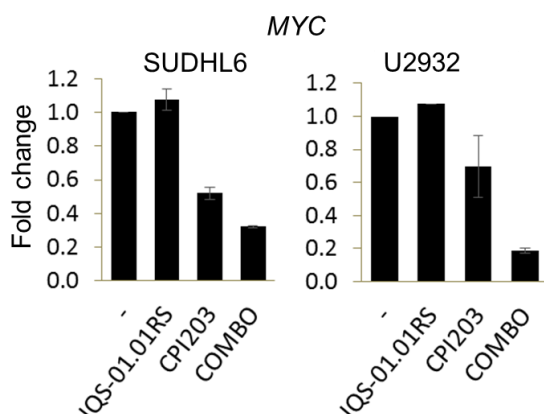


Figure 34.- Effect of the treatment on *MYC* transcription. Relative *MYC* transcript levels in SUDHL6 and U2932 cells upon a 6 hours treatment with 100 μ M IQS-01.01RS, 0.5 μ M CPI203 and the combination of both. Control untreated cells were used as a reference. β -ACTIN was used a housekeeping control.

4.4.3 CXCR4 levels are not affected by CPI203

Excluding that the synergistic effect of the combination was not consequent to a BRD4 inhibition-mediated alteration in CXCR4 expression as previously described in T lymphocytes following JQ1 treatment (Banerjee et al., 2012), **figure 33** shows that CPI203 addition did not alter CXCR4 protein levels either in the presence or absence of IQS-01.01RS. Flow cytometry analysis further confirmed that surface levels of CXCR4 were unmodified by BET bromodomain inhibition (**Figure 35A**). **Figure 35B** shows an increase in CXCR4 mRNA levels in SUDHL6 upon exposure to IQS-01.01RS, which was not observed in the presence of CPI203 or in U2932 cells.

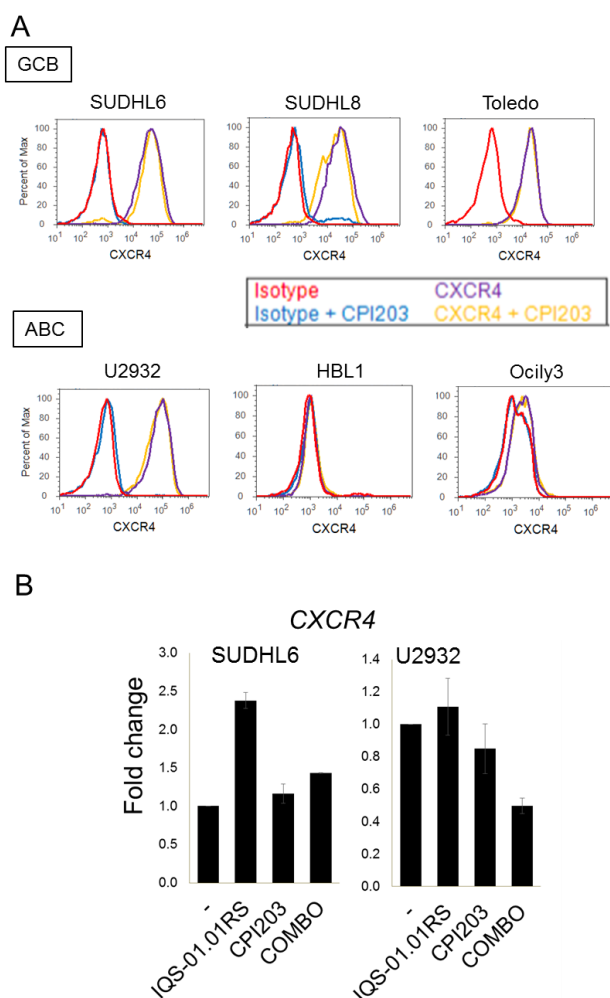


Figure 35.- Effect of CPI203 on CXCR4 levels. A) CXCR4 surface levels assessed by flow cytometry. **B)** Relative *CXCR4* transcript levels in SUDHL6 and U2932 cells upon a 6 hours treatment with 100 μ M IQS-01.01RS, 0.5 μ M CPI203, and the combination of both. Control untreated cells were used as a reference. β -*ACTIN* was used a housekeeping gene.

Considering these results altogether, we concluded that there were no significant changes in CXCR4 protein levels in DLBCL cells exposed to CPI203 and that the synergistic effect of the combination was due to the activity of the effect of both drugs towards MYC.

4.5 IQS-01.01RS cooperates with BET-bromodomain inhibition *in vivo*

To further assess the efficacy of the drug combination *in vivo*, NSG mice were subcutaneously injected with SUDHL6-GFP+/Luc+ cells and randomized into four groups receiving either 2 mg/kg IQS-01.01RS, 1.5 mg/kg CPI203, the combination of both agents, or the equivalent volume of vehicle for 13 days on a 5 on/2 off schedule.

4.5.1 IQS-01.01RS and CPI203 combination reduces tumor burden

Tumor burden was evaluated twice a week by external calipers and weekly by bioluminescence signal recording. At the final time point, tumors were extracted and weighted. [Figure 36A](#) shows that CPI203 and IQS-01.01RS single agents induced a 27% and 4% reduction in tumor growth, respectively, while the combination of both drugs induced a 38% decrease in tumor burden. Accordingly, a reduced luciferase activity as well as a significant (38%, $p=0.05$) decrease in tumor weight was detected in COMBO-receiving mice, when compared to the vehicle group ([Figure 36B and C](#)).

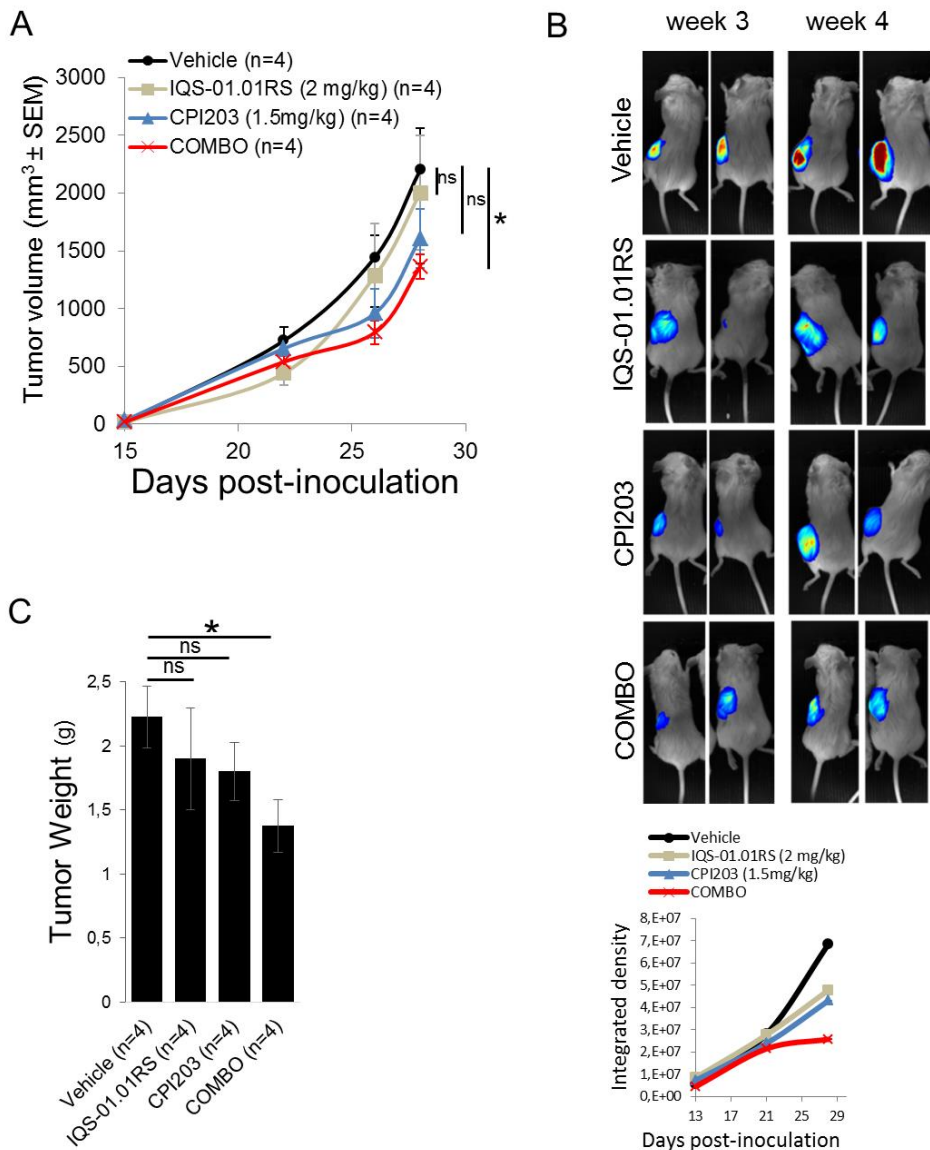


Figure 36.- IQS-01.01RS and CPI203 cooperate to reduce tumor growth in a subcutaneous mouse model of DLBCL. NSG mice were subcutaneously injected with SUDHL6-GFP+/Luc+ cells and tumor-bearing mice were randomly assigned to one of the following treatment arms: IQS-01.01RS 2 mg/kg daily (p.o.), CPI203 1.5 mg/kg (i.p.), both agents or equal volume of vehicle, for two weeks. n=4 mice per group. **A**) Tumor volume was evaluated twice a week using external calipers. **B**) Tumor burden was evaluated at week 3 and week 4 by analysis of the bioluminescence signal. Upper panel: color maps of 2 representative animals per group. Lower panel: quantification of Luc activity using the Image J software. **C**) Mean tumor weight in each treatment group at the final time point.

4.5.2 *In vivo* activity of IQS-01.01RS/CPI203 combination relies on CXCR4 downstream signaling blockade and subsequent triggering of apoptosis

To investigate the molecular events underlying the tumor reduction observed in COMBO-receiving mice, we performed a histological analysis by staining the corresponding tumors with the proliferation marker p-histone H3, the apoptotic activated caspase-3 (act. casp3), p-AKT and MYC. As shown in [figure 37](#), a decreased expression of p-histone H3 was seen in the tumors of the IQS-01.01RS, CPI203, and COMBO groups, highlighting an increased reduction of tumor mitotic index by the combination treatment, when compared to the single agent groups. In addition, IHC detection of activated-caspase-3 indicated an accumulation of apoptotic cells by the combination therapy, together with an enhanced reduction in MYC and p-AKT levels ([Figure 37](#)), in agreement with the *in vitro* results shown previously.

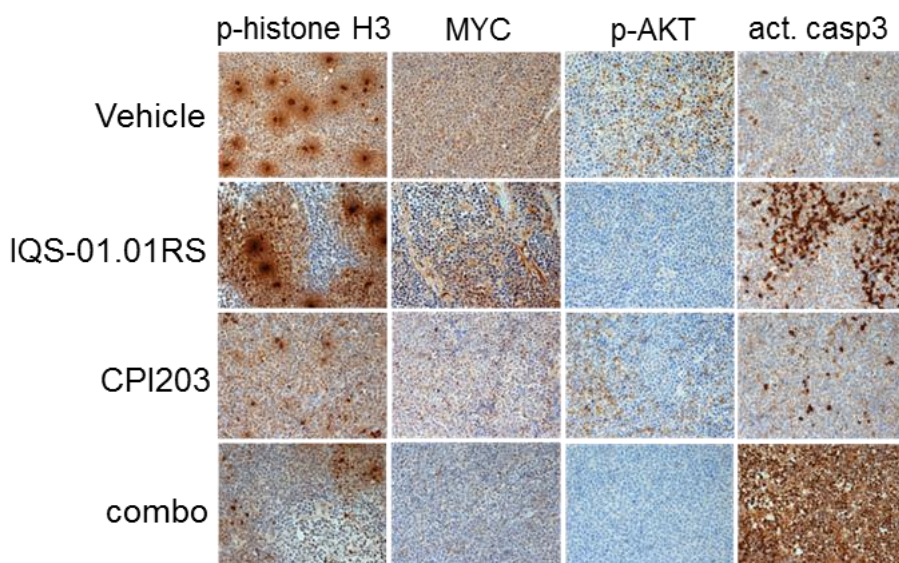


Figure 37.- Molecular effects underlying the combination of IQS-01.01RS and CPI203 in a subcutaneous model of DLBCL. Immunohistochemical labeling of p-histone H3, activated caspase-3 (act. casp3), MYC and p-AKT in consecutive tissue sections from four representative tumor specimens (magnification x200).

COLLECTIVELY, THESE RESULTS CONFIRMED our *in vitro* data, showing that the combination of IQS-01.01RS with the BET inhibitor CPI203 enhances the antitumor properties of each single agent, through to the blockade of CXCR4 signaling, followed by the abrogation of MYC expression and culminating in a synergistic proliferation blockade and sensitization to apoptosis.

5 Discussion

The rapid and important progress in the knowledge of the molecular and genetic factors responsible for cancer development and progression thanks to the advances in basic, preclinical and clinical research has provided clinicians with a broad range of new targeted therapies that has improved patient overall survival. However, long term survival in aggressive neoplasms still needs to be improved.

DLBCL is an aggressive neoplasm that represents the most common subtype of NHL. The establishment of immunochemotherapy as the standard of care in the early 2000s significantly improved the outcome of the disease, and at the present about two thirds of patients can be cured with R-CHOP. However, relapse is often observed and generally associated with dismal prognosis. Development of more effective strategies remains, therefore, an important objective (Pasqualucci, 2013).

Multiple GEP, functional, and clinical studies have translated to a better knowledge of the pathobiology of DLBCL and have served to improve its classification and stratification. For instance, these studies have enabled the classification of DLBCL, NOS into the subgroups GCB and ABC. In addition, the 2016 revision of the WHO classification considers the cases that carry simultaneous *MYC* and *BCL2* and/or *BCL6* aberrations as "High-grade B-cell lymphoma with *MYC* and *BCL2* and/or *BCL6* rearrangements" shortened as "double or triple hit" (DH or TH) as a new entity separated from DLBCL, NOS (Campo, 2017; Swerdlow et al., 2016). Yet, DLBCL, NOS still remains a heterogeneous disease with the same standard of care regardless its sub-classification and stratification. A better understanding of the molecular pathways involved in DLBCL pathogenesis should translate into the discovery of new pharmacological strategies and widen therapeutic options to improve patients outcome. This thesis has focused on investigating the relevance of targeting simultaneously the *MYC* oncogene, with a crucial role in DLBCL development and maintenance, and the chemokine receptor CXCR4, which is gaining an emerging role in cancer and DLBCL.

Although the CXCR4-CXCL12 axis has been recently proposed as an adverse prognostic marker in DLBCL (Chen et al., 2015; Lenz et al., 2008b; Moreno et al., 2015; Xu et al., 2017), its biological relevance remains underexplored. Additionally, as stated in the introduction, the FDA-approved CXCR4 inhibitor, AMD3100/Plerixafor presents serious limitations that could preclude its use as an anticancer drug (De Clercq, 2009). Thus, the lack of a CXCR4 inhibitor suitable to be administered as a standard regimen, together with the emerging role of CXCR4 in tumor pathogenesis, supports the development of a less toxic and more stable CXCR4-targeting agent.

The first part of this doctoral thesis aimed at shedding light into the effect of targeting the CXCR4-CXCL12 axis in DLBCL, and at the characterization of a new CXCR4 inhibitor, IQS-01.01. Our results show that the stereoisomer IQS-01.01RS is a potent CXCR4 inhibitor with the capacity to downregulate MYC. We have seen for the first time a connection between CXCR4, AKT, and MYC in DLBCL.

We have shown that the stereoisomer IQS-01.01RS presents a higher activity than IQS-01.01RR, IQS-01.01SS, or the racemate. We hypothesized that the position of the chiral carbons in the RS stereoisomer is responsible for reduced allosteric impediments as it provides this molecule with the most flexible structure. However, the fact that the separated stereoisomers present a higher cAMP release inhibitory profile than the racemic mixture is somewhat striking as one would expect the activity of each single stereoisomers to add up when administered together. Numerous stereo-selective drug-drug interactions have been reported (Fassihi, 1993) and the generation of non-covalent bonds between the stereoisomers of the racemate could be a plausible explanation for their activity loss.

Inhibition of CXCR4 has been recurrently suggested as an emerging sensitizer for anticancer therapies, as it favors the peripheral mobilization of malignant cells and increases their exposure to chemotherapy in different types of cancer (Calinescu et al., 2017; Rios et al., 2016). AMD3100 is used in the clinics for HSC mobilization and is under clinical trials for mobilization of tumor cells and consequent chemo-sensitization (see introduction). In our *in vivo* DLBCL systemic model however, 12 hours after the last administration, IQS-01.01RS, but not AMD3100, efficiently mobilized xenografted tumor cells into the blood current. This is in agreement with published data where mice treated with AMD3100 exhibited a peak of AML cell mobilization 3 hours after AMD3100 administration, with cell count returning to basal levels within 12 hours (Nervi et al., 2009). Our results indicate that IQS-01.01RS has a longer-term effect that might be due to its oral bioavailability and to a higher stability of the molecule. This evidences the short half-life of AMD3100 as one of its pharmacological drawbacks. It would be of interest to analyze tumor cell content in the blood at time points closer to drug administration to further compare the kinetics of both drugs.

Supporting the better pharmacology of IQS-01.01RS, it appears to be less toxic than AMD3100 in NSG mice. Previous data shows a higher toxicity of IQS-01.01RS compared to AMD3100 intravenously administrated to CD-1 mice (Ros-Blanco et al., 2012). Nonetheless, both drugs differ in administration routes. In the clinics, the administration route of AMD3100 is intraperitoneal (i.p), while IQS-01.01 was designed

to be orally available. Our data shows how at MTD, cell mobilization by AMD3100 is inferior to that of IQS-01.01RS. We can therefore conclude that at least in our model, AMD3100 presents a higher toxicity than IQS-01.01RS.

Moreno *et al.* claimed that pharmacological inhibition of CXCR4 by AMD3100 impairs the propagation of tumor B cells in a systemic mouse model of DLBCL (Moreno *et al.*, 2015). In our systemic model, we observed only a mild tendency of tumor load reduction in the brain and no differences in ovary tumor content upon treatment with either IQS-01.01RS or AMD3100. The variations in the models used might explain this difference. Moreno *et al.* pretreated the cells before inoculation and used a different cell line. In addition, we use NSG mice, characterized by a superior immune-suppression and better engraftment-promoting properties than the SCID mice used in their study.

Since its discovery in the 90s, CXCL12 is described as a potent chemo-attractant that induces cell migration towards a CXCL12 concentration gradient (Bleul *et al.*, 1996). The initial concept that the CXCL12-CXCR4 axis exclusively induced cell chemotaxis, leads to the belief that cells should remain static upon exposure to a CXCR4 inhibitor. This is in accordance with our *in vitro* results where CXCR4 inhibition reduces the trans-migration induced by CXCL12. However, since the first decade of the 2000s and the discovery of the secondary effect of AMD3100 toward HSC mobilization into the peripheral blood, it is widely accepted in the clinics, that inhibition of the CXCL12-CXCR4 axis, disrupts cells retention leading to cell mobilization into peripheral blood (Karpova *et al.*, 2017). This is in accordance with the results of our *in vivo* systemic model where IQS-01.01RS induces mobilization of tumor cells. Conceptually, these two apparent opposite effects of CXCR4 inhibition seem incoherent, but have a simple explanation. The effect of CXCR4 triggering by CXCL12 depends on the localization of the cells in relation to CXCL12, and so does the effect of inhibiting this signaling axis. Using a metal and a magnet as an analogy, CXCR4 expressing cells would represent a metal, and a CXCL12 secreting site a magnet. In the CXCL12-induced chemotaxis experiments performed *in vitro*, the metal (cells) is artificially positioned close enough the magnet (CXCL12) for it to exert an attraction force. It would be like starting the experiment with the metal inside the magnetic field and thus being instantly attracted to the magnet (CXCR4 expressing cells immediately migrate towards a CXCL12 gradient). Inhibiting CXCR4 would be like disrupting the magnetic field and stop cell migration. However, in the clinical context where AMD3100 is administered, the scenario differs. In this setting HSC are already attached to the CXCL12 secreting BM (the metal is attached to the magnet) and cells are retained in a static way. If the inhibition of the axis is forced in this setting, disruption of the "magnetic field" leads to detachment of the cells that are now vulnerable to being carried away (mobilized) into

the blood flow. These two effects of CXCR4 inhibition need to be clearly distinguished by the accurate use of the words **migration** and **mobilization**.

It seems logical that in the context of a tumor both settings co-occur. CXCR4 has been linked to metastasis in several cancer types (Zlotnik et al., 2011) and CXCR4 inhibition reduces engraftment of tumor cells in a systemic mouse model of DLBCL (Moreno et al., 2015). In fact, in this mouse model, like in ours, injected circulating cells home to the brain, the ovary, and the BM where they form detectable metastasis. Interestingly, all those metastatic sites have been reported to express high levels of CXCL12 (Zlotnik et al., 2011). Based on the bibliography and on our observations, the mechanism we propose for the colonization of these sites, that should be translational to human cases, is the following: Once cells are inoculated, they freely circulate through the blood torrent until, by chance, a single cell (or more than one) finds itself close enough to a CXCL12-secreting site or organ. This tumor cell (or cells) is then trapped by the CXCL12 "magnetic field", migrates towards the CXCL12 concentration gradient and gets retained there. If it encounters a favorable microenvironment, a metastatic tumor will be further formed. This attachment to a CXCL12 rich site with a favorable microenvironment is responsible for CAM-DR. Accordingly, the use of CXCR4 inhibition as an antitumor strategy should impair colonization of new organs and therefore metastasis as described by Moreno *et al* and others (Juarez et al., 2007; Moreno et al., 2015). Unexpectedly, as discussed earlier, we do not see a significant reduction of tumor cell engraftment upon inhibition of CXCR4 suggesting that, in our model, CXCR4 inhibition is not sufficient to impair engraftment and tissue colonization. This might be also due to the complexity of the metastatic mechanism which is regulated by many other pathways and molecules that could be replaceable (Gandalovičová et al., 2017). Retained tumor cells in a metastatic site, takes us to the second scenario where the cells are already attached to the magnet. In fact, inhibition of CXCR4 is currently being investigated in the clinics, mainly due to the subsequent mobilization of tumor cell. AMD3100 is under 5 clinical trials as an anticancer agent in different cancer types (see introduction, section 1.5.6.2), and is mainly used to mobilize the malignant cells that are located in a protective microenvironment or niche, with the aim to sensitize them to chemotherapy or other antitumor treatments. This approach is well established in different cancer models and may lead to promising results for CXCR4 inhibition as an anti-cancer therapy. Yet, it is unclear if CXCR4 inhibition would reduce metastasis in a clinical setting and clinical trials should include assessment of metastasis to elucidate this possible antitumor effect.

CXCR4 inhibition through IQS-01.01RS lead to a cytotoxic effect of 40% in tumor cells *in vitro*. Nevertheless, this toxic effect was not detected in our *in vivo*

systemic model as IQS-01.01RS treatment induced no significant differences in tumor load compared to mice treated with AMD3100 or the vehicle. It is worth pointing out that due to the type of animal model used in these experiments, the toxic effect of IQS-01.01RS could be underestimated. We use NSG immunodeficient mice and the toxic effect in a fully immunized organism could possibly be more notable as it should induce an inflammatory response that would collaborate in the removal of malignant cells (Dunn et al., 2004; Palucka and Coussens, 2016). Anyhow, our current data supports the direction that CXCR4 inhibitors are taking in the clinics, in combination with a more potent tumoricidal agent like Rituximab (Reinholdt et al., 2016).

While it has been previously published that levels of sCXCR4 correlate with CXCL12-induced migration in DLBCL cell lines both *in vitro* and *in vivo*, and in other tumors (Crazzolaro et al., 2001; Moreno et al., 2015), our findings in this regard are inconclusive. We have observed that basal *in vitro* migration of cells determined by transwell migration assays is variable, possibly because it may depend on several factors (not only CXCR4 expression level), that could mask this correlation. Nevertheless, the cytotoxic effect of IQS-01.01RS was consistently replicated in all the cell lines studied, and we were able to predict a lack of correlation between sCXCR4 levels and antiproliferative effect, illustrated by the fact that cells that express very low levels of CXCR4 harbored a high sensitivity to the compound. Upon its ligation by CXCL12, CXCR4 is internalized into the cytoplasm (Marchese, 2014), and in addition, nuclear CXCR4 has been reported and associated with poor prognosis in different cancer types (Masuda et al., 2014; Speetjens et al., 2009; Wang et al., 2009). Nevertheless the cytotoxic effect of the drug did not correlate with the levels of iCXCR4 in permeabilized DLBCL cells either. Globally, this lack of relationship between CXCR4 expression level and cell sensitivity to our compound, puts forward for consideration a possible off-target effect of this latest. However, this small inhibitor was designed to bind to a transmembrane receptor and, due to its chemical characteristics, it is plausible that it has not the capacity to cross the cell membrane, an observation which reduces the possible off-target molecules to transmembrane cell receptors. In addition, our and previous occupancy studies have confirmed that IQS-01.01 binds specifically to CXCR4, while it lacks affinity to other lymphoid receptors (Pettersson et al., 2008). Finally, beside cell chemotaxis, the CXCR4 pathway triggers different survival and proliferation signaling, making plausible that a CXCR4 inhibitor can exert a cytotoxic activity in malignant B cells. Several CXCR4 inhibitors have been reported to exert *in vitro* and *in vivo* antitumor activity (Abraham et al., 2017; Kim et al., 2010), supporting our belief that IQS-01.01RS cytotoxic effect is due to the specific inhibition of CXCR4. However, and given the relevance of the observed toxicity especially in the combinatorial part of this study, further studies of the

effect of genetic depletion of CXCR4 in cell viability are currently being performed in our laboratory.

AN INTERESTING INSIGHT gained from this study is the post-transcriptional modulation of MYC levels, through regulation of protein stability by the CXCR4-AKT axis in DLBCL cells. Our data show a CXCL12-mediated upregulation of MYC protein that can be counteracted *in vitro* by treatment with IQS-01.01RS, in both ABC- and GCB-DLBCL cell lines.

MYC is tightly regulated at a transcriptional, translational and post-translational level (Kress et al., 2015) and overexpression of this oncogene is associated with poorer survival in DLBCL patients (Karube and Campo, 2015; Nguyen et al., 2017; Valera et al., 2013). CXCR4 is also overexpressed in cancer and might contribute to the aberrant increment of MYC levels. In agreement with our results, MYC has been found to be stabilized by CXCR4 in prostate cancer cells via the pro-survival MAPK, ERK1/2 (Hatano et al., 2013) (see section 1.7.2 in the introduction). However, our data suggest that this loop is not active in our DLBCL model. It is well established that CXCR4 activates the PI3K/AKT pathway as well as ERK. Accordingly, in pancreatic cancer, CXCR4 promotes proliferation and invasion due to CXCL12-induced activating phosphorylation of ERK and AKT (Shen et al., 2010). As detailed in the introduction section 1.7, AKT may also stabilize MYC post-transcriptionally by inhibiting the GSK-3 β kinase that mediates MYC ubiquitination. AKT-mediated inhibitory phosphorylation of GSK-3 β at Ser9 is responsible for the increase of MYC protein stability. In an attempt to further investigate the molecular mechanisms by which CXCR4 contributes to human pancreatic cancer, Ma *et al.* confirmed that overexpression of CXCR4 promotes p-AKT expression and found, in addition, an overexpression of GSK-3 β (Ma et al., 2015).

GSK-3 β is a major regulator of protein stability with over a hundred substrates that are degraded in response to its phosphorylation. This kinase is active in most cells and regulated through decreasing its activity through phosphorylation by, for instance, p-AKT. MYC, NF- κ B and β -catenin proto-oncogenes, among others, are known to be destabilized by GSK-3 β (Robertson et al., 2017). As highlighted in several reviews focused on the functions of GSK-3 β (Mancinelli et al., 2017; Maurer et al., 2014; Patel and Woodgett, 2008), the role of this protein in cancer is controversial. As a deactivator of potent proto-oncogenes, such as MYC, its overexpression results in cell death and negative regulation of cell proliferation or self-renewal (Robertson et al., 2017). Conversely, it has been found to be overexpressed in some cancers (Ma et al., 2015) and GSK-3 inhibition induces apoptosis in different leukemia cell lines (Mirlashari et al.,

2012). GSK-3 inhibitors have been tested clinically for cancer treatment (NCT01632306) (NCT01287520) (NCT01214603), with no available results yet. Recent findings indicate that repression of GSK-3 restores NK cell cytotoxicity in AML patients through activation of NF- κ B, suggesting that the antitumor effect of GSK-3 inhibition may be due to the activation of the immune response against tumor cells and not to a direct tumoricidal effect (Guillerey et al., 2016; Parameswaran et al., 2016). In favor of an antitumor role of GSK-3 β in DLBCL, we have seen that AKT phosphorylation correlates well with GSK-3 β -pSer9 levels. In that sense, PI3K/AKT inhibition leads to a reduced inhibitory phosphorylation of GSK-3 β and consequent apoptosis induction (Uddin et al., 2006). Independently, activation of GSK-3 β through cMet/AKT inhibition induced apoptosis in DLBCL cell lines (Uddin et al., 2010). Accordingly, in our model, GSK-3 β activation consequent to IQS-01.01RS-mediated blockade of CXCR4/AKT signaling, leads to an antitumor effect mediated by the downregulation of, at least, MYC oncoprotein. As a broad regulator of protein stability, this effect of GSK-3 β on cell fate and behavior may be cell type-dependent. The reason why its overexpression in some cancers is related to a worst prognostic, and why its inhibition leads to apoptotic effects, is still to be clearly defined. Our results point out for the first time a possible relationship between CXCR4 signaling and AKT/GSK-3 β -dependent regulation of MYC protein stability in DLBCL, shedding some light in the misty role of GSK-3 β in cancer.

In this doctoral thesis, we focused our attention on the impact of this new axis on the stability of MYC. However, GSK-3 β also regulates the NF- κ B pathway, providing a new rationale towards the effectiveness of IQS-01.01RS in the ABC-DLBCL subtype, that should be further investigated.

Supporting the link between CXCR4 signaling and MYC protein levels in DLBCL, our results have shown how the first-in-class and FDA-approved CXCR4 inhibitor destabilized MYC protein, as IQS-01.01RS does, but to a lower extent. Accordingly, in osteosarcoma cells AMD3100 alone and in combination also induced MYC downregulation (Jiang et al., 2017), suggesting that the role of CXCR4 toward MYC stability levels may be extrapolated to other types of malignant neoplasm.

IN THE SECOND PART of this thesis, we have proposed the combination of CXCR4 and BET inhibition as a synergic therapeutic strategy to treat DLBCL.

MYC is an oncogene with a prominent role in the development of DLBCL as well as many other tumors. As previously commented, the total abrogation of MYC still remains a challenge. BET inhibition is one of the most successful strategies for MYC inhibition currently used in clinical settings (Whitfield et al., 2017). Responding to the

second aim of this thesis, our data show that ABC and GCB DLBCL cells are highly sensitive to the BET inhibitor CPI203 when used in monotherapy, and that the transcriptional downregulation of *MYC* achieved by this compound allows to an almost complete abrogation of *MYC* protein expression in cells exposed to the IQS-01.01RS/CPI203 combination. We attribute this rapid abrogation of *MYC* protein levels (after only 6 hours of treatment) to the simultaneous BET inhibition-mediated transcriptional and CXCR4 inhibition-mediated post-translational targeting of this oncogene. This dual approach underlies the synergistic interaction of the two compounds and consequent sensitization to apoptosis *in vitro* and *in vivo*.

Extensive research has been performed regarding *MYC* gene alterations in DLBCL, however limited information is available about the prognostic impact of *MYC* total protein levels in this disease. Valera *et al.* analyzed the clinical impact of *MYC* genetic alterations and protein expression. In agreement with other studies, the authors found that in a cohort of DLBCL patients, 7% presented *MYC* rearrangements, 2% amplifications, and 19% gains of *MYC* copy number. They also concluded that *MYC* translocations and amplifications, but not gains (less than four copies), conferred an unfavorable prognosis to DLBCL patients (Valera *et al.*, 2013). Additionally analysis of *MYC* expression by IHC revealed an overexpression of the protein in 50% of patients. According to other studies (Horn *et al.*, 2013; Tapia *et al.*, 2011), *MYC* protein overexpression correlated with *MYC* rearrangements. However, 20% of the cases that overexpressed *MYC* lacked any kind of *MYC* gene alteration, but yet presented a similar poor prognosis. Altogether, these results confirm the impact of *MYC* oncogene in DLBCL patients' survival and reinforce the fact that apart from genetically, *MYC* is also aberrantly regulated through other mechanisms in DLBCL. Of note, almost 20% of DLBCL cases with *MYC* rearrangement harbor an unchanged expression of the oncogene. These observations, together with our results, strengthen the immunohistochemical evaluation of *MYC* protein as a reliable strategy prior to the stratification of DLBCL patients in the clinics. Another aspect to take into account is that in the new WHO classification of aggressive mature B-cell lymphomas, those cases that carry simultaneous *MYC* and *BCL2* and/or *BCL6* aberrations are now excluded from DLBCL, NOS and are classified as DH or TH. In our study, we have included DH and TH cell lines (see Table 8), following the methodology of Valera *et al.*. Between 40 and 80% of the cases that present *MYC* rearrangements are accompanied by an additional rearrangement of *BCL2* or *BCL6* (Salaverria and Siebert, 2011). It would be of interest to 1) evaluate the impact of removing this cases from the study, 2) analyze whether the percentage of cases with *MYC* protein overexpression and no genetic aberrations would increment if DLBCL, NOS cases were studied separately, and 3) assess in these settings

whether the targeting of MYC protein would gain even more relevance in this type of lymphoma.

It is interesting to point out that the effect of IQS-01.01RS and CPI203 combination was independent of the translocational status of the cell line. For instance, OCI-Ly8, a TH cell line, and SUDHL8, a *MYC*-translocated cell line, responded poorly to IQS-01.01RS/CPI203 combination with a CI over the mean value. In contrast, Toledo, another *MYC*-translocated cell line, presented a CI below the mean value, indicating a high sensitivity of the cells to the combination. These results reinforce the idea that although genetic aberrations are relevant tumorigenic factors, the most relevant feature is the aberrant MYC protein expression and the many other, translocation-independent, factors involved in its regulation. All these observations provide a robust rationale for the dual MYC-targeting approach proposed herein, and suggest that more efforts should be made in the clinics to evaluate MYC protein expression, rather than *MYC* genetic deregulations.

BET inhibitors are known to regulate multiple other genes apart from *MYC* (Whitfield et al., 2017). For instance, JQ1 has been reported to reduce *CXCR4* levels (Banerjee et al., 2012). Our results show that *CXCR4* mRNA levels are not modified by treatment with CPI203. In contrast, an upregulation of the gene was observed in SUDHL6 upon exposure to IQS-01.01RS, a phenomenon which was counteracted in the presence of CPI203. Enhancement of *CXCR4* promoter activity by MYC has been previously reported (Hatano et al., 2013; Moriuchi et al., 1999) and could explain a process that is, however, cell line-specific, as it was not seen in U2932 cells. In any case, we concluded that there were no significant changes in *CXCR4* protein levels in DLBCL cells exposed to CPI203, confirming that the effect of the combination was due to the synergistic effect of both drugs towards MYC expression. BET inhibition may also downregulate the transcription of other oncogenic transcription factors such as NF- κ B, BCL6 and BCL2. In this thesis, we have focused on the effects of the combination over MYC.

Regarding *CXCR4*, there is controversy on the possible prognostic impact of its expression, as it may depend on the subgroup of DLBCL considered. Xu *et al.* reported that in a cohort of DLBCL patients, *CXCR4* expression correlated with high IPI score, high LDH levels and non-GCB subtype (Xu et al., 2017), whereas Chen *et al.* linked *CXCR4* expression with the progression of GCB-DLBCL patients (Chen et al., 2015). Independently, Moreno *et al.* found that the worst prognosis conferred by *CXCR4* expression was subtype-independent (Moreno et al., 2015). In the present work, we

observed that the response to both single agent CXCR4 inhibition, and CXCR4 inhibition in combination with BET inhibition was subtype-independent.

IN SUMMARY, IN THIS THESIS a new potent orally available CXCR4 inhibitor with antitumor properties has been described. Our work has uncovered a new CXCR4-AKT-GSK-3 β -MYC axis in DLBCL. In addition, this study offers the first rational basis for the potential clinical evaluation of a dual approach combining BET inhibition and CXCR4 blockade in DLBCL. Thus, this doctoral thesis has contributed to the knowledge on the relevance of the CXCL12-CXCR4 axis in DLBCL and pointed out a new therapeutic interest in disrupting this axis, due to its role in the post-transcriptional regulation of MYC. As presented along this discussion, we have encountered some questions that still remain open, warranting further research on this topic.

Of importance, this study has been possible thanks to previous knowledge, derived from both basic and clinical research, and resulted from a collaboration with the Molecular Engineering Group (GEM) at IQS School of Engineering whose members synthesized the CXCR4 inhibitor evaluated in this thesis. Cancer, including DLBCL, is a very complex and multifactorial disease, reflecting a malignancy driven by mutations and genomic instability. It is a side effect of evolution and a consequence of aging, and the hope of its eradication will remain a utopia. Pharmacological treatment is crucial to slow, block, or reverse progression of aggressive cancers and may even lead to complete remission in some cases. Anti-cancer drug development has experienced a great advance since the discovery of chemotherapy in the 40s of the XX century, thanks to the identification of new molecular targets that have led to the generation of new targeted therapies. These studies have also evidenced the complexity of the disease, and have illustrated the notion that joining efforts of multidisciplinary teams, with the aim to achieve a more complete understanding of cancer and to attack it through different perspectives should dictate the future of cancer research.

6 Conclusions

The main conclusions derived from this doctoral thesis are the following:

1. IQS-01.01 is a potent orally available CXCR4 inhibitor with antitumor properties in preclinical models of DLBCL.
 - 1.1. IQS-01.01RS is the most potent stereoisomer of the IQS-01.01 racemic mixture.
 - 1.2. IQS-01.01RS mimics some aspects of AMD3100, holds better pharmacological properties, and exerts a superior blockade of CXCR4 signaling, together with an improved antitumor activity.
 - 1.3. CXCR4 inhibition by means of IQS-01.01RS affects MYC at a post-translational level by decreasing the stability of the protein.

2. IQS-01.01RS and the BET-bromodomain inhibitor CPI203 cooperate in DLBCL.
 - 2.1. The combination reduces MYC expression through simultaneous CPI203-induced transcriptional repression of *MYC* and an IQS-01.01RS-mediated MYC protein destabilization. This culminates in a synergistic proliferation blockade and sensitization to apoptosis.
 - 2.2. *In vivo*, it enhances the effect of both compounds as single agents by triggering apoptosis through simultaneous inhibition of CXCR4 survival signaling and downregulation of MYC consequently reducing tumor burden of DLBCL mice xenografts.

As a general conclusion, that answers our broad aim, CXCR4 inhibition using IQS-01.01RS in combination with an antitumor agent like CPI203 is a promising novel therapeutic approach in DLBCL.

7 References

Abraham, M., Klein, S., Bulvik, B., Wald, H., Weiss, I., Olam, D., Weiss, L., Beider, K., Eizenberg, O., and Wald, O. (2017). The CXCR4 inhibitor BL-8040 induces the apoptosis of AML blasts by downregulating ERK, BCL-2, MCL-1 and cyclin-D1 via altered miR-15a/16-1 expression. *Leukemia* 31, 2336-2346.

Abbas, A.K., Lichtman, A.H., Pallei, S. (2010). *Cellular and Molecular Immunology* Sixth edition. Philadelphia (PA): Saunders Elsevier.

Adhikary, S., and Eilers, M. (2005). Transcriptional regulation and transformation by Myc proteins. *Nature reviews Molecular cell biology* 6, 635-645.

Alizadeh, A. A., Eisen, M. B., Davis, R. E., Ma, C., Lossos, I. S., Rosenwald, A., Boldrick, J. C., Sabet, H., Tran, T., and Yu, X. (2000). Distinct types of diffuse large B-cell lymphoma identified by gene expression profiling. *Nature* 403, 503-511.

Allen, C. D., Ansel, K. M., Low, C., Lesley, R., Tamamura, H., Fujii, N., and Cyster, J. G. (2004). Germinal center dark and light zone organization is mediated by CXCR4 and CXCR5. *Nature immunology* 5, 943-952.

Amaya-Chanaga, C. I., Jones, H., AlMahasnah, E. A., Choi, M. Y., Kuhne, M. R., Cohen, L., Sabbatini, P., Kipps, T. J., Cardarelli, P. M., and Castro, J. E. (2013). BMS-936564 (anti-CXCR4 antibody) induces specific leukemia cell mobilization and objective clinical responses in CLL patients treated under a phase I clinical trial. In, (Am Soc Hematology).

Anders, H.-J., Romagnani, P., and Mantovani, A. (2014). Pathomechanisms: homeostatic chemokines in health, tissue regeneration, and progressive diseases. *Trends in molecular medicine* 20, 154-165.

Annibali, D., Whitfield, J. R., Favuzzi, E., Jauset, T., Serrano, E., Cuartas, I., Redondo-Campos, S., Folch, G., González-Juncà, A., and Sodir, N. M. (2014). Myc inhibition is effective against glioma and reveals a role for Myc in proficient mitosis. *Nature communications* 5, 4632.

Balkwill, F. (2004). Cancer and the chemokine network. *Nature Reviews Cancer* 4, 540-550.

Banerjee, C., Archin, N., Michaels, D., Belkina, A. C., Denis, G. V., Bradner, J., Sebastiani, P., Margolis, D. M., and Montano, M. (2012). BET bromodomain inhibition as a novel strategy for reactivation of HIV - 1. *Journal of leukocyte biology* 92, 1147-1154.

Bannard, O., Horton, R. M., Allen, C. D., An, J., Nagasawa, T., and Cyster, J. G. (2013). Germinal center centroblasts transition to a centrocyte phenotype according to a timed program and depend on the dark zone for effective selection. *Immunity* 39, 912-924.

7-REFERENCES

Basso, K., and Dalla-Favera, R. (2012). Roles of BCL6 in normal and transformed germinal center B cells. *Immunological reviews* 247, 172-183.

Basso, K., and Dalla-Favera, R. (2015). Germinal centres and B cell lymphomagenesis. *Nature reviews Immunology* 15, 172-184.

Bea, S., Zettl, A., Wright, G., Salaverria, I., Jehn, P., Moreno, V., Burek, C., Ott, G., Puig, X., and Yang, L. (2005). Diffuse large B-cell lymphoma subgroups have distinct genetic profiles that influence tumor biology and improve gene-expression-based survival prediction. *Blood* 106, 3183-3190.

Béguelin, W., Popovic, R., Teater, M., Jiang, Y., Bunting, K. L., Rosen, M., Shen, H., Yang, S. N., Wang, L., and Ezponda, T. (2013). EZH2 is required for germinal center formation and somatic EZH2 mutations promote lymphoid transformation. *Cancer cell* 23, 677-692.

Berson, J. F., Long, D., Doranz, B. J., Rucker, J., Jirik, F. R., and Doms, R. W. (1996). A seven-transmembrane domain receptor involved in fusion and entry of T-cell-tropic human immunodeficiency virus type 1 strains. *Journal of virology* 70, 6288-6295.

Bleul, C. C., Fuhlbrigge, R. C., Casasnovas, J. M., Aiuti, A., and Springer, T. A. (1996). A highly efficacious lymphocyte chemoattractant, stromal cell-derived factor 1 (SDF-1). *The Journal of experimental medicine* 184, 1101-1109.

Boi, M., Gaudio, E., Bonetti, P., Kwee, I., Bernasconi, E., Tarantelli, C., Rinaldi, A., Testoni, M., Cascione, L., and Ponzoni, M. (2015). The BET bromodomain inhibitor OTX015 affects pathogenetic pathways in preclinical B-cell tumor models and synergizes with targeted drugs. *Clinical Cancer Research* 21, 1628-1638.

Borthakur, G., Dawson, M. A., Stein, E. M., Karadimitris, A., Huntly, B. J., Dickinson, M. J., Chaidos, A., Horner, T., Brennan, J., and Baron, J. (2016). A phase I/II open-label, dose escalation study to investigate the safety, pharmacokinetics, pharmacodynamics and clinical activity of GSK525762 in subjects with relapsed, refractory hematologic malignancies. In, (Am Soc Hematology).

Bosch, R., Dieguez-Gonzalez, R., Céspedes, M. V., Parreño, M., Pavón, M. Á., Grañena, A., Sierra, J., Mangues, R., and Casanova, I. (2011). A novel inhibitor of focal adhesion signaling induces caspase-independent cell death in diffuse large B-cell lymphoma. *Blood* 118, 4411-4420.

Brach, D., Johnston-Blackwell, D., Drew, A., Lingaraj, T., Motwani, V., Warholic, N. M., Feldman, I., Plescia, C., Smith, J. J., and Copeland, R. A. (2017). EZH2 inhibition by

tazemetostat results in altered dependency on B-cell activation signaling in DLBCL. *Molecular cancer therapeutics* 16, 2586-2597.

Brelot, A., Heveker, N., Montes, M., and Alizon, M. (2000). Identification of residues of CXCR4 critical for human immunodeficiency virus coreceptor and chemokine receptor activities. *Journal of Biological Chemistry* 275, 23736-23744.

Brown, J. R., Byrd, J. C., Coutre, S. E., Benson, D. M., Flinn, I. W., Wagner-Johnston, N. D., Spurgeon, S. E., Kahl, B. S., Bello, C., and Webb, H. K. (2014). Idelalisib, an inhibitor of phosphatidylinositol 3-kinase $\text{p110}\delta$, for relapsed/refractory chronic lymphocytic leukemia. *Blood* 123, 3390-3397.

Bueno, B. A., Martínez-Chamorro, C., Andrés, I. V., and Amor, A. A. (2011). Tratamiento del mieloma múltiple en recaída o refractario. *Cuadernos de Hematología*.

Burger, J. A., Burger, M., and Kipps, T. J. (1999). Chronic lymphocytic leukemia B cells express functional CXCR4 chemokine receptors that mediate spontaneous migration beneath bone marrow stromal cells. *Blood* 94, 3658-3667.

Burger, J. A., and Kipps, T. J. (2006). CXCR4: a key receptor in the crosstalk between tumor cells and their microenvironment. *Blood* 107, 1761-1767.

Busillo, J. M., and Benovic, J. L. (2007). Regulation of CXCR4 signaling. *Biochimica et Biophysica Acta (BBA)-Biomembranes* 1768, 952-963.

Calinescu, A.-A., Yadav, V. N., Carballo, E., Kadiyala, P., Tran, D., Zamler, D. B., Doherty, R., Srikanth, M., Lowenstein, P. R., and Castro, M. G. (2017). Survival and Proliferation of Neural Progenitor-Derived Glioblastomas Under Hypoxic Stress is Controlled by a CXCL12/CXCR4 Autocrine-Positive Feedback Mechanism. *Clinical Cancer Research* 23, 1250-1262.

Camicia, R., Winkler, H. C., and Hassa, P. O. (2015). Novel drug targets for personalized precision medicine in relapsed/refractory diffuse large B-cell lymphoma: a comprehensive review. *Molecular cancer* 14, 207.

Campo, E. (2017). Pathology and classification of aggressive mature B - cell lymphomas. *Hematological oncology* 35, 80-83.

Campo, E., Swerdlow, S. H., Harris, N. L., Pileri, S., Stein, H., and Jaffe, E. S. (2011). The 2008 WHO classification of lymphoid neoplasms and beyond: evolving concepts and practical applications. *Blood* 117, 5019-5032.

7-REFERENCES

Cardenas, M. G., Oswald, E., Yu, W., Xue, F., MacKerell, A. D., and Melnick, A. M. (2017). The expanding role of the BCL6 oncoprotein as a cancer therapeutic target. *Clinical Cancer Research* 23, 885-893.

Cardesa-Salzmann, T. M., Colomo, L., Gutierrez, G., Chan, W. C., Weisenburger, D., Climent, F., González-Barca, E., Mercadal, S., Arenillas, L., and Serrano, S. (2011). High microvessel density determines a poor outcome in patients with diffuse large B-cell lymphoma treated with rituximab plus chemotherapy. *Haematologica* 96, 996-1001.

Coiffier, B., Lepage, E., Brière, J., Herbrecht, R., Tilly, H., Bouabdallah, R., Morel, P., Van Den Neste, E., Salles, G., and Gaulard, P. (2002). CHOP chemotherapy plus rituximab compared with CHOP alone in elderly patients with diffuse large-B-cell lymphoma. *New England Journal of Medicine* 346, 235-242.

Coiffier, B., Thieblemont, C., Van Den Neste, E., Lepeu, G., Plantier, I., Castaigne, S., Lefort, S., Marit, G., Macro, M., and Sebban, C. (2010). Long-term outcome of patients in the LNH-98.5 trial, the first randomized study comparing rituximab-CHOP to standard CHOP chemotherapy in DLBCL patients: a study by the Groupe d'Etudes des Lymphomes de l'Adulte. *Blood* 116, 2040-2045.

Cojoc, M., Peitzsch, C., Trautmann, F., Polishchuk, L., Telegeev, G. D., and Dubrovskaya, A. (2013). Emerging targets in cancer management: role of the CXCL12/CXCR4 axis. *OncoTargets and therapy* 6, 1347.

Colomo, L., López-Guillermo, A., Perales, M., Rives, S., Martínez, A., Bosch, F., Colomer, D., Falini, B., Montserrat, E., and Campo, E. (2003). Clinical impact of the differentiation profile assessed by immunophenotyping in patients with diffuse large B-cell lymphoma. *Blood* 101, 78-84.

Colvin, M., Brundrett, R. B., Kan, M.-N. N., Jardine, I., and Fenselau, C. (1976). Alkylating properties of phosphoramidate mustard. *Cancer research* 36, 1121-1126.

Coutinho, R., Clear, A. J., Mazzola, E., Owen, A., Greaves, P., Wilson, A., Matthews, J., Lee, A., Alvarez, R., and da Silva, M. G. (2015). Revisiting the immune microenvironment of diffuse large B-cell lymphoma using a tissue microarray and immunohistochemistry: robust semi-automated analysis reveals CD3 and FoxP3 as potential predictors of response to R-CHOP. *Haematologica* 100, 363-369.

Crazzolara, R., Kreczy, A., Mann, G., Heitger, A., Eibl, G., Fink, F. M., Möhle, R., and Meister, B. (2001). High expression of the chemokine receptor CXCR4 predicts extramedullary organ infiltration in childhood acute lymphoblastic leukaemia. *British journal of haematology* 115, 545-553.

Cunningham, D., Hawkes, E. A., Jack, A., Qian, W., Smith, P., Mouncey, P., Pocock, C., Ardeschna, K. M., Radford, J. A., and McMillan, A. (2013). Rituximab plus cyclophosphamide, doxorubicin, vincristine, and prednisolone in patients with newly diagnosed diffuse large B-cell non-Hodgkin lymphoma: a phase 3 comparison of dose intensification with 14-day versus 21-day cycles. *The Lancet* *381*, 1817-1826.

Challa-Malladi, M., Lieu, Y. K., Califano, O., Holmes, A. B., Bhagat, G., Murty, V. V., Dominguez-Sola, D., Pasqualucci, L., and Dalla-Favera, R. (2011). Combined genetic inactivation of β 2-Microglobulin and CD58 reveals frequent escape from immune recognition in diffuse large B cell lymphoma. *Cancer cell* *20*, 728-740.

Chen, J., Xu-Monette, Z. Y., Deng, L., Shen, Q., Manyam, G. C., Martinez-Lopez, A., Zhang, L., Montes-Moreno, S., Visco, C., and Tzankov, A. (2015). Dysregulated CXCR4 expression promotes lymphoma cell survival and independently predicts disease progression in germinal center B-cell-like diffuse large B-cell lymphoma. *Oncotarget* *6*, 5597.

Choi, W. W., Weisenburger, D. D., Greiner, T. C., Piris, M. A., Banham, A. H., Delabie, J., Braziel, R. M., Geng, H., Iqbal, J., and Lenz, G. (2009). A new immunostain algorithm classifies diffuse large B-cell lymphoma into molecular subtypes with high accuracy. *Clinical Cancer Research* *15*, 5494-5502.

Dalla-Favera, R., Bregni, M., Erikson, J., Patterson, D., Gallo, R. C., and Croce, C. M. (1982). Human c-myc onc gene is located on the region of chromosome 8 that is translocated in Burkitt lymphoma cells. *Proceedings of the National Academy of Sciences* *79*, 7824-7827.

Dani, C., Blanchard, J., Piechaczyk, M., El Sabouty, S., Marty, L., and Jeanteur, P. (1984). Extreme instability of myc mRNA in normal and transformed human cells. *Proceedings of the National Academy of Sciences* *81*, 7046-7050.

Davis, R. E., Ngo, V. N., Lenz, G., Tolar, P., Young, R., Romesser, P. B., Kohlhammer, H., Lamy, L., Zhao, H., and Yang, Y. (2010). Chronic active B cell receptor signaling in diffuse large B cell lymphoma. *Nature* *463*, 88-92.

De Clercq, E. (2009). The AMD3100 story: the path to the discovery of a stem cell mobilizer (Mozobil). *Biochemical pharmacology* *77*, 1655-1664.

De Silva, N. S., and Klein, U. (2015). Dynamics of B cells in germinal centres. *Nature reviews Immunology* *15*, 137-148.

Deeks, E. D. (2016). Venetoclax: first global approval. *Drugs* *76*, 979-987.

7-REFERENCES

Delarue, R., Tilly, H., Mounier, N., Petrella, T., Salles, G., Thieblemont, C., Bologna, S., Ghesquières, H., Hacini, M., and Fruchart, C. (2013). Dose-dense rituximab-CHOP compared with standard rituximab-CHOP in elderly patients with diffuse large B-cell lymphoma (the LNH03-6B study): a randomised phase 3 trial. *The lancet oncology* *14*, 525-533.

Devaiah, B. N., Lewis, B. A., Cherman, N., Hewitt, M. C., Albrecht, B. K., Robey, P. G., Ozato, K., Sims, R. J., and Singer, D. S. (2012). BRD4 is an atypical kinase that phosphorylates serine2 of the RNA polymerase II carboxy-terminal domain. *Proceedings of the National Academy of Sciences* *109*, 6927-6932.

Díaz, T., Rodríguez, V., Lozano, E., Mena, M.-P., Calderón, M., Rosiñol, L., Martínez, A., Tovar, N., Pérez-Galán, P., and Bladé, J. (2017). The BET bromodomain inhibitor CPI203 improves lenalidomide and dexamethasone activity in in vitro and in vivo models of multiple myeloma by blockade of Ikaros and MYC signaling. *Haematologica* *102*, 1776-1784.

Discoverex SL. HitHunter® cAMP Assay Platform. From <https://www.discoverx.com/products-applications/camp-assays>.

Dreyling, M., Morschhauser, F., Bouabdallah, K., Bron, D., Cunningham, D., Assouline, S., Verhoef, G., Linton, K., Thieblemont, C., and Vitolo, U. (2017). Phase II study of copanlisib, a PI3K inhibitor, in relapsed or refractory, indolent or aggressive lymphoma. *Annals of Oncology* *28*, 2169-2178.

Duan, S., Cermak, L., Pagan, J. K., Rossi, M., Martinengo, C., di Celle, P. F., Chapuy, B., Shipp, M., Chiarle, R., and Pagano, M. (2012). FBXO11 targets BCL6 for degradation and is inactivated in diffuse large B-cell lymphomas. *Nature* *481*, 90-93.

Dunleavy, K., Pittaluga, S., Czuczman, M. S., Dave, S. S., Wright, G., Grant, N., Shovlin, M., Jaffe, E. S., Janik, J. E., and Staudt, L. M. (2009). Differential efficacy of bortezomib plus chemotherapy within molecular subtypes of diffuse large B-cell lymphoma. *Blood* *113*, 6069-6076.

Dunn, G. P., Old, L. J., and Schreiber, R. D. (2004). The three Es of cancer immunoeediting. *Annu Rev Immunol* *22*, 329-360.

Ember, S. W., Zhu, J.-Y., Olesen, S. H., Martin, M. P., Becker, A., Berndt, N., Georg, G. I., and Schönbrunn, E. (2014). Acetyl-lysine binding site of bromodomain-containing protein 4 (BRD4) interacts with diverse kinase inhibitors. *ACS chemical biology* *9*, 1160-1171.

Esteve-Arenys, A., Valero, J., Chamorro-Jorganes, A., Gonzalez, D., Rodriguez, V., Dlouhy, I., Salaverria, I., Campo, E., Colomer, D., and Martinez, A. (2018). The BET bromodomain inhibitor CPI203 overcomes resistance to ABT-199 (venetoclax) by downregulation of BFL-1/A1 in in vitro and in vivo models of MYC+/BCL2+ double hit lymphoma. *Oncogene* 37, 1830-1844.

European Medicines Agency (EMA). EU Clinical Trials Register. From: <https://www.clinicaltrialsregister.eu>.

European Medicines Agency (EMA). (2017). Mozobil. Summary of product characteristics. From: http://www.ema.europa.eu/ema/index.jsp?curl=pages/medicines/human/medicines/01030/human_med_000910.jsp&mid=WC0b01ac058001d124

Fassihi, A. (1993). Racemates and enantiomers in drug development. *International journal of pharmaceutics* 92, 1-14.

Feng, Y., Broder, C. C., Kennedy, P. E., and Berger, E. A. (1996). HIV-1 entry cofactor: functional cDNA cloning of a seven-transmembrane, G protein-coupled receptor. *Science Reports* 272, 872-877.

Filippakopoulos, P., and Knapp, S. (2014). Targeting bromodomains: epigenetic readers of lysine acetylation. *Nature reviews Drug discovery* 13, 337-356.

Filippakopoulos, P., Picaud, S., Mangos, M., Keates, T., Lambert, J.-P., Barsyte-Lovejoy, D., Felletar, I., Volkmer, R., Müller, S., and Pawson, T. (2012). Histone recognition and large-scale structural analysis of the human bromodomain family. *Cell* 149, 214-231.

Filippakopoulos, P., Qi, J., Picaud, S., Shen, Y., Smith, W. B., Fedorov, O., Morse, E. M., Keates, T., Hickman, T. T., and Felletar, I. (2010). Selective inhibition of BET bromodomains. *Nature* 468, 1067.

Fisher, R. I., Gaynor, E. R., Dahlborg, S., Oken, M. M., Grogan, T. M., Mize, E. M., Glick, J. H., Coltman Jr, C. A., and Miller, T. P. (1993). Comparison of a standard regimen (CHOP) with three intensive chemotherapy regimens for advanced non-Hodgkin's lymphoma. *New England Journal of Medicine* 328, 1002-1006.

French, C., Ramirez, C., Kolmakova, J., Hickman, T., Cameron, M., Thyne, M., Kutok, J., Toretsky, J., Tadavarthy, A., and Kees, U. (2008). BRD-NUT oncoproteins: a family of closely related nuclear proteins that block epithelial differentiation and maintain the growth of carcinoma cells. *Oncogene* 27, 2237.

7-REFERENCES

Gandalovičová, A., Rosel, D., Fernandes, M., Veselý, P., Heneberg, P., Čermák, V., Petruželka, L., Kumar, S., Sanz-Moreno, V., and Brábek, J. (2017). Migrastatics—anti-metastatic and anti-invasion drugs: promises and challenges. *Trends in cancer* 3, 391-406.

Garapaty-Rao, S., Nasveschuk, C., Gagnon, A., Chan, E. Y., Sandy, P., Busby, J., Balasubramanian, S., Campbell, R., Zhao, F., and Bergeron, L. (2013). Identification of EZH2 and EZH1 small molecule inhibitors with selective impact on diffuse large B cell lymphoma cell growth. *Chemistry & biology* 20, 1329-1339.

García, Y. R., Pabon-Martinez, Y. V., Smith, C. E., and Madder, A. (2017). Specific dsDNA recognition by a mimic of the DNA binding domain of the c-Myc/Max transcription factor. *Chemical Communications* 53, 6653-6656.

GLOBOCAN (2012) (IARC). Estimated Cancer Incidence, Mortality and Prevalence Worldwide in 2012. From <http://globocan.iarc.fr>.

Goy, A., Ramchandren, R., Ghosh, N., Munoz, J., Morgan, D. S., Dang, N. H., Knapp, M., Delioukina, M., Kingsley, E. C., and Tran, A. (2016). A Multicenter Open-Label, Phase 1b/2 Study of Ibrutinib in Combination with Lenalidomide and Rituximab in Patients with Relapsed or Refractory (R/R) Diffuse Large B-Cell Lymphoma (DLBCL). In, (Am Soc Hematology).

Grande, C. (2011). Actualización del tratamiento del linfoma difuso de células grandes B. Cuadernos de Hematología.

Greb, A., Bohlius, J., Schiefer, D., Schwarzer, G., Schulz, H., and Engert, A. (2008). High - dose chemotherapy with autologous stem cell transplantation in the first line treatment of aggressive Non - Hodgkin Lymphoma (NHL) in adults. *The Cochrane Library* 23.

Gregory, M. A., and Hann, S. R. (2000). c-Myc proteolysis by the ubiquitin-proteasome pathway: stabilization of c-Myc in Burkitt's lymphoma cells. *Molecular and cellular biology* 20, 2423-2435.

Guillerey, C., Huntington, N. D., and Smyth, M. J. (2016). Targeting natural killer cells in cancer immunotherapy. *Nature immunology* 17, 1025-1036.

Gutiérrez-García, G., Cardesa-Salzmán, T., Climent, F., González-Barca, E., Mercadal, S., Mate, J. L., Sancho, J. M., Arenillas, L., Serrano, S., and Escoda, L. (2011). Gene-expression profiling and not immunophenotypic algorithms predicts prognosis in patients with diffuse large B-cell lymphoma treated with immunochemotherapy. *Blood* 117, 4836-4843.

Habermann, T. M., Weller, E. A., Morrison, V. A., Gascoyne, R. D., Cassileth, P. A., Cohn, J. B., Dakhil, S. R., Woda, B., Fisher, R. I., and Peterson, B. A. (2006). Rituximab-CHOP versus CHOP alone or with maintenance rituximab in older patients with diffuse large B-cell lymphoma. *Journal of Clinical Oncology* *24*, 3121-3127.

Hann, S. R. (2006). Role of post-translational modifications in regulating c-Myc proteolysis, transcriptional activity and biological function. *Seminars in cancer biology* (Elsevier) *16*, 288-302.

Hans, C. P., Weisenburger, D. D., Greiner, T. C., Gascoyne, R. D., Delabie, J., Ott, G., Müller-Hermelink, H. K., Campo, E., Braziel, R. M., and Jaffe, E. S. (2004). Confirmation of the molecular classification of diffuse large B-cell lymphoma by immunohistochemistry using a tissue microarray. *Blood* *103*, 275-282.

Hatano, K., Yamaguchi, S., Nimura, K., Murakami, K., Nagahara, A., Fujita, K., Uemura, M., Nakai, Y., Tsuchiya, M., and Nakayama, M. (2013). Residual prostate cancer cells after docetaxel therapy increase the tumorigenic potential via constitutive signaling of CXCR4, ERK1/2 and c-Myc. *Molecular cancer research* *11*, 1088-1100.

Hayward, W. S., Neel, B. G., and Astrin, S. M. (1981). Activation of a cellular onc gene by promoter insertion in ALV-induced lymphoid leukosis. *Nature* *290*, 475-480.

Hendrix, C. W., Collier, A. C., Lederman, M. M., Schols, D., Pollard, R. B., Brown, S., Jackson, J. B., Coombs, R. W., Glesby, M. J., and Flexner, C. W. (2004). Safety, pharmacokinetics, and antiviral activity of AMD3100, a selective CXCR4 receptor inhibitor, in HIV-1 infection. *JAIDS Journal of Acquired Immune Deficiency Syndromes* *37*, 1253-1262.

Hendrix, C. W., Flexner, C., MacFarland, R. T., Giandomenico, C., Fuchs, E. J., Redpath, E., Bridger, G., and Henson, G. W. (2000). Pharmacokinetics and safety of AMD-3100, a novel antagonist of the CXCR-4 chemokine receptor, in human volunteers. *Antimicrobial agents and chemotherapy* *44*, 1667-1673.

Hennessy, B. T., Hanrahan, E. O., and Daly, P. A. (2004). Non-Hodgkin lymphoma: an update. *The lancet oncology* *5*, 341-353.

Hernandez - Ilizaliturri, F. J., Deeb, G., Zinzani, P. L., Pileri, S. A., Malik, F., Macon, W. R., Goy, A., Witzig, T. E., and Czuczman, M. S. (2011). Higher response to lenalidomide in relapsed/refractory diffuse large B - cell lymphoma in nongerminal center B - cell-like than in germinal center B - cell-like phenotype. *Cancer* *117*, 5058-5066.

7-REFERENCES

Herrick, D., and Ross, J. (1994). The half-life of c-myc mRNA in growing and serum-stimulated cells: influence of the coding and 3'untranslated regions and role of ribosome translocation. *Molecular and cellular biology* *14*, 2119-2128.

Horn, H., Ziepert, M., Becher, C., Barth, T. F., Bernd, H.-W., Feller, A. C., Klapper, W., Hummel, M., Stein, H., and Hansmann, M.-L. (2013). MYC status in concert with BCL2 and BCL6 expression predicts outcome in diffuse large B-cell lymphoma. *Blood* *121*, 2253-2263.

Jiang, C., Fang, X., Zhang, H., Wang, X., Li, M., Jiang, W., Tian, F., Zhu, L., and Bian, Z. (2017). AMD3100 combined with triptolide inhibit proliferation, invasion and metastasis and induce apoptosis of human U2OS osteosarcoma cells. *Biomedicine & Pharmacotherapy* *86*, 677-685.

Jóźwiak, P., Forma, E., Bryś, M., and Krześlak, A. (2014). O-GlcNAcylation and metabolic reprogramming in cancer. *Frontiers in endocrinology* *5*, 145.

Juarez, J., Pena, A. D., Baraz, R., Hewson, J., Khoo, M., Cisterne, A., Fricker, S., Fujii, N., Bradstock, K., and Bendall, L. (2007). CXCR4 antagonists mobilize childhood acute lymphoblastic leukemia cells into the peripheral blood and inhibit engraftment. *Leukemia* *21*, 1249-1257.

Kahl, B. S., Spurgeon, S. E., Furman, R. R., Flinn, I. W., Coutre, S. E., Brown, J. R., Benson, D. M., Byrd, J. C., Peterman, S., and Cho, Y. (2014). A phase 1 study of the PI3K δ inhibitor idelalisib in patients with relapsed/refractory mantle cell lymphoma (MCL). *Blood* *123*, 3398-3405.

Karpova, D., Ritchey, J. K., Holt, M. S., Abou-Ezzi, G., Monlish, D., Batoon, L., Millard, S., Spohn, G., Wiercinska, E., and Chendamarai, E. (2017). Continuous blockade of CXCR4 results in dramatic mobilization and expansion of hematopoietic stem and progenitor cells. *Blood* *129*, 2939-2949.

Karube, K., and Campo, E. (2015). MYC alterations in Diffuse Large B-cell Lymphomas. Paper presented at: *Seminars in hematology* *52*, 97-106.

Kawano, Y., Kobune, M., Yamaguchi, M., Nakamura, K., Ito, Y., Sasaki, K., Takahashi, S., Nakamura, T., Chiba, H., and Sato, T. (2003). Ex vivo expansion of human umbilical cord hematopoietic progenitor cells using a coculture system with human telomerase catalytic subunit (hTERT)-transfected human stromal cells. *Blood* *101*, 532-540.

Kim, J. M., Lee, Y.-h., Ku, C. R., and Lee, E. J. (2010). The cyclic pentapeptide d-Arg3FC131, a CXCR4 antagonist, induces apoptosis of somatotrope tumor and inhibits tumor growth in nude mice. *Endocrinology* *152*, 536-544.

Kipshidze, N., Iversen, P., Overlie, P., Dunlap, T., Titus, B., Lee, D., Moses, J., O'Hanley, P., Lauer, M., and Leon, M. B. (2007). First human experience with local delivery of novel antisense AVI-4126 with Infiltrator catheter in de novo native and restenotic coronary arteries: 6-month clinical and angiographic follow-up from AVAIL study. *Cardiovascular Revascularization Medicine* 8, 230-235.

Klein, U., and Dalla-Favera, R. (2008). Germinal centres: role in B-cell physiology and malignancy. *Nature reviews Immunology* 8, 22-33.

Kress, T. R., Sabò, A., and Amati, B. (2015). MYC: connecting selective transcriptional control to global RNA production. *Nature Reviews Cancer* 15, 593-607.

Kubuschok, B., Held, G., and Pfreundschuh, M. (2015). Management of diffuse large B-cell lymphoma (DLBCL). *Cancer Treatment Research* 165, 271-288.

Kuhne, M. R., Mulvey, T., Chen, S., Pan, C., Chong, C., Niekro, W., Kempe, T., Henning, K. A., Cohen, L., and Korman, A. (2011). BMS-936564/MDX-1338: a fully human anti-cxcr4 antibody induces apoptosis in vitro and shows anti tumor activity in vivo. In, (Am Soc Hematology).

Kumar, K., Raza, S. S., Knab, L. M., Chow, C. R., Kwok, B., Bentrem, D. J., Popovic, R., Ebine, K., Licht, J. D., and Munshi, H. G. (2015). GLI2-dependent c-MYC upregulation mediates resistance of pancreatic cancer cells to the BET bromodomain inhibitor JQ1. *Scientific reports* 5, 9489.

Küppers, R. (2005). Mechanisms of B-cell lymphoma pathogenesis. *Nature Reviews Cancer* 5, 251-262.

Lampson, B. L., and Brown, J. R. (2017). PI3K δ -selective and PI3K α/δ -combinatorial inhibitors in clinical development for B-cell non-Hodgkin lymphoma. *Expert opinion on investigational drugs* 26, 1267-1279.

Lamy, T., Damaj, G., Soubeyran, P., Gyan, E., Cartron, G., Bouabdallah, K., Gressin, R., Cornillon, J., Banos, A., and Le Du, K. (2017). R-CHOP 14 with or without radiotherapy in non-bulky limited-stage diffuse large B-cell lymphoma (DLBCL). *Blood*, blood-2017-2007-793984.

Lenz, G., Davis, R. E., Ngo, V. N., Lam, L., George, T. C., Wright, G. W., Dave, S. S., Zhao, H., Xu, W., and Rosenwald, A. (2008a). Oncogenic CARD11 mutations in human diffuse large B cell lymphoma. *Science* 319, 1676-1679.

7-REFERENCES

Lenz, G., Wright, G., Dave, S., Xiao, W., Powell, J., Zhao, H., Xu, W., Tan, B., Goldschmidt, N., and Iqbal, J. (2008b). Stromal gene signatures in large-B-cell lymphomas. *New England Journal of Medicine* 359, 2313-2323.

Liles, W. C., Broxmeyer, H. E., Rodger, E., Wood, B., Hübel, K., Cooper, S., Hangoc, G., Bridger, G. J., Henson, G. W., and Calandra, G. (2003). Mobilization of hematopoietic progenitor cells in healthy volunteers by AMD3100, a CXCR4 antagonist. *Blood* 102, 2728-2730.

Liles, W. C., Rodger, E., Broxmeyer, H. E., Dehner, C., Badel, K., Calandra, G., Christensen, J., Wood, B., Price, T. H., and Dale, D. C. (2005). Augmented mobilization and collection of CD34+ hematopoietic cells from normal human volunteers stimulated with granulocyte-colony-stimulating factor by single-dose administration of AMD3100, a CXCR4 antagonist. *Transfusion* 45, 295-300.

Liu, S.-H., Gu, Y., Pascual, B., Yan, Z., Hallin, M., Zhang, C., Fan, C., Wang, W., Lam, J., and Spilker, M. E. (2017). A novel CXCR4 antagonist IgG1 antibody (PF-06747143) for the treatment of hematologic malignancies. *Blood advances* 1, 1088-1100.

Lunning, M., Vose, J., Bierman, P., Bociek, G., Schreeder, M., Siddiqi, T., Blumel, S., Cutter, K., Pauli, E., and Bui, D. (2017). Combination of TGR-1202, Ublituximab, and Bendamustine is Safe and Highly Active in Patients with Advanced DLBCL and Follicular Lymphoma. *Hematological Oncology* 35, 266-267.

Ma, S., Li, Q., and Pan, F. (2015). CXCR4 promotes GSK3 β expression in pancreatic cancer cells via the Akt pathway. *International journal of clinical oncology* 20, 525-530.

Maloney, D. G., Grillo-López, A. J., White, C. A., Bodkin, D., Schilder, R. J., Neidhart, J. A., Janakiraman, N., Foon, K. A., Liles, T.-M., and Dallaire, B. K. (1997). IDEC-C2B8 (Rituximab) Anti-CD20 Monoclonal Antibody Therapy in Patients With Relapsed Low-Grade Non-Hodgkin's Lymphoma. *Blood* 90, 2188-2195.

Mancinelli, R., Carpino, G., Petrunaro, S., Mammola, C. L., Tomaipitnca, L., Filippini, A., Facchiano, A., Ziparo, E., and Giampietri, C. (2017). Multifaceted Roles of GSK-3 in Cancer and Autophagy-Related Diseases. *Oxidative Medicine and Cellular Longevity* 2017.

Marchese, A. (2014). Endocytic trafficking of chemokine receptors. *Current opinion in cell biology* 27, 72-77.

Masuda, T., Nakashima, Y., Ando, K., Yoshinaga, K., Saeki, H., Oki, E., Morita, M., Oda, Y., and Maehara, Y. (2014). Nuclear expression of chemokine receptor CXCR4 indicates poorer prognosis in gastric cancer. *Anticancer research* 34, 6397-6403.

Maurer, U., Preiss, F., Brauns-Schubert, P., Schlicher, L., and Charvet, C. (2014). GSK-3— at the crossroads of cell death and survival. *J Cell Sci* 127, 1369-1378.

McCabe, M. T., Graves, A. P., Ganji, G., Diaz, E., Halsey, W. S., Jiang, Y., Smitheman, K. N., Ott, H. M., Pappalardi, M. B., and Allen, K. E. (2012a). Mutation of A677 in histone methyltransferase EZH2 in human B-cell lymphoma promotes hypertrimethylation of histone H3 on lysine 27 (H3K27). *Proceedings of the National Academy of Sciences* 109, 2989-2994.

McCabe, M. T., Ott, H. M., Ganji, G., Korenchuk, S., Thompson, C., Van Aller, G. S., Liu, Y., Graves, A. P., Diaz, E., and LaFrance, L. V. (2012b). EZH2 inhibition as a therapeutic strategy for lymphoma with EZH2-activating mutations. *Nature* 492, 108.

Meyer, P. N., Fu, K., Greiner, T. C., Smith, L. M., Delabie, J., Gascoyne, R. D., Ott, G., Rosenwald, A., Braziel, R. M., and Campo, E. (2010). Immunohistochemical methods for predicting cell of origin and survival in patients with diffuse large B-cell lymphoma treated with rituximab. *Journal of clinical oncology* 29, 200-207.

Miller, T. P., Dahlberg, S., Cassady, J. R., Adelstein, D. J., Spier, C. M., Grogan, T. M., LeBlanc, M., Carlin, S., Chase, E., and Fisher, R. I. (1998). Chemotherapy alone compared with chemotherapy plus radiotherapy for localized intermediate-and high-grade non-Hodgkin's lymphoma. *New England Journal of Medicine* 339, 21-26.

Mirlashari, M. R., Randen, I., and Kjeldsen-Kragh, J. (2012). Glycogen synthase kinase-3 (GSK-3) inhibition induces apoptosis in leukemic cells through mitochondria-dependent pathway. *Leukemia research* 36, 499-508.

Miyazaki, K. (2016). Treatment of diffuse large B-cell lymphoma. *Journal of Clinical and Experimental Hematopathology* 56, 79-88.

Monti, S., Savage, K. J., Kutok, J. L., Feuerhake, F., Kurtin, P., Mihm, M., Wu, B., Pasqualucci, L., Neuberg, D., and Aguiar, R. C. (2005). Molecular profiling of diffuse large B-cell lymphoma identifies robust subtypes including one characterized by host inflammatory response. *Blood* 105, 1851-1861.

Moreno, A., Colon-Otero, G., and Solberg, L. A. (2000). The prednisone dosage in the CHOP chemotherapy regimen for non-Hodgkin's lymphomas (NHL): is there a standard? *The oncologist* 5, 238-249.

Moreno, M. J., Bosch, R., Dieguez - Gonzalez, R., Novelli, S., Mozos, A., Gallardo, A., Pavón, M. Á., Céspedes, M. V., Grañena, A., and Alcoceba, M. (2015). CXCR4 expression enhances diffuse large B cell lymphoma dissemination and decreases patient survival. *The Journal of pathology* 235, 445-455.

7-REFERENCES

Moriuchi, M., Moriuchi, H., Margolis, D. M., and Fauci, A. S. (1999). USF/c-Myc enhances, while Yin-Yang 1 suppresses, the promoter activity of CXCR4, a coreceptor for HIV-1 entry. *The Journal of Immunology* *162*, 5986-5992.

Moros, A., Rodriguez, V., Saborit-Villarroya, I., Montraveta, A., Balsas, P., Sandy, P., Martinez, A., Wiestner, A., Normant, E., and Campo, E., Pérez-Galán, P., Colomer, D., Roué, G. (2014a). Synergistic antitumor activity of lenalidomide with the BET bromodomain inhibitor CPI203 in bortezomib-resistant mantle cell lymphoma. *Leukemia* *28*, 2049-2059.

Moros, A., Bustany, S., Cahu, J., Saborit-Villarroya, I., Martínez, A., Colomer, D., Sola, B., and Roué, G. (2014b). Antitumoral activity of lenalidomide in in vitro and in vivo models of mantle cell lymphoma involves the destabilization of cyclin D1/p27KIP1 complexes. *Clinical Cancer Research* *20*, 393-403.

Muris, J., Meijer, C., Vos, W., van Krieken, J., Jiwa, N., Ossenkoppele, G., and Oudejans, J. (2006). Immunohistochemical profiling based on Bcl - 2, CD10 and MUM1 expression improves risk stratification in patients with primary nodal diffuse large B cell lymphoma. *The Journal of pathology* *208*, 714-723.

Nagasawa, T., Hirota, S., Tachibana, K., Takakura, N., Nishikawa, S.-i., Kitamura, Y., Yoshida, N., Kikutani, H., and Kishimoto, T. (1996). Defects of B-cell lymphopoiesis and bone-marrow myelopoiesis in mice lacking the CXC chemokine PBSF/SDF-1. *Nature* *382*, 635-638.

Nagasawa, T., Kikutani, H., and Kishimoto, T. (1994). Molecular cloning and structure of a pre-B-cell growth-stimulating factor. *Proceedings of the National Academy of Sciences* *91*, 2305-2309.

National Center for Biotechnology Information (NCBI). Standard Protein BLAST. <https://blast.ncbi.nlm.nih.gov/Blast.cgi?PAGE=Proteins>.

National Comprehensive Cancer Network (2014). NCCN CLinical Practice Guidelines in Oncology. Non-Hodking Lymphomas. From <https://www.nccn.org>.

National Institute of Health a (NIH). Cancer Statistics.

National Institute of Health b (NIH). National Cancer Institute. US National Library of Medicine Clinical Trials. <https://clinicaltrials.gov>.

National Institute of Health (2017a). Dailymed. YESCARTA- axicabtagene ciloleucel suspension. From:

<https://dailymed.nlm.nih.gov/dailymed/drugInfo.cfm?setid=9b70606e-b99c-4272-a0f1-b5523cce0c59>

National Institute of Health (NIH). National Cancer Institute (2017b). CAR T Cells: Engineering Patients' Immune Cells to Treat Their Cancers. From <https://www.cancer.gov/about-cancer/treatment/research/car-t-cells>.

Neelapu, S. S., Locke, F. L., Bartlett, N. L., Lekakis, L. J., Miklos, D. B., Jacobson, C. A., Braunschweig, I., Oluwole, O. O., Siddiqi, T., and Lin, Y. (2017). Axicabtagene ciloleucel CAR T-cell therapy in refractory large B-cell lymphoma. *New England Journal of Medicine* 377, 2531-2544.

Nervi, B., Ramirez, P., Rettig, M. P., Uy, G. L., Holt, M. S., Ritchey, J. K., Prior, J. L., Piwnica-Worms, D., Bridger, G., and Ley, T. J. (2009). Chemosensitization of acute myeloid leukemia (AML) following mobilization by the CXCR4 antagonist AMD3100. *Blood* 113, 6206-6214.

Ngo, V. N., Young, R. M., Schmitz, R., Jhavar, S., Xiao, W., Lim, K.-H., Kohlhammer, H., Xu, W., Yang, Y., and Zhao, H. (2011). Oncogenically active MYD88 mutations in human lymphoma. *Nature* 470, 115-119.

Nguyen, L., Papenhausen, P., and Shao, H. (2017). The role of c-MYC in B-cell lymphomas: diagnostic and molecular aspects. *Genes* 8, 116.

Nowakowski, G. S., Laplant, B. R., Pederson, L., Maurer, M. J., Macon, W. R., King, R. L., Storhoff, J., Dennis, S., Gandhi, A. K., and Thakurta, A. (2016). Lenalidomide combined with R-CHOP (R2CHOP) overcomes negative prognostic impact of ABC molecular subtype in newly diagnosed diffuse large B-cell lymphoma. In, (Am Soc Hematology).

Oken, M. M., Creech, R. H., Tormey, D. C., Horton, J., Davis, T. E., McFadden, E. T., and Carbone, P. P. (1982). Toxicity and response criteria of the Eastern Cooperative Oncology Group. *American journal of clinical oncology* 5, 649-656.

Palucka, A. K., and Coussens, L. M. (2016). The basis of oncoimmunology. *Cell* 164, 1233-1247.

Parameswaran, R., Ramakrishnan, P., Moreton, S. A., Xia, Z., Hou, Y., Lee, D. A., Gupta, K., Beck, R. C., and Wald, D. N. (2016). Repression of GSK3 restores NK cell cytotoxicity in AML patients. *Nature communications* 7, 11154.

Pasqualucci, L. (2013). The genetic basis of diffuse large B cell lymphoma. *Current opinion in hematology* 20, 336-344.

7-REFERENCES

Pasqualucci, L., and Dalla-Favera, R. (2014). SnapShot: diffuse large B cell lymphoma. *Cancer cell* 25, 132-132e1.

Pasqualucci, L., and Dalla-Favera, R. (2015). The genetic landscape of diffuse large B-cell lymphoma. Paper presented at: Seminars in hematology 52, 67-76.

Patel, S., and Woodgett, J. (2008). Glycogen synthase kinase-3 and cancer: good cop, bad cop? *Cancer cell* 14, 351-353.

Pawig, L., Klasen, C., Weber, C., Bernhagen, J., and Noels, H. (2015). Diversity and inter-connections in the CXCR4 chemokine receptor/ligand family: molecular perspectives. *Frontiers in immunology* 6, 429.

Peled, A., Petit, I., Kollet, O., Magid, M., Ponomaryov, T., Byk, T., Nagler, A., Ben-Hur, H., Many, A., and Shultz, L. (1999). Dependence of human stem cell engraftment and repopulation of NOD/SCID mice on CXCR4. *Science* 283, 845-848.

Pettersson, S., Pérez - Nueno, V. I., Ros - Blanco, L., Puig de La Bellacasa, R., Rabal, M. O., Batllori, X., Clotet, B., Clotet - Codina, I., Armand - Ugón, M., and Esté, J. (2008). Discovery of Novel Non - Cyclam Polynitrogenated CXCR4 Coreceptor Inhibitors. *ChemMedChem* 3, 1549-1557.

Pfreundschuh, M., Kuhnt, E., Trümper, L., Österborg, A., Trneny, M., Shepherd, L., Gill, D. S., Walewski, J., Pettengell, R., and Jaeger, U. (2011). CHOP-like chemotherapy with or without rituximab in young patients with good-prognosis diffuse large-B-cell lymphoma: 6-year results of an open-label randomised study of the MabThera International Trial (MInT) Group. *The lancet oncology* 12, 1013-1022.

Pfreundschuh, M., Trümper, L., Österborg, A., Pettengell, R., Trneny, M., Imrie, K., Ma, D., Gill, D., Walewski, J., and Zinzani, P.-L. (2006). CHOP-like chemotherapy plus rituximab versus CHOP-like chemotherapy alone in young patients with good-prognosis diffuse large-B-cell lymphoma: a randomised controlled trial by the MabThera International Trial (MInT) Group. *The lancet oncology* 7, 379-391.

Qi, W., Chan, H., Teng, L., Li, L., Chuai, S., Zhang, R., Zeng, J., Li, M., Fan, H., and Lin, Y. (2012). Selective inhibition of Ezh2 by a small molecule inhibitor blocks tumor cells proliferation. *Proceedings of the National Academy of Sciences* 109, 21360-21365.

Recasens-Zorzo, C., Cardesa-Salzmann, T., Ros-Blanco, L., Esteve-Arenys, A., Clot, G., Guerrero-Hernández, M., Valera, A., Moros, A., Gutierrez, G., Casanova, I., *et al.* (2017). Abstract 2169: Pharmacological modulation of CXCL12-CXCR4 intracellular trafficking potentiates the in vitro and in vivo activity of the BET bromodomain inhibitor CPI203 in diffuse large B-cell lymphoma. *Cancer Research* 77, 2169.

Reinholdt, L., Laursen, M. B., Schmitz, A., Bødker, J. S., Jakobsen, L. H., Bøgsted, M., Johnsen, H. E., and Dybkær, K. (2016). The CXCR4 antagonist plerixafor enhances the effect of rituximab in diffuse large B-cell lymphoma cell lines. *Biomarker Research* 4, 12.

Rios, A., Hsu, S. H., Blanco, A., Buryanek, J., Day, A. L., McGuire, M. F., and Brown, R. E. (2016). Durable response of glioblastoma to adjuvant therapy consisting of temozolomide and a weekly dose of AMD3100 (plerixafor), a CXCR4 inhibitor, together with lapatinib, metformin and niacinamide. *Oncoscience* 3, 156-163.

Robertson, H., Hayes, J. D., and Sutherland, C. (2017). A partnership with the proteasome; the destructive nature of GSK3. *Biochemical pharmacology* 147, 77-92.

Ros-Blanco, L., Anido, J., Bosser, R., Esté, J., Clotet, B., Kosoy, A., Ruíz-Ávila, L., Teixidó, J., Seoane, J., and Borrell, J. I. (2012). Noncyclam Tetraamines Inhibit CXC Chemokine Receptor Type 4 and Target Glioma-Initiating Cells. *Journal of medicinal chemistry* 55, 7560-7570.

Rosenwald, A., Wright, G., Chan, W. C., Connors, J. M., Campo, E., Fisher, R. I., Gascoyne, R. D., Muller-Hermelink, H. K., Smeland, E. B., and Giltnane, J. M. (2002). The use of molecular profiling to predict survival after chemotherapy for diffuse large-B-cell lymphoma. *New England Journal of Medicine* 346, 1937-1947.

Ruan, J., Martin, P., Furman, R. R., Lee, S. M., Cheung, K., Vose, J. M., LaCasce, A., Morrison, J., Elstrom, R., and Ely, S. (2010). Bortezomib plus CHOP-rituximab for previously untreated diffuse large B-cell lymphoma and mantle cell lymphoma. *Journal of Clinical Oncology* 29, 690-697.

Saenz, D., Fiskus, W., Manshouri, T., Mill, C., Sun, B., Verstovsek, S., and Bhalla, K. (2017). BET Protein Proteolysis Targeting Chimera (BETP-PROTACs) Exert Potent Activity Against Post-Myeloproliferative Neoplasm (MPN) Secondary (s)-AML Cells. *Clinical Lymphoma, Myeloma and Leukemia* 31 1951-1961.

Salaverria, I., and Siebert, R. (2011). The gray zone between Burkitt's lymphoma and diffuse large B-cell lymphoma from a genetics perspective. *Journal of clinical oncology* 29, 1835-1843.

Salles, G., Barrett, M., Foà, R., Maurer, J., O'Brien, S., Valente, N., Wenger, M., and Maloney, D. G. (2017). Rituximab in B-Cell Hematologic Malignancies: A Review of 20 Years of Clinical Experience. *Advances in Therapy* 34, 2232-2273.

Scala, S. (2015). Molecular pathways: targeting the CXCR4–CXCL12 axis—untapped potential in the tumor microenvironment. *Clinical Cancer Research* 21, 4278-4285.

7-REFERENCES

Scott, D. W., and Gascoyne, R. D. (2014). The tumour microenvironment in B cell lymphomas. *Nature Reviews Cancer* 14, 517-534.

Scott, D. W., Wright, G. W., Williams, P. M., Lih, C.-J., Walsh, W., Jaffe, E. S., Rosenwald, A., Campo, E., Chan, W. C., and Connors, J. M. (2014). Determining cell-of-origin subtypes of diffuse large B-cell lymphoma using gene expression in formalin-fixed paraffin-embedded tissue. *Blood* 123, 1214-1217.

Scheaffer, R. L., and McClave, J. T. (1993). *Probabilidad y Estadística para Ingeniería*. Tercera edición. México. Grupo editorial Iberoamérica.

Sears, R., Nuckolls, F., Haura, E., Taya, Y., Tamai, K., and Nevins, J. R. (2000). Multiple Ras-dependent phosphorylation pathways regulate Myc protein stability. *Genes & development* 14, 2501-2514.

Shain, K., Dalton, W., and Tao, J. (2015). The tumor microenvironment shapes hallmarks of mature B-cell malignancies. *Oncogene* 34, 4673-4682.

Sheiness, D., Fanshier, L., and Bishop, J. M. (1978). Identification of nucleotide sequences which may encode the oncogenic capacity of avian retrovirus MC29. *Journal of virology* 28, 600-610.

Shen, X., Artinyan, A., Jackson, D., Thomas, R. M., Lowy, A. M., and Kim, J. (2010). Chemokine receptor CXCR4 enhances proliferation in pancreatic cancer cells through AKT and ERK dependent pathways. *Pancreas* 39, 81-87.

Siegel, M. B., Liu, S. Q., Davare, M. A., Spurgeon, S. E., Loriaux, M. M., Druker, B. J., Scott, E. C., and Tyner, J. W. (2015). Small molecule inhibitor screen identifies synergistic activity of the bromodomain inhibitor CPI203 and bortezomib in drug resistant myeloma. *Oncotarget* 6, 18921-18932.

Soucek, L., Whitfield, J., Martins, C. P., Finch, A. J., Murphy, D. J., Sodik, N. M., Karnezis, A. N., Swigart, L. B., Nasi, S., and Evan, G. I. (2008). Modelling Myc inhibition as a cancer therapy. *Nature* 455, 679-683.

Soucek, L., Whitfield, J. R., Sodik, N. M., Massó-Vallés, D., Serrano, E., Karnezis, A. N., Swigart, L. B., and Evan, G. I. (2013). Inhibition of Myc family proteins eradicates KRas-driven lung cancer in mice. *Genes & development* 27, 504-513.

Speetjens, F. M., Liefers, G. J., Korbee, C. J., Mesker, W. E., van de Velde, C. J., van Vlierberghe, R. L., Morreau, H., Tollenaar, R. A., and Kuppen, P. J. (2009). Nuclear localization of CXCR4 determines prognosis for colorectal cancer patients. *Cancer Microenvironment* 2, 1-7.

Staudt, L. M., and Dave, S. (2005). The biology of human lymphoid malignancies revealed by gene expression profiling. *Advances in immunology* 87, 163-208.

Stiff, P. J., Unger, J. M., Cook, J. R., Constine, L. S., Couban, S., Stewart, D. A., Shea, T. C., Porcu, P., Winter, J. N., and Kahl, B. S. (2013). Autologous transplantation as consolidation for aggressive non-Hodgkin's lymphoma. *New England Journal of Medicine* 369, 1681-1690.

Sun, X., Cheng, G., Hao, M., Zheng, J., Zhou, X., Zhang, J., Taichman, R. S., Pienta, K. J., and Wang, J. (2010). CXCL12/CXCR4/CXCR7 chemokine axis and cancer progression. *Cancer and Metastasis Reviews* 29, 709-722.

Swerdlow, S. H., Campo, E., Harris, N., Jaffe, E., Pileri, S., Stein, H., Thiele, J. (2008). *WHO Classification of Tumors of Hematopoietic and Lymphoid Tissues* 4th Ed.

Swerdlow, S. H., Campo, E., Pileri, S. A., Harris, N. L., Stein, H., Siebert, R., Advani, R., Ghielmini, M., Salles, G. A., and Zelenetz, A. D. (2016). The 2016 revision of the World Health Organization classification of lymphoid neoplasms. *Blood* 127, 2375-2390.

Tachibana, K., Hirota, S., Iizasa, H., Yoshida, H., Kawabata, K., Kataoka, Y., Kitamura, Y., Matsushima, K., Yoshida, N., and Nishikawa, S. (1998). The chemokine receptor CXCR4 is essential for vascularization of the gastrointestinal tract. *Nature* 393, 591-594.

Tapia, G., Lopez, R., Muñoz - Mármol, A. M., Mate, J. L., Sanz, C., Marginet, R., Navarro, J. T., Ribera, J. M., and Ariza, A. (2011). Immunohistochemical detection of MYC protein correlates with MYC gene status in aggressive B cell lymphomas. *Histopathology* 59, 672-678.

Tashiro, K., Tada, H., Heilker, R., Shirozu, M., Nakano, T., and Honjo, T. (1993). Signal sequence trap: a cloning strategy for secreted proteins and type I membrane proteins. *Science* 261, 600-603.

Teicher, B. A., and Fricker, S. P. (2010). CXCL12 (SDF-1)/CXCR4 pathway in cancer. *Clin Cancer Res* 16, 2927-2931.

Testoni, M., Zucca, E., Young, K., and Bertoni, F. (2015). Genetic lesions in diffuse large B-cell lymphomas. *Annals of Oncology* 26, 1069-1080.

Tilly, H., Gomes da Silva, M., Vitolo, U., Jack, A., Meignan, M., Lopez-Guillermo, A., Walewski, J., Andre, M., Johnson, P., and Pfreundschuh, M. (2015). Diffuse large B-cell lymphoma (DLBCL): ESMO Clinical Practice Guidelines for diagnosis, treatment and follow-up. *Annals of Oncology* 26, v116-v125.

7-REFERENCES

Tomayko, M. M., and Reynolds, C. P. (1989). Determination of subcutaneous tumor size in athymic (nude) mice. *Cancer chemotherapy and pharmacology* 24, 148-154.

Tsai, W.-B., Aiba, I., Long, Y., Lin, H.-K., Feun, L., Savaraj, N., and Kuo, M. T. (2012). Activation of Ras/PI3K/ERK pathway induces c-Myc stabilization to upregulate argininosuccinate synthetase, leading to arginine deiminase resistance in melanoma cells. *Cancer research* 72, 2622-2633.

Uddin, S., Hussain, A. R., Ahmed, M., Al-Dayel, F., Bu, R., Bavi, P., and Al-Kuraya, K. S. (2010). Inhibition of c-MET is a potential therapeutic strategy for treatment of diffuse large B-cell lymphoma. *Laboratory investigation* 90, 1346-1356.

Uddin, S., Hussain, A. R., Siraj, A. K., Manogaran, P. S., Al-Jomah, N. A., Moorji, A., Atizado, V., Al-Dayel, F., Belgaumi, A., and El-Solh, H. (2006). Role of phosphatidylinositol 3'-kinase/AKT pathway in diffuse large B-cell lymphoma survival. *Blood* 108, 4178-4186.

Valera, A., López-Guillermo, A., Cardesa-Salzmann, T., Climent, F., González-Barca, E., Mercadal, S., Espinosa, Í., Novelli, S., Briones, J., and Mate, J. L. (2013). MYC protein expression and genetic alterations have prognostic impact in patients with diffuse large B-cell lymphoma treated with immunochemotherapy. *Haematologica* 98, 1554-1562.

Van Aller, G. S., Pappalardi, M. B., Ott, H. M., Diaz, E., Brandt, M., Schwartz, B. J., Miller, W. H., Dhanak, D., McCabe, M. T., and Verma, S. K. (2013). Long residence time inhibition of EZH2 in activated polycomb repressive complex 2. *ACS chemical biology* 9, 622-629.

Vervoorts, J., Lüscher-Firzlaff, J., and Lüscher, B. (2006). The ins and outs of MYC regulation by posttranslational mechanisms. *Journal of Biological Chemistry* 281, 34725-34729.

Wang, L., Wang, Z., Yang, B., Yang, Q., Wang, L., and Sun, Y. (2009). CXCR4 nuclear localization follows binding of its ligand SDF-1 and occurs in metastatic but not primary renal cell carcinoma. *Oncology reports* 22, 1333-1339.

Whitfield, J. R., Beaulieu, M.-E., and Soucek, L. (2017). Strategies to inhibit Myc and their clinical applicability. *Frontiers in cell and developmental biology* 5, 10.

Wilson, W. H., Young, R. M., Schmitz, R., Yang, Y., Pittaluga, S., Wright, G., Lih, C.-J., Williams, P. M., Shaffer, A. L., and Gerecitano, J. (2015). Targeting B cell receptor signaling with ibrutinib in diffuse large B cell lymphoma. *Nature medicine* 21, 922-926.

Wong, C., Laddha, S., Tang, L., Vosburgh, E., Levine, A., Normant, E., Sandy, P., Harris, C., Chan, C., and Xu, E. (2014). The bromodomain and extra-terminal inhibitor CPI203 enhances the antiproliferative effects of rapamycin on human neuroendocrine tumors. *Cell death & disease* *5*, e1450.

Xu, Z.-Z., Shen, J.-K., Zhao, S.-Q., and Li, J.-M. (2017). Clinical significance of chemokine receptor CXCR4 and mammalian target of rapamycin (mTOR) expression in patients with diffuse large B-cell lymphoma. *Leukemia & lymphoma*, 1-10.

Ying, C. Y., Dominguez-Sola, D., Fabi, M., Lorenz, I. C., Hussein, S., Bansal, M., Califano, A., Pasqualucci, L., Basso, K., and Dalla-Favera, R. (2013). MEF2B mutations lead to deregulated expression of the oncogene BCL6 in diffuse large B cell lymphoma. *Nature immunology* *14*, 1084-1092.

Yoon, N., Ahn, S., Yoo, H. Y., Kim, S. J., Kim, W. S., and Ko, Y. H. (2017). Cell-of-origin of diffuse large B-cell lymphomas determined by the Lymph2Cx assay: better prognostic indicator than Hans algorithm. *Oncotarget* *8*, 22014-22022.

Younes, A., Thieblemont, C., Morschhauser, F., Flinn, I., Friedberg, J. W., Amorim, S., Hivert, B., Westin, J., Vermeulen, J., and Bandyopadhyay, N. (2014). Combination of ibrutinib with rituximab, cyclophosphamide, doxorubicin, vincristine, and prednisone (R-CHOP) for treatment-naïve patients with CD20-positive B-cell non-Hodgkin lymphoma: a non-randomised, phase 1b study. *The lancet oncology* *15*, 1019-1026.

Zhu, H., Bengsch, F., Svoronos, N., Rutkowski, M. R., Bitler, B. G., Allegranza, M. J., Yokoyama, Y., Kossenkov, A. V., Bradner, J. E., and Conejo-Garcia, J. R. (2016). BET bromodomain inhibition promotes anti-tumor immunity by suppressing PD-L1 expression. *Cell reports* *16*, 2829-2837.

Zlotnik, A., Burkhardt, A. M., and Homey, B. (2011). Homeostatic chemokine receptors and organ-specific metastasis. *Nature Reviews Immunology* *11*, 597-606.

Zou, Y.-R., Kottmann, A. H., Kuroda, M., Taniuchi, I., and Littman, D. R. (1998). Function of the chemokine receptor CXCR4 in haematopoiesis and in cerebellar development. *Nature* *393*, 595-599.

Acknowledgements

Firstly, I would like to thank my supervisors Dr. Gaël Roué and Dr. Patricia Pérez-Galán for directing this doctoral thesis and for trusting me with this project. *Gracias Gaël por dírígmme a las duras y a las maduras. Gracias Patri por estar ahí.* My most sincere thank you to Dr. Dolors Colomer and Dr. Elías Campo for their valuable support in times of uncertainty.

To all the former and current members of the Physiopathology and Molecular Bases in Hematology lab, thank you for being SO AMAZING! *Gràcies Teresa Rubió per posar-me en contacte amb el Gaël. Laura M, fue un placer tenerte en el lab y trabajar y aprender contigo mano a mano. Martina, companya de CXCR4, gràcies per les discussions crítiques sobre ciència (i sobre la vida). Anna E, companya de tesis, congressos i viatges. Gràcies per ser-hí. En tot. Arí, que hauria fet sense la teva UCI on ressusciten les cèl·lules? Vaní, Anna E, gràcies por enseñarme a poder trabajar independiente con los ratones. Neus S, que en seria dels meus dubtes existencials d'immunología sense les teves respostes? Silvia, Sandra M, Jocabed, Arancha, Laura J, Nuria, Sandra C, Ivan, Alba, Arnau, Anna V, vaní, Arí, Juan, Neus J, Eriong, Anna E, Mònica, Martina, Fabian, Neus S, Morihiro, Laia, Irene, Laura M, Rupal, Carlota, Javi, David...The memories and anecdotes I take with me would write an entire book. Thank you all for being the best lab mates one could ever have. Let's never stop cheering for this at Broders with an after work mojito! Jaunito, brindo per jugar-nos-en molts més. Vaní, Ivan, Laura, por todos mis próximos mates que me harán recordaros. Arí, Laia, com esmorzaré tots els dies sense vosaltres?*

Marta, thanks for managing the IDIBAPS, CEK, Planta 2. To all the members of the *planta 2*, thank you for your everyday smiles and for being so easy to work with.

Without the work of our collaborators this thesis would not have been possible. This includes Dr. Teresa Cardesa and Dr. Lluís Colomo who, in collaboration with Gaël, initiated the research of CXCR4 in DLBCL in our institution. *Gràcies Lluís pel teu temps, paciència i esperit crític.* The Molecular Engineering Group (GEM) (IQS School of Engineering) synthesized the small molecule evaluated in this thesis. *Gràcies Vera Uixó per l'ajuda amb el docking i Dr. Albert Gibert per estar*

sempre disposat a resoldre els meus dubtes sobre la química de l'IQSS-01.01. The Oncogenesis and Antitumor Drug Group (IIB-Sant Pau) welcomed me to their lab for the generation of GFP+/Luc+ cell lines. Gràcies Cristina Suárez pel suport tècnic i Dra. Isolda Casanova per la teva sempre disponibilitat per col·laborar, aportar noves idees i discutir sobre CXCR4.

I would also like to thank all the patients that have collaborated in this and other studies, and to mention the mice that have unwillingly given their life for the benefit of cancer research.

It is only fair to thank my previous mentors and colleagues that have helped me push my career towards this PhD. Thank you Bigas' lab (IMIM, 2010) for presenting me with high quality public research, and for encouraging me to believe in my qualities as a researcher in science. Thanks Aliaga's lab (University of Cambridge, 2012) for making me aware of the necessity of high quality basic research for scientific and clinical progress. I can't not mention my Biology and Biochemistry professors, and undergraduate classmates: Ignasi, Edu, Irene, David, Emma, Ferràn, Quim, Albert... thanks for some of the most fun years of my life (Faculty of Biosciences, UAB, 2005-2010). Thanks to all the teachers and schools that have positively collaborated in my education since 1989.

I wouldn't have possibly survived these 4 years of hard work, ups and downs, and long working hours without the multitude of support from people outside of the lab:

Oscar, això va començar amb la teva espelmeta.

*Gràcies Cor Aglepta, per les vostres veus i per l'alegria de cada assaig que m'ha ajudat a desconectar per poder seguir endavant. "Ohne Musik wäre das Leben ein Irrtum".***

**Without music, life would be a mistake, Federich Nietzsche.*

Gràcies Maria del Mar i Irene per camímar plegades. Juntas arribarem al CIM.

Merce, píxi, gràcies per ser-hi sempre.

Catina, companya de carrera i de vida. Gràcies per ser la meua imatge especular. Lola, Roser gràcies pels sopars fugaços i per seguir al meu costat. Prometem-nos que a partir d'ara seran menys dispersos.

Gràcies als dels partits de volley patxanga, als de Sencu, Mirasol, valldoreix. Al Brosa i al Dani. A les Nenes, sorry per les meves semi bombes de fum durant la tesis i gràcies per respectar-les.

Gràcies Montse per no deixar mai de visitar-me quan vens a Barcelona.

Thank you Natasha and Vanessa for keeping in touch after so long, for your help with my sudden grammatical questions, and for being such an important part of my life.

To my friends from "Cambridge" (with a special mention for Artur), thanks for the business times. I look forward to many more.

Albert, gràcies per existir, pel teu suport incalculable. Ara sí que ja pots dir "I survived my GF's PhD dissertation!"

Infinite thanks to my parents to whom I dedicate this dissertation. Thank you for having always emphasized the importance of culture and education as a path towards personal growth and independence, and for encouraging critical thinking at home. Thank you for your love and caring.

To everyone who, one way or another, has contributed to the fulfillment of this thesis,

THANK YOU



Barcelona, 23rd April 2018

Sant Jordi

ANNEX

Scientific publications produced during this thesis

Clara Recasens-Zorzo, Teresa Cardesa-Salzmann, Laia Ros-Blanco, Anna Esteve-Arenys, Guillem Clot, Martina Guerrero-Hernández, Vanina Rodríguez, Davide Soldini, Alexandra Valera, Alexandra Moros, Fina Climent, Eva González-Barca, Santiago Mercadal, Leonor Arenillas, Xavier Calvo, José Luís Mate, Gonzalo Gutiérrez-García, Isolda Casanova, Ramón Mangués, Alejandra Sanjuan-Pla, Pablo Menéndez, Antonio Martínez, Dolors Colomer, Roger Estrada Tejedor, Jordi Teixidó, Elias Campo, Armando López-Guillermo, José Ignacio Borrell, Luis Colomo, Patricia Pérez-Galán, and Gaël Roué. (2018). Pharmacological modulation of CXCR4 cooperates with BET bromodomain inhibition in diffuse large B-cell lymphoma. *Manuscript submitted for publication*.

Scholar-in-Training Award recipient for Abstract 2169 presented in a Poster Session at the AACR Annual Meeting 2017:

Clara Recasens-Zorzo, Teresa Cardesa-Salzmann, Laia Ros-Blanco, Anna Esteve-Arenys, Guillem Clot, Martina Guerrero-Hernández, Alejandra Valera, Alejandra Moros, Gonzalo Gutierrez, Isolda Casanova, Ramón Mangués, Alejandra Sanjuan, Pablo Menéndez, Vanina Rodriguez, Antonio Martínez, Pedro Jares, Dolors Colomer, Jordi Teixidó, José Ignacio Borrell, Elias Campo, Armando López-Guillermo, Luís Colomo, Patricia Pérez-Galán and Gaël Roué. (2017). Abstract 2169: Pharmacological modulation of CXCL12-CXCR4 intracellular trafficking potentiates the *in vitro* and *in vivo* activity of the BET bromodomain inhibitor CPI203 in diffuse large B-cell lymphoma. *Cancer Research*. DOI: 10.1158/1538-7445.AM2017-2169

Simon Body, Anna Esteve-Arenys, Hadjer Miloudi, **Clara Recasens-Zorzo**, Guergana Tchakarska, Alexandra Moros, Sophie Bustany, Anna Vidal-Crespo, Vanina Rodriguez, Régis Lavigne, Emmanuelle Com, Isolda Casanova, Ramón Mangués, Oliver Weigert, Alejandra Sanjuan-Pla, Pablo Menéndez, Bénédicte Marcq, Jean-Michel Picquenot, Patricia Pérez-Galán, Fabrice Jardin, Gaël Roué & Brigitte Sola. (2017). Cytoplasmic cyclin D1 controls the migration and invasiveness of mantle lymphoma cells. *Scientific Reports*. DOI: 10.1038/s41598-017-14222-1

Simon Body, Anna Esteve-Arenys, **Clara Recasens-Zorzo**, Xavier Troussard, Gaël Roué & Brigitte Sola. (2017). A mouse model of disseminated mantle cell lymphoma highlights a

ANNEX

lack of activity of estrogen receptor β agonists toward tumor burden. *Leukemia & Lymphoma*. DOI: 10.1080/10428194.2017.1399313

